Dipl.-Ing. Alexandra Binter

Enzymes of Nikkomycin Biosynthesis

DISSERTATION

zur Erlangung des akademischen Grades einer

Doktorin der technischen Wissenschaften (Dr. *techn.*)

erreicht an der

Technischen Universität Graz

Betreuer: Univ.-Prof. Mag. *rer. nat.* Dr. *rer. nat.* Peter Macheroux

Institut für Biochemie

Technische Universität Graz

Graz, 2011

Acknowledgment

I would like to thank all people who have helped and inspired me during my doctoral study.

I especially want to thank my supervisor, Prof. Peter Macheroux, for his guidance and support during my research and for giving me the opportunity to work on such an interesting topic.

I am grateful to all present and former members of our working group who inspired me in research and life through our interactions during the long hours in the lab. They were not only always helpful, they also really made me enjoy coming to work each morning. In particular, I would like to thank Steve Stipsits and Martin Puhl for their expert support in matters of practical lab work and handling of equipment.

It was delightful to work in cooperation with Gustav Oberdorfer, whose unswerving optimism provided a great source of motivation for me. Discussing problems and observations with Gustav not only provided me with insights into the field of structural biology but also was a lot of fun!

During the last years I had the pleasure to guide several very talented and highly motivated students through the work on their bachelor thesis. Thanks to Georg Altenbacher, Stefanie Nerstheimer, Patrik Fladischer, and Heinz Hammerlindl, essential contributions to the nikkomycin project were made.

Prof. Karl Gruber, Prof. Kurt Faber and Prof. Anton Glieder deserve special thanks as my thesis committee members for dedicating time and knowledge to advise and support me.

I would also like to thank Prof. Bertolt Gust from the University of Tübingen for providing me with information, protocols and materials for working with *Streptomyces* and for immediately trying to help and advise me whenever I contacted him with questions.

Furthermore, I would like to say thank you to Prof. Hans-Jörg Weber for performing NMR measurements, to Prof. Tanja Wrodnigg and Verena Schenk for their attempts to synthesise the keto acid substrate for NikK, to Prof. Michael Murkovic for MS measurements, to Prof. Dennis Dean (Virginia Tech) for sending me the plasmid for NifS expression and to Dr. Tobias Gräwert (TU Munich) for the *isc*-plasmid.

My deepest gratitude goes to my family and to Juan. It is their unflagging love and support that gives me the confidence and strength to face the challenges and overcome the difficulties that come up in my way.

Abstract

Nikkomycins are peptide nucleosides which can be isolated from the fermentation broth of *Streptomyces tendae* and *S. ansochromogenes*. Due to their inhibition of chitin synthase they have fungicidal properties and a great potential as antibiotics. The peptide moiety is formed by hydroxypyridylhomothreonine, the nucleoside moiety consists of aminohexuronic acid with an N-glycosidically linked uracil or 4-formyl-4-imidazoline-2-one base. This work is intended to shed light onto the biosynthetic pathway that leads to the aminohexuronic acid moiety of nikkomycins. Commencing with the transfer of an enolpyruvyl moiety to the 3´-position of UMP, which is catalyzed by NikO, a series of reactions leads to a rearrangement of the carbon skeleton and finally to the formation of aminohexuronic acid. The enzymes involved in these reactions are encoded on the *nikIJKLMNO* operon of *S. tendae*. The enzymes NikI, NikJ, NikK, NikL, NikM, and NikO were expressed heterologously in *Escherichia coli*, in order to characterize them biochemically and determine their role in the biosynthesis of nikkomycins. Furthermore, nikkomycin intermediates produced by *Streptomyces* mutants featuring disruptions of the respective genes should be analyzed, but no nikkomycins could be detected in their fermentation media. Comparisons of Nik enzyme sequences to those of known enzymes in the databases allow some predictions on the reactions each *nik* enzyme might catalyze. None of the enzymes was observed to convert 3´-EPUMP, the product of the NikO catalyzed reaction, so far. NikK is a pyridoxal-5-phosphate dependent aminotransferase, which is expected to introduce the amino group into the aminohexuronic acid moiety. Several amino acids were shown to serve as amino group donors, and L-glutamate was the most efficient one. NikJ possesses an iron-sulfur cluster and probably belongs to the family of radical SAM enzymes. Its role in nikkomycin biosynthesis is unclear, but it is expected to function as an oxidoreductase. Cleavage of S-adenosylmethionine could not be observed. Furthermore, NikS was expressed, an enzyme that is expected to play a role in the assembly of nikkomycins.

Kurzfassung

Nikkomycine sind Peptidnucleoside, welche aus dem Fermentationsmedium von *Streptomyces tendae* und *S. ansochromogenes* isoliert werden können. Aufgrund ihrer Hemmung der Chitinsynthase besitzen sie fungizide Eigenschaften und haben ein beachtliches Potential als Antibiotika. Der Peptidrest wird aus Hydroxypyridylhomothreonin gebildet, der Nukleosidrest besteht aus Aminohexuronsäure mit einer N-glykosidisch verknüpften Uracil- oder 4-Formyl-4-imidazoline-2-on-Base. Diese Arbeit soll zur Aufklärung des Biosyntheseweges beitragen, der zur Bildung des Aminohexuronsäurerestes von Nikkomycinen führt. Beginnend mit dem Transfer eines Enolpyruvylrestes an die 3´-Position von UMP, der von dem NikO Enzym katalysiert wird, führt eine Reihe von Reaktionen zu einer Umordnung des Kohlenstoffgerüsts und schliesslich zur Bildung der Aminohexuronsäure. Die an diesen Reaktionen beteiligten Enzyme sind am *nikIJKLMNO* Operon von *S. tendae* codiert. Die Enzyme NikI, NikJ, NikK, NikL, NikM und NikO wurden in *Escherichia coli* exprimiert, um sie biochemisch zu charakterisieren und ihre Rolle in der Nikkomycinbiosynthese zu untersuchen. Weiters sollten Intermediate untersucht werden, die von *Streptomyces* Deletionsmutanten der jeweiligen Gene segregiert werden, jedoch konnten keine Nikkomycine in den Fermentationsmedien dieser Mutanten nachgewiesen werden. Sequenzvergleiche mit bekannten Proteinen in Datenbanken ermöglichen hypothetische Vorhersagen über die Reaktionen, die von den *nik* Enzymen katalysiert werden. Keines der Enzyme setzte bisher 3´-EPUMP, das Produkt der NikO-katalysierten Reaktion, um. NikK ist eine Pyridoxal-5-phoshphat-abhängige Aminotransferase, und katalysiert vermutlich den Einbau der Aminogruppe in den Aminohexuronsäurerest. Es wurde festgestellt, dass verschiedene Aminosäuren als Aminogruppendonoren fungieren können, am effizientesten ist jedoch L-Glutaminsäure. NikJ weist einen Eisen-Schwefel Cluster auf und gehört vermutlich zur Familie der Radical SAM Enzyme. Seine Rolle in der Nikkomycinbiosynthese ist unklar, vermutlich fungiert es als Oxidoreduktase. Spaltung von S-Adenosylmethionin konnte keine beobachtet werden. Weiters wurde das Enzym NikS exprimiert, welches wahrscheinlich an der Verknüpfung des Peptid- und Nukleosidrestes beteiligt ist.

EIDESSTATTLICHE ERKLÄRUNG

Ich erkläre an Eides statt, dass ich die vorliegende Arbeit selbstständig verfasst, andere als die
angegebenen Quellen/Hilfsmittel nicht benutzt, und die den benutzten Quellen wörtlich und inhaltlich entnommenen Stellen als solche kenntlich gemacht habe.

STATUTORY DECLARATION

I declare that I have authored this thesis independently, that I have not used other than the declared sources / resources, and that I have explicitly marked all material which has been quoted either literally or by content from the used sources.

Graz, September 2011

Contents

CHAPTER 1

1 Introduction

1.1 Nucleoside antibiotics targeting cell wall assembly in fungi

Nikkomycins belong to a group of nucleoside natural product antibiotics which target fungal chitin cell wall biosynthesis. Fungal cells possess a chitin polysaccharide on the outside of the cytoplasmic membrane, to which further β-glucan and mannoprotein layers are attached. Chitin, the second most common polysaccharide found in nature, is required for fungal cell wall structural rigidity. It consists of a β-1,4-linked polymer of *N*-acetylglucosamine sugars, which are formed biosynthetically from UDP-*N*-acetylglucosamine (UDPGlcNAc). This reaction is catalyzed by chitin synthase (UDP-2-acetamido-2-deoxy-D-glucose: chitin 4-β-acetamidodeoxy-D-glucosyltransferase; EC 2.4.1.16) (1). In *Saccharomyces cerevisiae*, three chitin synthase enzymes are present, each having a different role in cell division. No single chitin synthase is essential for viability, but complete loss of chitin synthase activity is lethal to the cell (2). Chitin synthase represents an attractive antifungal target, considering that chitin is absent from mammalian cells. Chitin synthase is inhibited by uridine nucleoside natural product antibiotics which bind in place of UDPGlcNAc. This inhibition causes osmotic sensivity and growth arrest, which leads to cell death (3). Nikkomycins and polyoxins represent attractive compounds for study as they are effective inhibitors of chitin biosynthesis (4). Considering the increase in life-threatening fungal infections particularly occuring in immuno-compromised patients, the growing restistance of fungi to clinically used antifungal drugs, and the toxicity of antifungal drugs, nikkomycins and polyoxins have a great potential for drug development (5).

1.2 The history of nikkomycins and polyoxins

Nikkomycins and polyoxins represent two structurally related groups of fermentation secondary metabolites that act as specific inhibitors of chitin synthase. The polyoxins, produced by *Streptomyces cacaoi* were first described in 1965 (6) and the nikkomycins, produced by *Streptomyces tendae*, were described in 1976 (4). Both groups of peptide-nucleoside compounds were isolated during the search for new agricultural fungicides and pesticides. The polyoxins were discovered in a screen against a fungus which causes sheath blight in rice plants, *Pellicularia filamentosa* f. sp. *sasakii* (7). A crude mixture of polyoxins was marketed as a fungicide for a variety of agricultural applications. *Streptomyces tendae* Tü901 was the first nikkomycin producing strain, isolated in 1970 from a soil sample collected at the famous five-storey pagoda in Nikko,

Japan (8). A few years later, a subspecies of *S. cacaoi* was discovered to produce a number of secondary metabolites termed neopolyoxins, which were identical in structure to nikkomycins (9). More recently, nikkomycins were also discovered in the fermentation broth of *S. ansochromogenes* (10). 13 naturally occurring polyoxins (polyoxins A through M) and 14 naturally derived nikkomycins (nikkomycins B_x, B_z, C_x, C_z, D, E, I, J, M, N, X, Z, pseudo-J, pseudo-Z) have been described (4;11-16). Despite excellent *in vitro* results of inhibition of chitin synthase, nikkomycins and polyoxins show low *in vivo* activity, due to poor uptake. Consequently, a number of synthetic studies have been performed to generate their analogues to probe structure-activity relationships and design new antifungals with improved physicochemical properties. Those studies include the synthesis of nikkomycin Z analogues from uracil polyoxin C, in which the peptidyl chain is modified (17) and the generation of a carbohydrate ring-enlarged pyranosyl nikkomycin B analogue (18).

1.3 The structures of nikkomycins and polyoxins

1.3.1 Nikkomycins produced by wild type *Streptomyces tendae* and *ansochromogenes*

Structurally, nikkomycins can be classified as peptide nucleosides. The peptidyl side chain of the biologically active nikkomycins I, J, X, and Z, 4-hydroxy-3-methyl-4-(3'-hydroxy-6'-pyridyl)butanoic acid (hydroxypyridylhomothreonine, HPHT, or nikkomycin D), is linked to the nucleoside moiety *via* a peptide bond. The nucleoside moiety (nikkomycin C_x or C_z) consists of 5-aminohexuronic acid with an *N*-glycosidically linked base. The base is uracil in nikkomycins Z and J, and 4-formyl-4-imidazoline-2-one in nikkomycins X and I. Nikkomycins I and J have glutamic acid peptidically bound to the 6'-carboxyl group of the aminohexuronic acid moiety (19) (Figure 1). From the fermentation broth of the wild type strain *S. tendae* Tü901, nikkomycins Z, X, J and I, as well as the biologically inactive nikkomycins C_x, C_z and D can be isolated.

Nikkomycin	R₁	R₂	R₃
X			OH
Z			OH
I			Glu
J			Glu
Cₓ		H	OH
Cᴢ		H	OH
D			
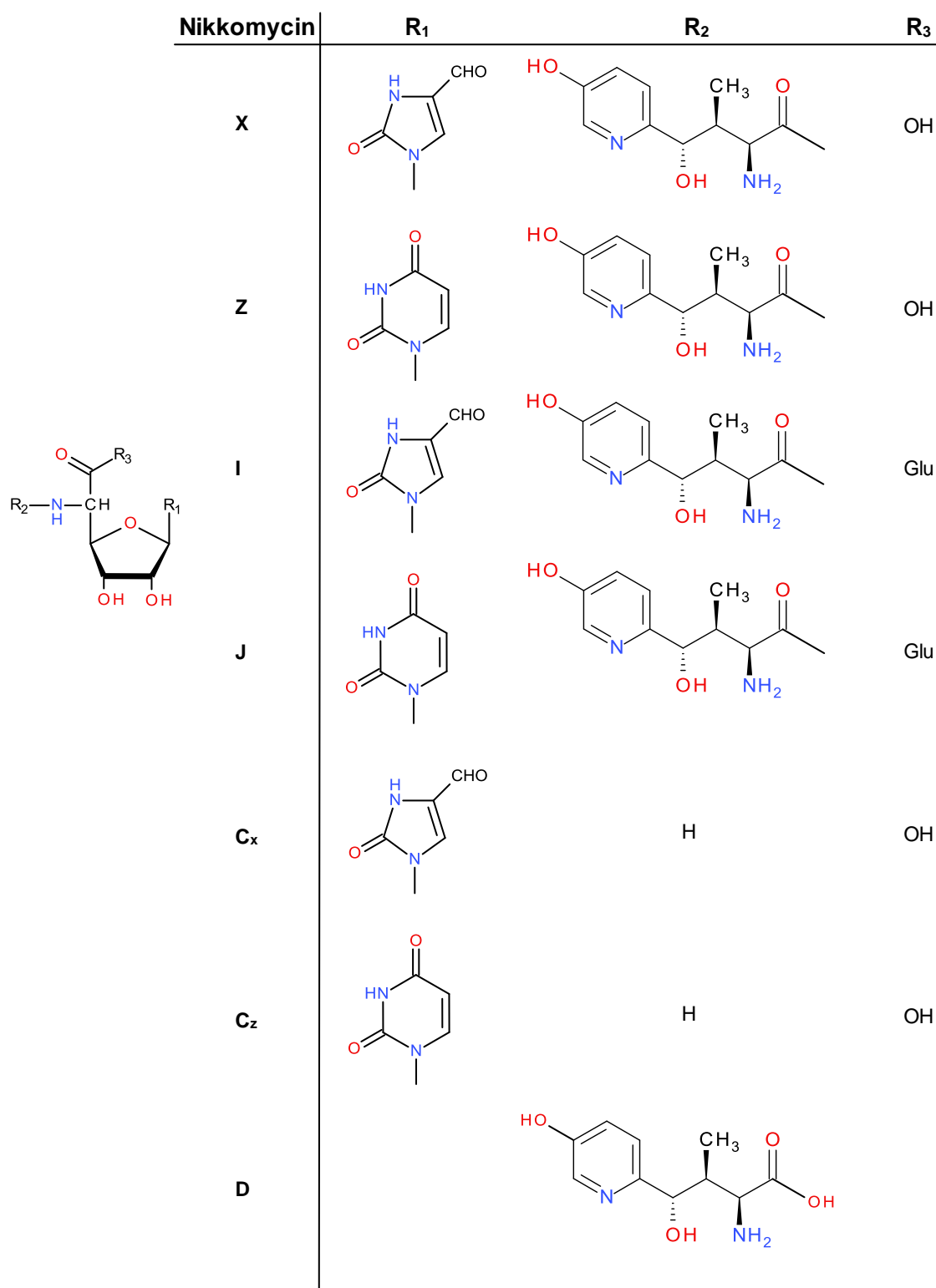
Figure 1: Chemical structures of nikkomycins isolated from *S. tendae* Tü901 culture broth

4

1.3.2 Nikkomycins produced by mutants of *Streptomyces tendae* and *ansochromogenes*

More than 20 biologically active nikkomycin structures have been generated by mutasynthesis, directed fermentation and enzymatic modification, or have been isolated as minor components from the culture filtrate of *Streptomyces tendae* Tü901 or from mutant strains (11;19-22).
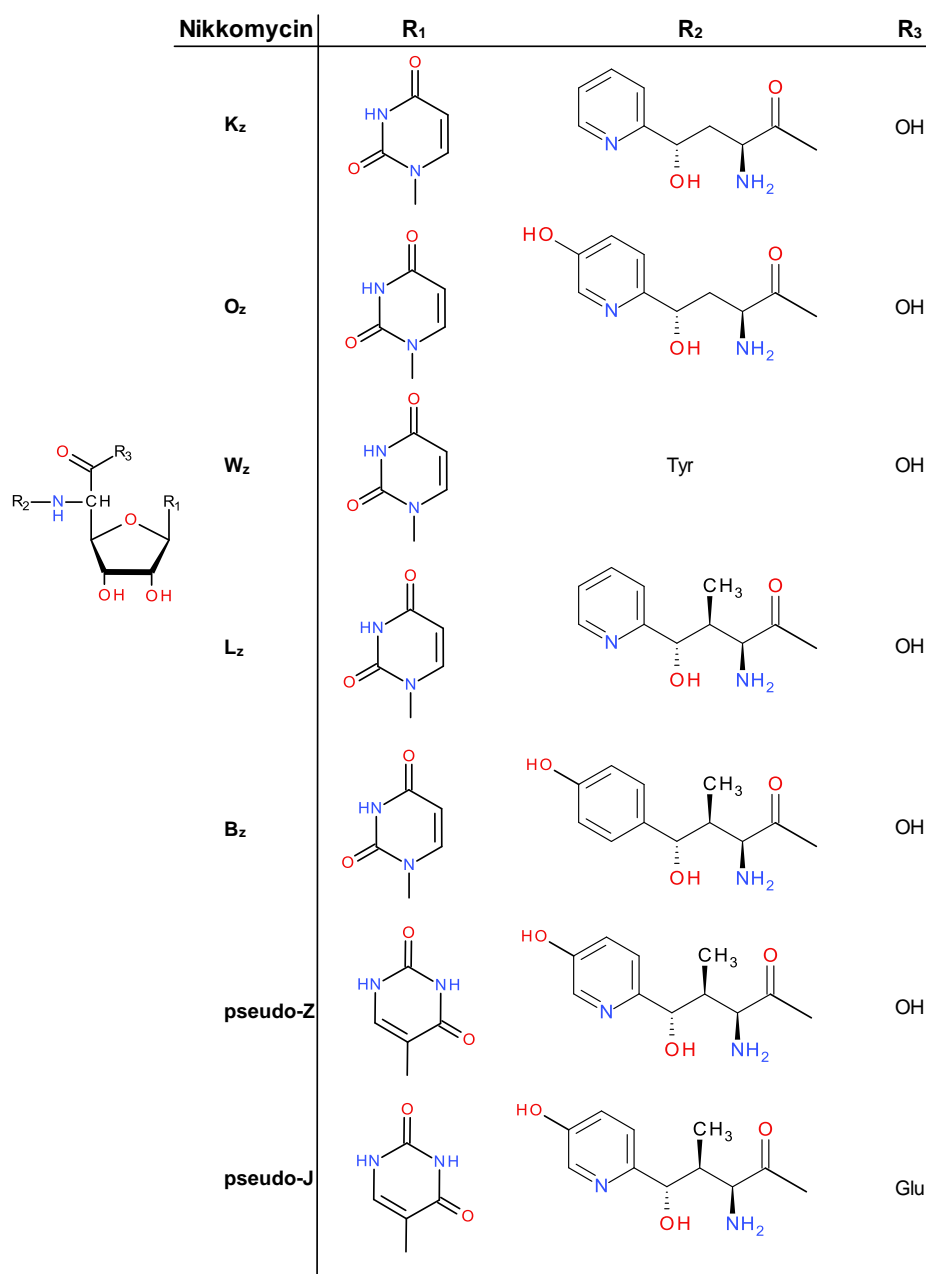
Figure 2: Chemical structures of nikkomycins produced by mutants of *Streptomyces tendae* Tü901

Nikkomycins K_z, K_x, O_z, and O_x were obtained from the mutant strain *S. tendae* Tü 901/395 (20). Further mutations led to the strain *S. tendae* Tü901/395-11/32, which additionally produced nikkomycins W_z and W_x (22). A genetically engineered mutant was obtained by inserting a kanamycin resistance gene in the nikkomycin biosynthesis gene *nikF*. Nikkomycins L_z and L_x were isolated from the fermentation broth of this mutant (19). When fed with benzoic acid, resting cell cultures of a genetically engineered *S. tendae* Tü901 strain deficient in nikkomycin biosynthesis gene *nikC*, produced nikkomycins B_x and B_z, which exhibit a significantly higher pH stability than nikkomycins X and Z (23). The mutant strain *S. tendae* Tü901/PF 53$^+$ -3 was shown to produce nikkomycins pseudo-Z and pseudo-J, which have a C-glycosidic linkage to the uracil base (11) (Figure 2).

1.3.3 Polyoxins

Polyoxins, which are produced by *Streptomyces cacaoi* var. *asoensis* (14;24) and *S. aureochromogenes* are composed of three moieties (Figure 3), including a nucleoside skeleton and the two modified amino acids polyoximic acid and carbamoylpolyoxamic acid (25).

Polyoxin	R_1	R_2
B	CH_2OH	OH
K	H	
H	CH_3	
A	CH_2OH	
F	COOH	
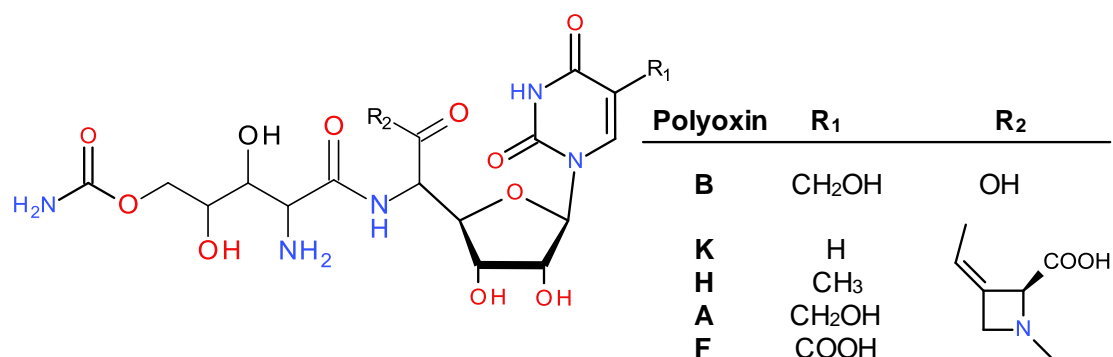
Figure 3: Chemical structures of several polyoxins

1.3.4 Nikkomycin-polyoxin hybrid antibiotics

The hybrid antibiotics polyoxin N and polynik A (Figure 4) were generated by introduction of the genes required for the dipeptidyl moiety of polyoxin from *Streptomyces cacaoi* into a *S. ansochromogenes* mutant. Polynik A was identified as a potent antifungal agent, polyoxin N is a naturally occurring compound. The hybrid antibiotics exhibited improved properties, compared to both their parents: they had better inhibitory activity against phytopathogenic fungi than polyoxin B, and were more stable under different pH and temperature conditions than nikkomycin X.
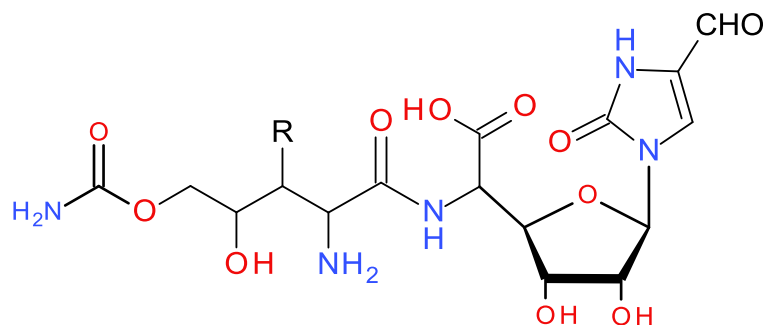
Figure 4: Structure of polyoxin N (R=OH) and polynik A (R=H)

1.4   Polyoxins and nikkomycins: biochemical aspects

Polyoxins and nikkomycins bear striking structural similarity to UDP-*N*-acetylglucosamine (Figure 5), the precursor for chitin. The biologically active compounds of each group act as competitive inhibitors of fungal chitin synthase (26;27). Thereby they differ from previously described aminoacyl nucleoside antibiotics, which act by the inhibition of protein biosynthesis (28).
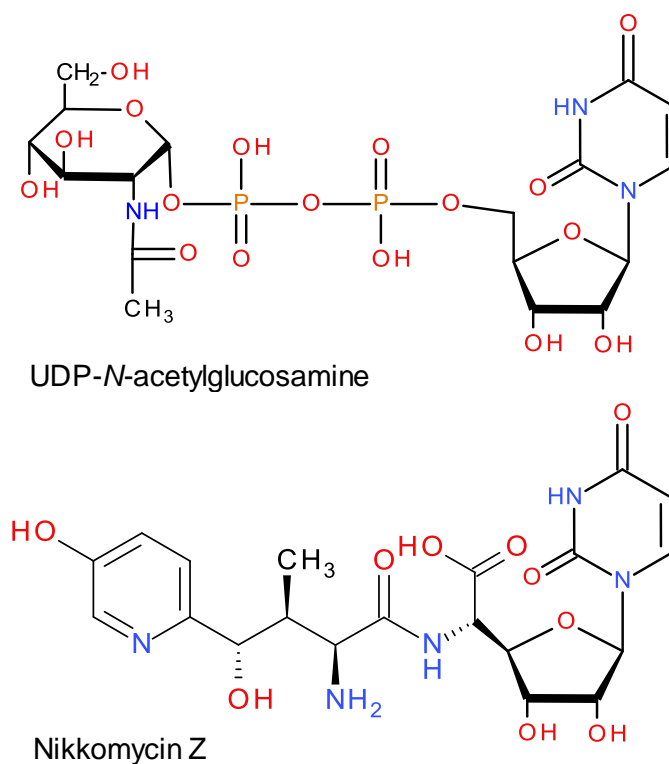
Figure 5: Structures of UDP-N-acetylglucosamine and nikkomycin Z

The nikkomycins and polyoxins have rather similar *in vitro* activity against isolated chitin synthases from various fungi, with K_i values in the range of 0.5 to 3.5 µM for nikkomycins X and Z (29;30). The ability to inhibit chitin synthesis is not limited to fungi, nikkomycins were also evaluated for potential use as insecticidal agents (8).

Nikkomycins have been studied with respect to their actual mechanisms of action. To elucidate structure-function relationships, variations in the peptide and nucleoside components were created. In contrast to polyoxins, nikkomycins have a subclass which possesses a 4-formyl-4-imidazoline-2-one base instead of uracil. This group, with nikkomycin X as its most important representative, exhibits a higher binding affinity and lower K_i for chitin synthase *in vitro* than nikkomycin Z derivatives which contain uracil (31). Hydrophobic substitutions by methylating the hydroxy group of the phenyl ring of the peptidyl moiety led to approximately twice the inhibition by the parent compound *in vitro*. Substitutions of HPHT for the natural amino acids L-tyrosine and L-arginine reduced the binding affinity to chitin synthase (31).

Certain derivatives which are active in *in vitro* inhibition assays are inactive against intact fungi. Transport via peptide transport mechanisms is likely to be the limiting factor in their activity. Dipeptides were shown to interfere with the antifungal activity of polyoxin, acting as competitors for penetration across the cell membrane (32;33). However, a peptide-containing medium does not interfere with susceptibility of *Candida albicans* for nikkomycin Z. In this yeast, at least two distinct peptide transport systems facilitate the entry of di- and tripeptides (34). The finding that chitin synthase from *C. albicans* was susceptible to nikkomycins in a submilligram range, and that the susceptibility of intact yeast was in the high milligram range because peptide transport was the limiting factor in the uptake of these substances, led to several efforts to obtain active derivatives of these compounds. A number of polyoxin derivatives with different amino acid or amino fatty acid compositions were generated with the hope of improving uptake and biological activity (35-39). In the case of nikkomycins, Zähner *et al* used a different approach by mutagenesis of the producing strain of *Streptomyces tendae* and running a directed fermentation. In this way new derivatives were produced which involved substitutions for the nucleoside as well as the peptide moieties (20-22;31;40). Neither of those approaches led to derivatives which were sufficiently more active

against intact fungal cells than their parent compounds, although several candidates showed improved properties in transport, stability and *in vitro* inhibition of chitin synthase. The reason for the lack of improved activity might be that inhibition of chitin synthase is not sufficient to kill fungal cells (36). However, results from susceptibility tests and efficacy experiments demonstrated that this is the case for certain fungi but not for others (8).

An additional complication is that several medically important fungi possess multiple forms of chitin synthase which are of different importance to the growth of the cell (41). It is likely that they also show differential susceptibilities to the inhibitory effects of nikkomycins and polyoxins, as shown for Chs1 and Chs2 from *Saccharomyces cerevisiae* (42). All this may explain the broad range in susceptibilities.

Furthermore, genetic control of nikkomycin biosynthesis in *Streptomyces tendae* is of interest, as the ability to selectively control the expression of the more active nikkomycin forms would greatly improve the economics of the fermentation product (8).

1.5   Use of nikkomycins and polyoxins against pathogenic fungi

Shortly after the discovery of polyoxins in 1965, reports on their effects on various saprophytic fungi appeared (27;32;43). In 1977, inhibitors of chitin synthesis were proposed as therapeutic agents for fungal infections (44) and in 1983 the first reports on the effects of polyoxin D on medically important fungi were published. The discovery that polyoxin D was active *in vitro* against the parasitic phase of *Coccidioides immitis* in the microgram-per-milliliter range rendered the use of these compounds as antifungal agents plausible. It was found that immature spherules of *C. immitis* were highly susceptible to the effects of polyoxin D, which made them swell and burst at lower concentrations and die immediately at concentrations of 200 µg/mL. The drug did not show any effect on the mycelial phase of the fungus (45).

Candida albicans was also shown to be susceptible to polyoxin D in the range of 500 to 2,000 µg/mL, causing swelling and "chaining" of cells and a block of germ tube formation (46;47).

While the dimorphic fungus *Coccidioides immitis* is highly succeptible towards nikkomycin X and Z, *Candida albicans* has only moderate susceptibility toward these compounds and *Candida tropicalis* was found to be resistant against them (8).

In vitro, nikkomycins were also found to be effective agains the highly chitinous dimorphic fungus *Blastomyces dermatidis*, but less effective against yeasts and showed virtually no effect on *Aspergillus fumigatus*, a filamentous fungus (48). Unlike the dimorphic fungi mentioned above, in which chitin represents 10-20% of their cell wall in the parasitic phase (49-53), *Candida albicans* has a lower chitin content, which might be the reason for its decreased susceptibility. The issue of susceptibility seems to be rather complex, as the mycelial fungi as well as *Cryptococcus neoformans* are less susceptible in spite of their higher chitin content. An additional factor which has to be considered are the differences among different fungi in cellular uptake and intracellular transport of chitin synthase inhibitors (34;54). However, for the susceptible fungi, the inhibition of chitin as an important component of the cell wall has negative consequences. It was shown that the inhibition of septum formation in the endosporulation process of *Coccidioides immitis* interferes with the reproduction of these cells (8).

To further investigate the chitin synthase inhibitors, several studies of animal models of mycoses were performed. Becker *et al* found that polyoxin D offered no protection against candidiasis in mice, while a mixture of nikkomycins X and Z was able to delay, but not prevent deaths (55). That finding might partially be explained by the fact that in yeast, the highest concentration of chitin can be found in the bud septum (46). Nikkomycins X and Z were also evaluated in mouse models of coccidioidomycosis, histoplasmosis and blastomycosis, with much more promising results, by Hector *et al* (48). They found that *in vivo*, nikkomycin Z was more effective than nikkomycin X. In the models of pulmonary coccidioidomycosis and systemic blastomycosis, orally administered nikkomycin Z appeared to be fungicidal, while the effect of nikkomycins against histoplasmosis was only moderate. In comparison to conventional antifungal agents, like fluconazole and amphotericin B, nikkomycin Z resulted in greater killing of *Coccidioides* ssp. In the ranges tested, no adverse effects were observed. Those findings invited continuous efforts into the development of drugs against mycoses. In 2009, Nix *et al* described the results of the first administration of nikkomycin Z to twelve healthy humans (56). Their goal was to determine the safety, tolerance and pharmacokinetics, following single rising oral doses. They did not observe serious or dose-related adverse events and provided a base for pharmacokinetic simulations and continued studies on the administration of nikkomycin Z in multiple doses.

Phase I clinical trials on "Safety and PK of Nikkomycin Z in Healthy Subjects" have been completed, (http://clinicaltrials.gov/ct2/show/NCT00834184), but, unfortunately, Phase I and Phase II clinical trials on the "Pharmacokinetics and Safety of Nikkomycin Z for Coccidioides Pneumonia Treatment" at the University of Arizona were prematurely terminated due to recruitment challenges and lack of funding (http://clinicaltrials.gov/ct2/show/NCT00614666).

Nikkomycin Z also showed efficacy against pulmonary blastomycosis in murine models, which could result in biological cure (57).

Although nikkomycin Z is still under investigation and not yet approved clinically, combinations of this compound and other antifungal compounds may open additional possibilities for the treatment of mycoses. Sandovsky-Losica *et al* reported a study on the assessment of *in vitro* activity of nikkomycin Z with voriconazole or caspofungin against *Candida albicans* and showed that they had a synergistic effect. Whether combinations of antifungals which either affect the cell wall or the cell membrane would enhance the therapeutic efficacy should be investigated in animal models (58).

1.6   Fungal diseases that could potentially be cured by nikkomycin Z

As described above, nikkomycin Z shows antifungal activity against *Coccidioides immitis*, the fungus causing coccidioidomycosis, against *Blastomyces dermatitidis*, which causes blastomycosis, and the agent of candidiasis, *Candida albicans* (8). Keeping in mind the increase in life-threatening fungal infections, especially in immuno-compromised patients, the growing resistance of fungi to clinically used drugs, and the toxicity of antifungal drugs, the chitin synthase inhibitor nikkomycin Z is a very promising compound (5).

1.6.1   Coccidioidomycosis

Coccidioidomycosis, which is also called Valley Fever, is found only in the Western Hemisphere, especially in the semiarid areas of Mexico, and the southern part of the United States. It is caused by *Coccidioides immitis* and *C. posadii*, two nearly identical species which grow in dry, sandy soils. Soil disruptions release their spores into the air. Inhalation of the dust-borne reproductive spores leads to infection by the pathogenic fungus in humans and domestic and wild mammals (59). Manifestations of the disease range from a primary pulmonary infection to a progressive disease involving skin, bones, joints, the central nervous system and other organs. The most dangerous form is

meningeal infection, which occurs in about 0.15-0.75% of extrapulmonary coccidioidomycosis cases. Most patients with primary pulmonary infection recover spontaneously, but chronic and disseminated disease occurs in approximately 5% of infected individuals. Immunocompromised patients have a higher risk of severe infection (60;61).

Coccidioidomycosis is treated by two classes of antifungal therapeutics, the polyenes (amphothericin B), and the azoles (fluconazole, itraconazole, voriconazole) (62). Treatment of the progressive forms of the disease is often difficult, and relapse is common (63). As management of this chronic disease is problematic, there is an urgent need for new preventive or therapeutic options (59).

1.6.2   Blastomycosis

 The thermally dimorphic fungus *Blastomyces dermatitidis* exists in its mycelial form in soil rich in organic debris. It is found in the warm, moist, wooded areas in North America that border the Great Lakes and Mississippi and Ohio River (64-68). When the mycelia are disturbed, airborne conidia are inhaled and at body temperature they convert to thick-walled budding yeast (69;70). The common form is a pulmonary disease, but hematogenous dissemination results in extrapulmonary blastomycosis, with skin lesions, abscesses and osteomyelitis (71;72). Blastomycosis is clinically indistinguishable from tuberculosis. A long course of amphothericin B is usually curative, but itraconazole is highly effective and mainly used for treatment of the disease (73).

1.6.3   Candidiasis

Candidiasis encompasses a whole range of infections, from superficial diseases, like oral thrush and vaginitis, to systemic and potentially life-threatening diseases, which are referred to as candidemia. The ubiquitous yeast *Candida* spp. can cause fatal bloodstream infections in immunocompromised persons, despite the treatment with antifungal drugs (74). Candidiasis is treated with antimycotics like fluconazole (75). *C. albicans* was shown to develop resistance to antimycotic drugs (76), which also enhances the need for new therapies.

1.7   Biosynthesis of nikkomycins

1.7.1   Biosynthesis of secondary metabolites

Filamentous fungi, *Bacillus*, plant cells and actinomycetes, particularly *Streptomyces,* show an amazing capability to synthesize antibiotics. Multistep pathways lead from precursors, which are usually primary metabolic intermediates, to the specific moieties of secondary metabolites. The component moieties are activated in the form of adenylated, phosphorylated or CoA derivatives and linked together to form the final products. Enzymes that are specific for each antibiotic carry out the biosynthetic steps leading to the respective secondary metabolite (77). Usually, genes encoding pathways of secondary metabolism are located in clusters. Subclustering of antibiotic biosynthetic genes appears to be important for the timing of expression of each enzyme in the multistep pathway so that the intermediates appear in the proper sequence of reactions (78). In *Streptomyces* spp., gene transcription and mRNA translation are tightly coupled and each enzyme formed by coupled transcription-translation is enabled to act on the product of the previous enzyme (79).

1.7.2   Organization of the gene cluster for nikkomycin biosynthesis

Initially, proteins involved in nikkomycin biosynthesis were identified in expression studies using two-dimensional gel electrophoresis. *Streptomyces tendae* Tü901 and mutants blocked in nikkomycin biosynthesis were analyzed for gene expression during growth in production medium and ten proteins were found in the *S. tendae* Tü901 cell extract, which were absent in cell extracts of the non-producing mutants. By designing gene probes based on their amino acid sequence, nikkomycin biosynthetic genes could be isolated (80). Later, the whole nikkomycin biosynthesis gene cluster from *Streptomyces tendae* Tü901 was isolated and the entire set of structural (*nik*) genes was heterologously expressed in *S. lividans*. Transformants of *S. lividans* synthesized nikkomycins X, Z, I and J (81). Also from *S. ansochromogenes* nikkomycin biosynthetic (*san)* genes were isolated and characterized (10). The order of homologous genes from the *Streptomyces tendae* and *ansochromogenes* gene clusters appears to be similar and their gene products are 93 to 99 % identical. The length of the *nik* gene cluster is 29 kb and it consists of 23 genes which are organized in four transcription units. The 5'- boundary of the *nik* cluster is marked by the monocistronically transcribed *nikZ* gene which encodes a pathway-specific regulator. At the 3'- end of the

cluster lies probably the *nikO* gene. Within the operons (*nikABCDEFG, nikIJKLMNO,* and *nikP1P2QRSTUV),* the genes are closely spaced. Several times the stop codon of a gene overlaps with the start codon of the subsequent gene. Biosynthetic functions were assigned to the gene products by the detection of sequence similarities to proteins in databases, by the characterization of disruption mutants and by the heterologous expression of the genes and determination of enzymatic activities (82).
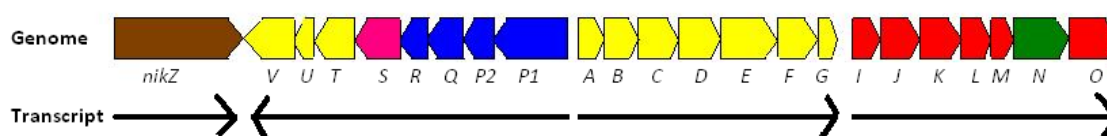
Figure 6: Organization of the nikkomycin biosynthetic gene cluster in *Streptomyces tendae* Tü901. Genes for hydroxypyridylhomothreonine biosynthesis are highlighted in yellow, genes which are thought to be involved in the biosynthesis of the aminohexuronic acid moiety are red, genes for 4-formyl-4-imidazolin-2-one biosynthesis and incorporation are blue, the *nikS* gene, which is probably involved in peptide bond formation is shown in pink, the putative membrane transport protein *nikN* in green and the regulator gene *nikZ* in brown.

1.7.3 Biosynthesis of the peptidyl moiety of nikkomycins

The peptidyl moiety of nikkomycins consists of hydroxypyridylhomothreonine (HPHT), it is also called nikkomycin D. Mutants with disruptions in the genes *nikA, nikB, nikC, nikD, nikE, nikF, nikT* and *nikV* were not able to produce neither HPHT, nor the biologically active nikkomycins X, Z, I and J. The *nikA, nikB, nikC, nikD, nikE* and *nikT* mutants accumulated the nucleoside moieties C_X and C_Z in their culture broths. The *nikF* mutant produced the nikkomycin derivatives L_X and L_Z, with pyridylhomothreonine as peptidyl moiety. From the culture broth of the *nikT* mutant, nikkomycins O_X and O_Z, which contain 2-amino-4-hydroxy-4-(3'-hydroxy-6'-pyridyl) butanoic acid as the peptidyl moiety, were isolated (see Figure 2) (83;84).

The initial step in the biosynthetic pathway of HPHT is catalyzed by the *nikC*-encoded, pyridoxal-5-phosphate-dependent enzyme L-lysine 2-aminotransferase (Scheme 1). The enzyme was shown to convert L-lysine to piperideine-2-carboxylic acid (P2C), the cyclic and dehydrated form of 2-oxo-6-aminohexanoic acid (85).
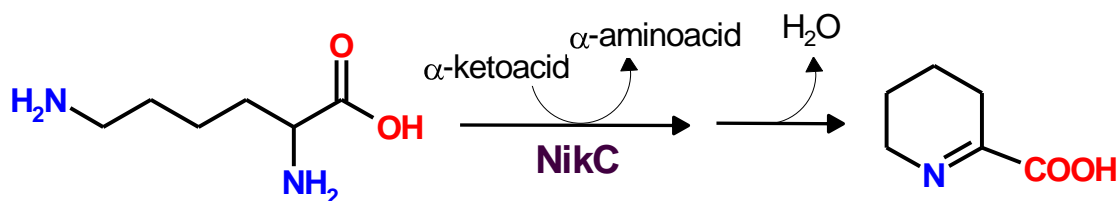
Scheme 1: NikC-catalyzed conversion of L-lysine to piperideine 2-carboxylic acid.

Piperideine-2-carboxylate can exist in two tautomeric forms, the imine form which is predominant at acid or neutral pH, and the enamine tautomer, which is the major species at alkaline pH and is thought to be the more easily oxidized form (86). The second step in the biosynthesis of the peptidyl moiety is catalyzed by the flavoenzyme NikD which contains covalently bound FAD, and catalyzes the oxidation of P2C (Scheme 2). The electron acceptor is oxygen, which is reduced to hydrogen peroxide (87). It was shown that NikD is an obligate 2-electron acceptor and catalyzes a 4-electron oxidation of P2C, via a dihydropicolinate intermediate (88).
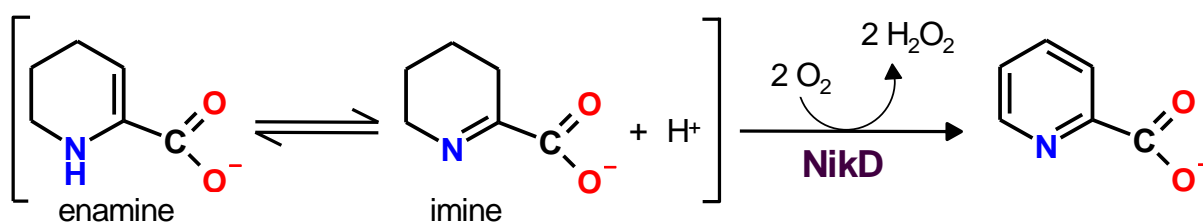
Scheme 2: The reaction catalyzed by NikD, a 4-electron oxidation of piperideine 2-carboxylate to picolinate.

In *S. tendae,* picolinic acid is activated as the CoA-thioester by NikE, before it is reduced to picolinaldehyde by NikA (Scheme 3) (89). Those reactions are well described for the analogous gene products from *S. ansochromogenes*, SanJ, which shows 96 % sequence identity to NikE and SanN, which shows 99 % sequence identity to NikA. SanJ shows sequence similarities to acyl-CoA ligases of adenylate-forming enzymes which activate carboxylic acids for subsequent biosynthetic steps. The enzyme functions in the activation of picolinate. First, the unstable intermediate picolinate-AMP is generated in the presence of ATP. When CoA-SH is present, AMP is released and the picolinate-CoA thioester is formed (90). The activated form of picolinate sets the stage for the next biosynthetic step, the reduction of picolinate-CoA to pyridine-2-aldehyde by the dehydrogenase SanN. This enzyme displays similarities to acetaldehyde dehydrogenases and was demonstrated to convert benzoate-CoA to benzaldehyde (91).

15
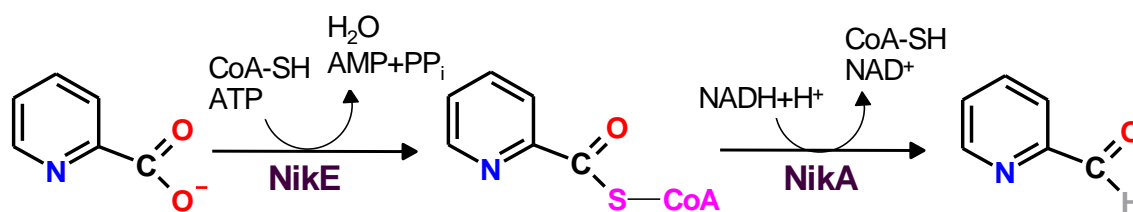
Scheme 3: Conversion of picolinate to picolinaldehyde.

SanN was shown to interact with the aldolase SanM, which is 97 % identical to NikB from *S. tendae*. The interaction is essential for the conversion of picolinaldehyde and 2-oxo-3-methylsuccinic acid to 4-pyridyl-2-oxo-4-hydroxyisovalerate (POHIV), but not for the dehydrogenase activity of SanN (92). In *S.* ansochromogenes, 2-oxo-3-methylsuccinic acid is generated by the enzymes SanU and SanV (corresponding to NikU and NikV in *S. tendae*), which assemble with coenzyme B_{12} to form a complete enzyme with glutamate mutase activity. This complex converts L-glutamate to 3-methylaspartic acid, which is probably deaminated to form 2-oxo-3-methylsuccinic acid (93). When *sanU* or *sanV* is knocked out, L-glutamate is converted to aspartic acid, finally resulting in the nikkomycins O_x and O_z, which do not contain the methyl group at C3 in HPHT (21).
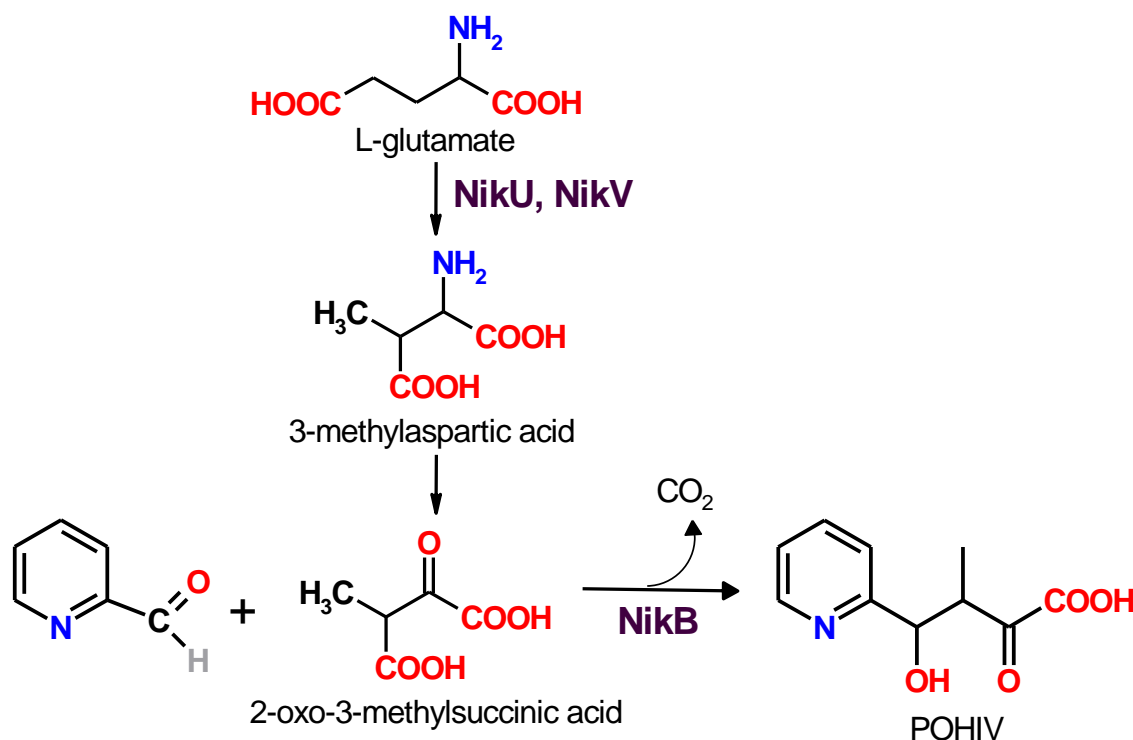
Scheme 4: Conversion of picolinaldehyde to POHIV.

POHIV is transaminated by NikT or SanT (the genes in *S. tendae* and *ansochromogenes* are 100 % identical) to form 4-(2'-pyridinyl)-homothreonine (PHT) (Scheme 5). SanT possesses an unusual domain structure, consisting of an N-terminal acyl carrier domain and a C-terminal aminotransferase domain. The two domains, which both are essential to nikkomycin biosynthesis, were shown to function independently. The aminotransferase domain transaminated POHIV in vitro, the role of the acyl carrier protein, which is posttranslationally modified with a phosphopantetheine prosthetic group, is unknown. It was suggested that it takes part in the assembly of nikkomycins (95).
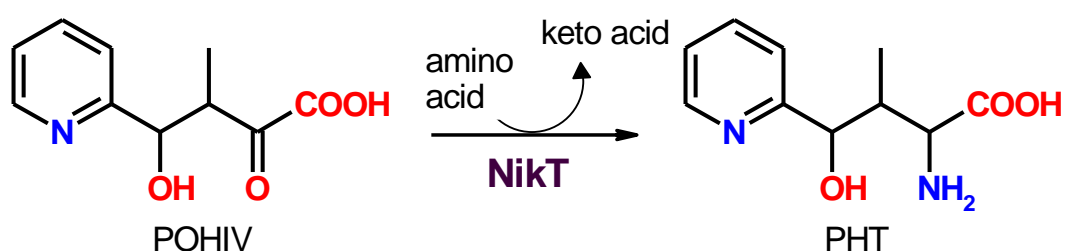
Scheme 5: Transamination of POHIV to PHT.

The hydroxylation of PHT to hydroxypyridylhomothreonine (HPHT) is catalyzed by a cytochrome P450 system, consisting of the hydroxylase NikF and the ferredoxin NikG (Scheme 6). Disruption of *nikF* led to the biosynthesis of nikkomycins L_x and L_z, analogues of nikkomycins X and Z that lack the hydroxyl group of the pyridyl residue (83). The analogous proteins of *S. ansochromogenes*, the cytochrome P450 monooxygenase SanH and the ferredoxin SanI were expressed heterologously and characterized. It was concluded that SanH is essential for the hydroxylation of the pyridyl residue and SanI works as an effective electron donor for SanH (95).
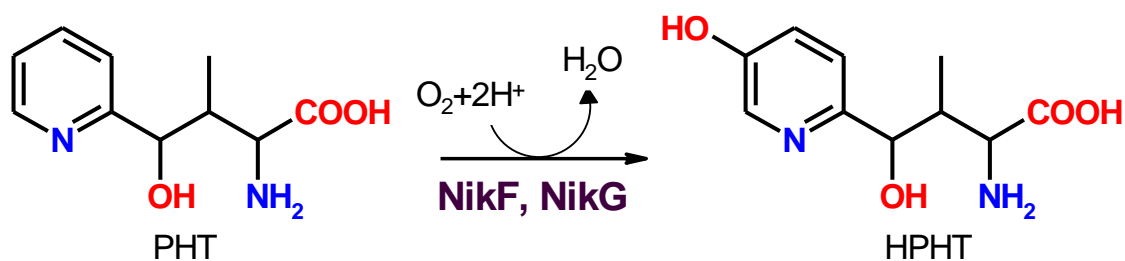
Scheme 6: Hydroxylation of PHT to HPHT.

1.7.4 Biosynthesis of the imidazolone base of nikkomycins

Nikkomycins X and I contain an aminohexuronic acid residue with an N-glycosidically linked 4-formyl-4-imidazoline-2-one (imidazolone) base. The proteins responsible for its biosynthesis are encoded by the first four genes of the *nikP1P2QRSTUV* operon (82). The initial step is covalent binding in a thioester linkage of L-histidine to the non-ribosomal peptide synthase NikP1. L-His-S-NikP1 serves as the substrate for the heme hydroxylase NikQ, and β-OH-His is hydrolytically released from NikP1 by the thioesterase NikP2 (96). NikQ is proposed to catalyze a second monooxygenation step at the C-2 of the imidazole ring, inducing fragmentation into 4-formyl-4-imidazolin-2-one and glycine (Scheme 7).
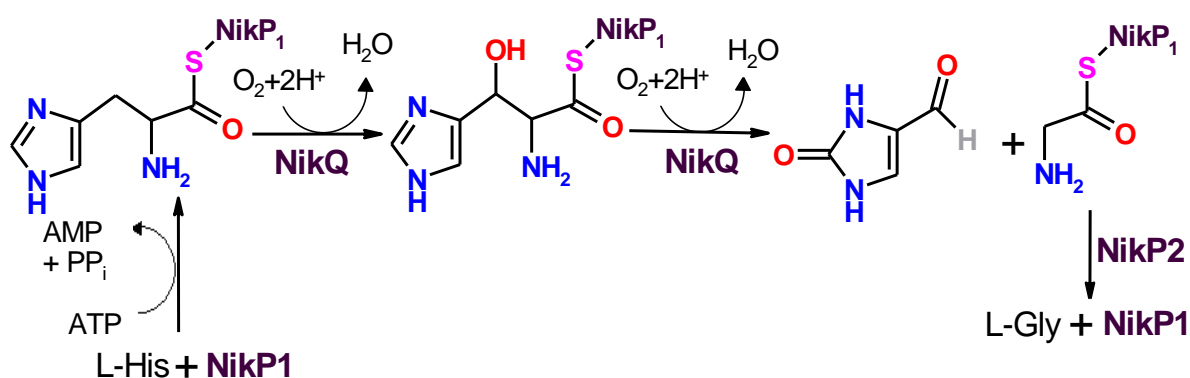
Scheme 7: Generation of the imidazolone base.

The transfer of the imidazolone base to 5'-phosphoribosyl-1-pyrophosphate to form 5'-phosphoribosyl-4-formyl-4-imidazoline-2-one (Scheme 8), is predicted to by catalyzed by NikR, which has sequence similarities to uracil-phosphoribosyl transferases of the uracil salvage pathway (82).
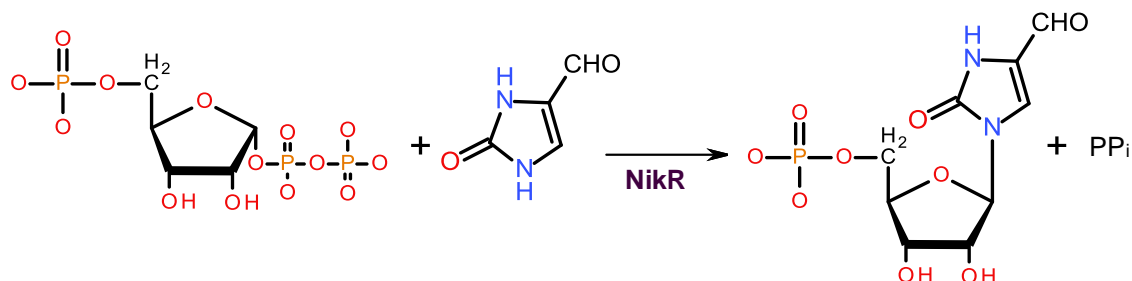
Scheme 8: Transfer of the imidazolone base to 5'-phosphoribosyl-1-pyrophosphate

1.7.5 Biosynthesis of the nucleoside moiety of nikkomycins

The biosynthetic pathway of the aminohexuronic acid moiety requires NikO, NikL, NikM, NikK, NikJ and NikI (82). The initial reaction is proposed to be catalyzed by NikO, which shows sequence similarity to UDP-*N*-acetylglucosamine enolpyruvyl transferases and 5-enolpyruvylshikimate-3-phosphate synthetases. Those enzymes catalyze the transfer of the intact enolpyruvyl moiety from phosphoenolpyruvate (PEP) to the 5'-hydroxyl group of shikimate 3-phosphate and the 3'-hydroxyl group of UDP-*N*-acetylglucosamine, respectively. A *nikO* deletion mutant did not produce the biologically active nikkomycins I, J, X and Z but accumulated the novel nucleoside ribofuranosyl-4-formyl-4-imidazolone. Therefore, NikO was proposed to catalyze the transfer of an enolpyruvyl moiety to the 5'-hydroxl group of uracil or its 4-formyl-4-imidazoline-2-one analog (97). However, recombinant NikO showed no enolpyruvyl transferase activity with uridine. Instead, UMP was found to serve as substrate for NikO, which catalyzes the generation of 3'-enolpyruvyl-UMP (3'-EPUMP) (Scheme 9), and not 5'-enolpyruvyl-uridine. Considering the introduction of the enolpyruvyl group at the 3'-position of UMP, a rearrangement of the carbon skeleton, catalysed by the enzymes which are cotranscribed with NikO, was postulated (98).
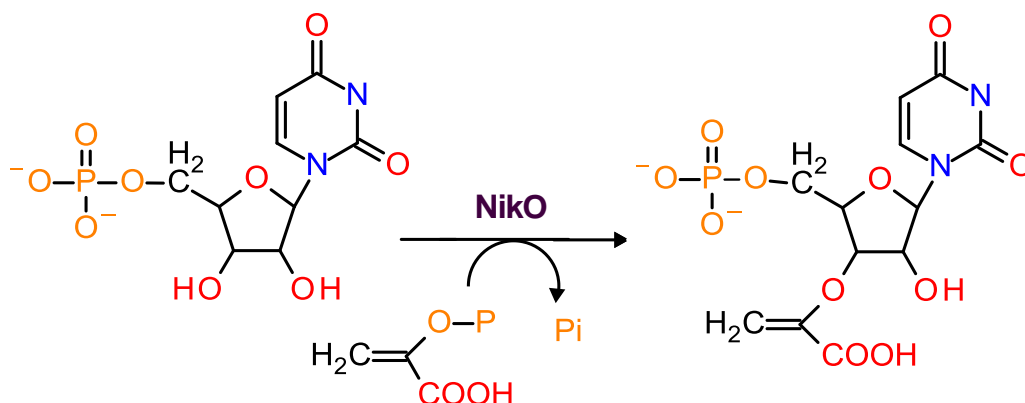
Scheme 9: Enolpyruvyl transfer reaction catalyzed by NikO

During the rearrangement reactions, the enolpyruvyl moiety is detached from its 3´- and transferred to the 5´-position of the ensuing aminohexuronic acid moiety. Interestingly, Schüz *et al* found the bicyclic nikkomycins S_x and S_z (Figure 7) in the fermentation medium of *S. tendae* Tü901/S 2566. Decreasing amounts of nikkomycins S_x and S_z in the culture broth, showed a significant correlation to increasing amounts of nikkomycins X and Z, depending on the increasing iron concentration. Apparently, the nikkomycin intermediates S_x and S_z are transformed into the nikkomycin target

structures in an iron-dependent fashion (99). However, it has to be taken into account that the bicyclic nikkomycins S_x and S_z, instead of being intermediates of aminohexuronic acid biosynthesis, could also be by-products of the biosynthetic pathway, as suggested by C. Bormann, who found these compounds in the culture broth of *nikK, nikL,* and *nikM* deletion mutants (82).
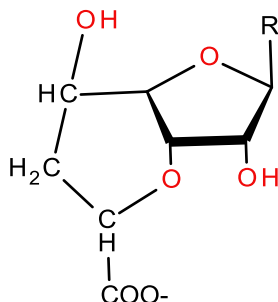
Figure 7: Nikkomycins S_x (R= 4-formyl-4-imidazoline-2-one) and S_z (R=uracil)

The enzymes NikI, NikJ, NikK, NikL, and NikM, which are co-transcribed with NikO are supposed to be involved in the reactions that transform 3´-EPUMP to aminohexuronic acid, but their functions are unclear. NikI and NikM share about 45% sequence similarity and show similarity to the iron-containing oxo-glutarate dependent prolyl-4-hydroxylase, NikL shows similarity to tyrosine phosphatases. NikJ shows similarities to S-adenosyl-methionine (SAM) and vitamin B_{12} binding proteins of bacterial origin and iron-sulfur oxidoreductases. Due to its sequence similarity to PLP-dependent aminotransferases, NikK was proposed to be responsible for the transfer of an amino group to an oxo group on C-5´of the nucleoside intermediates (82).

1.7.6 Assembly of nikkomycins

The formation of the amide bond between the peptidyl and aminohexuronic acid moieties was proposed to be catalyzed by the enzyme NikS, as *nikS* disruption mutants accumulated nikkomycins C_x, C_z, and HPHT in the culture broth (82). Lauer *et al* proposed that NikT-bound HPHT is involved in the condensation step (100), but C. Bormann suggested that peptide bond formation is catalyzed by NikS alone (82). NikS belongs to a superfamily of proteins with an unusual nucleotide-binding fold, the ATP-grasp fold (101;102). These enzymes catalyze the ATP-dependent ligation of a carboxylate-containing substrate to an amino- or thiol-containing molecule. NikS shows about 25% sequence identity over 235 amino acids to D-Ala-D-Ala ligases, which are

required for synthesis of bacterial cell walls. It is likely that the peptide bond formation reaction catalyzed by NikS is analogous to D-Ala-D-Ala formation (103).

S. ansochromogenes SanS is 97% identical to the *S. tendae* protein NikS. The function of the sans gene was investigated and SanS was expressed in *E. coli* and tested for ATPase activity by Li *et al* (104). Purified SanS did show ATPase activity, indicating activation of its substrates via phosphorylation in an ATP-dependent manner. Disruption mutants of *nikS* did not produce the bioactive nikkomycins X and Z, but accumulation of nikkomycins C_x, C_z and HPHT, as shown for *nikS* disruption mutants of *S. tendae*, was not reported by the authors.

Within the *nik* gene cluster, no gene responsible for peptide bond formation yielding the tripeptidyl nikkomycins J and I could be identified so far (82).

1.8 Transport of nikkomycins

The *nikN* gene of the *nikIJKLMNO* operon encodes a predicted membrane protein which consists of eight potential hydrophobic transmembrane regions and possesses a putative ATP/GTP binding site. It might be responsible for the export of nikkomycins through the cytoplasma membrane. In the culture broth of mutants where *nikN* is inactivated, only low levels of nikkomycins X, Z, I and J were detected (82).

1.9 Transcriptional regulation of nikkomycin biosynthesis

Streptomyces species produce a variety of secondary metabolites, in a strict coordination with cell growth and environmental conditions (105). The expression of individual antibiotic gene clusters is controlled by complex regulatory cascades that link environmental and physiological signals through pleiotropic and pathway-specific regulatory proteins (106).

Nikkomycin production occurs in a growth phase-dependent manner, as it is common for many secondary metabolites produced by *Streptomyces.* The growth curve of *Streptomyces tendae* shows biphasic exponential growth kinetics (82). Nikkomycins become detectable in the culture broth after 30 h of fermentation, at the transition from the second exponential growth phase to the stationary phase. After six to seven days of cultivation, their concentrations have increased to maximum amounts. Each of the three polycistronic *nik* operons is started to be transcribed during the second exponential growth phase, about 5 h before nikkomycins can be detected in the culture broth. The

transcripts accumulate and, during the stationary phase, they are maintained at maximal levels (83;100).

The gene product of *nikZ* was suggested to be a pathway-specific transcriptional activator. It consists of 1062 amino acids and contains two sequences resembling A- and B-type ATP binding consensus sequences in the N-terminal half (82). The N-terminal domain of NikZ shows sequence similarity to members of the SARP family (*Streptomyces* antibiotic regulatory proteins) (107). Many pathway-specific regulatory proteins belong to the SARPs, which bind to a direct repeat sequence which overlaps the -35 region of the target promoter (108). According to Bormann *et al*, NikZ positively controls the transcription of the *nikP1P2QRSTUV, nikABCDEFG,* and *nikIJKLMNO* operons. In the putative -10 regions of the promoters in front of the *nikP1, nikA* and *nikI* genes, the consensus sequence CAG/TGCT can be found. There is no similarity between the putative -35 regions, but well-conserved heptameric direct-repeat sequences of each promoter might function as binding sites for the *nikZ*-encoded regulator at the -35 regions (82).

Streptomyces tendae NikZ shows 89% amino acid sequence identity to its analogue in *S. ansochromogenes*, SanG. The transcriptional regulatory protein, which resembles other positive regulators involved in antibiotic biosynthesis, like PimR of *S. natalensis* (109) or PteR of *S. avermilitis* (110), was thoroughly characterized by the group of Huarong Tan (111;112). Disruption of the *sanG* gene abolished nikkomycin biosynthesis, which could be restored by complementation by a single copy *sanG*. Increasing the copy number of *sanG* resulted in an increase in nikkomycin production, which reinforced the evidence that *sanG* is an important activator gene for nikkomycin biosynthesis. Furthermore, *sanG* exhibits pleiotropic effects on colonial morphology and development, as its disruption reduced sporulation and led to brown pigment accumulation. At least three promoters (P1, P2 and P3) are involved in transcription of *sanG,* one of them (P1) being strongly upregulated when production of nikkomycin starts. The two operons starting from *sanN* and *sanO* are dependent on the expression of *sanG*, whereas the *sanFABCDEX* operon (resembling the *nikIJKLMNO* operon in *S. tendae*) is not regulated by *sanG* (112). SanG was expressed in *Escherichia coli* and shown to bind to the DNA fragment containing the *sanN-sanO* promoter region. The protein showed significant ATPase/GTPase activity and addition of ATP/GTP enhanced the affinity of SanG for target DNA. Apparently, ATPase/GTPase activity of SanG

modulated the transcriptional activation of SanG target genes during biosynthesis of nikkomycins (111).

SanG shows 32% identity to the pimaricin biosynthetic regulator PimR in *S. natalensis* and 33% identity to PteR from *S. avermilitis*, which is involved in filipin biosynthesis (109;110;112). Although pimaricin and filipin belong to the polyene antibiotics and their structures and biosynthetic pathways are different from those of nikkomycins which are nucleoside antibiotics, all of them have antifungal properties. The mechanisms of their regulation are supposed to be similar. Probably the regulators were acquired in the process of evolution against fungi (112).

The *sanG* promoter region may be the target for DNA binding by another regulatory protein, SabR. The γ-butyrolactone receptor homologous gene *sabR* was identified in *S. ansochromogenes* and disruption delayed nikkomycin production in media containing glucose or glycerol, but led to earlier sporulation. It had no effect in media containing mannitol as carbon source, suggesting that it is a pleiotropic regulatory gene that controls the onset of nikkomycin production and sporulation and is related to the carbon source (113). From nikkomycin producing *S. tendae* ATCC31160, the *tarA* (<u>t</u>endae <u>a</u>utoregulator <u>r</u>eceptor) gene was isolated. Disruption of the *tarA* gene also led to a delay in nikkomycin production. TarA shows strong similarity to γ-butyrolactone-binding proteins involved in the regulation of antibiotic biosynthesis in *Streptomyces*, where γ-butyrolactone autoregulators and the corresponding receptors play a crucial role in regulating the production of antibiotics and morphological differentiation (114).

1.10 Improvement of nikkomycin production

Nikkomycins X and Z are the main components produced by *Streptomyces tendae* and *S. ansochromogenes*. Generation of a high-producing strain has become very important to scale up nikkomycin production for clinical trials (115). Traditionally, the improvement of antibiotic-producing strains is achieved by random mutagenesis and selection. Another approach would be the overexpression of positive transcriptional regulators of a biosynthetic gene cluster or specific enzymes involving metabolic bottlenecks (116). An attempt to improve nikkomycin production by introducing an extra copy of *sanU* and *sanV* into *S. ansochromogenes* increased nikkomycin yield about 1.8-fold (93). The gene products of *sanU* and *sanV* are involved in the biosynthesis of the HPHT moiety of nikkomycins. In the biosynthetic pathways of secondary metabolites, there often exists more than one single rate-limiting step (117).

Overexpression of the entire biosynthetic gene cluster might therefore further improve the yields of the desired antibiotic. To improve nikkomycin production, Liao *et al* introduced an additional copy of the nikkomycin biosynthetic gene cluster into *S. ansochromogenes*, which led to enhanced production of nikkomycins X and Z (4-fold and 1.8-fold, respectively, compared to the wild type strain). The large (35 bp) gene cluster was first reassembled into an integrative plasmid by Red/ET technology combined with classic cloning methods and the resulting plasmid was introduced into *S. ansochromogenes* by conjugal transfer (118).

Nikkomycin Z is a potential fungicide with clinical significance. As the presence of its isomer, nikkomycin X, during fermentation interferes with its purification and increases the production cost, a nikkomycin producing strain of *S. ansochromogenes* was genetically modified to selectively produce nikkomycin Z. A complete block of nikkomycin X biosynthesis was achieved by deletion of *sanP*, whose gene product is involved in the imidazolone biosynthetic pathway of nikkomycin X (115). Earlier studies in *S. tendae* showed that disruption of *nikP2* almost abolished nikkomycin X production (100). Selective production of nikkomycin Z in high amounts was achieved by combining genetic manipulation with feeding of precursors to the fermentation medium. The *sanP* deletion mutant produced 2.6-fold higher yields of nikkomycin Z than the parent strain when uracil at the concentration of 2 g/L was present while suppressing nikkomycin X production by 85%. Possibly, UMP derived from uracil competed with imidazolone for incorporation into the molecule (115).

1.11 Aim of this work

The aim of this work has been to shed light onto the biosynthetic steps that lead to the generation of the aminohexuronic acid moiety of nikkomycins by heterologous expression and biochemical characterization of the involved enzymes and by the analysis of nikkomycin intermediates produced by *Streptomyces* mutants featuring disruptions of the respective genes. Investigations regarding the structural biology of nikkomycin biosynthetic enzymes were carried out by our cooperation partners at the Institute of Molecular Biosciences (University of Graz), and are described in the Doctoral Thesis of Gustav Oberdorfer, "Structural investigations on enzymes of nikkomycin biosynthesis" (119).

CHAPTER 2

2   NikO: An *enol*pyruvyltransferase catalyzing the first step in aminohexuronic acid biosynthesis

2.1 Introduction

2.1.1 *Enol*pyruvyltransferases

The NikO enzyme from *Streptomyces tendae* exhibits sequence similarity to *enol*pyruvyltransferases, which, after release of the phosphate group of phospho*enol*pyruvate (PEP) by C-O bond cleavage, transfer the intact *enol*pyruvyl moiety to their respective substrates. NikO is related to UDP-*N*-acetylglucosamine *enol*pyruvyltransferase (MurA) and, to a lesser extent, to 5-*enol*pyruvylshikimate-3-phosphate synthase (EPSPS) (120).

The enzyme UDP-*N*-acetylglucosamine *enol*pyruvyltransferase (MurA) catalyses transfer of an *enol*pyruvyl group from PEP to the 3´-OH group of UDP-*N*-acetylglucosamine, to form UDP-*N*-acetyl*enol*pyruvylglucosamine. This reaction constitutes the first committed step in the biosynthesis of bacterial cell wall peptidoglycan (121). Since MurA is an essential enzyme in all bacteria, its importance as an antibacterial target has been the subject of many investigations (122). The naturally occurring antibiotic fosfomycin, which is produced by some species of *Streptomyces* and *Pseudomonas* (123), alkylates the thiol group of the catalytically important cysteine residue C115 and thereby irreversibly inhibits MurA activity (124).

The enzyme 5-*enol*pyruvylshikimate-3-phosphate synthase (EPSPS) catalyzes the sixth step in the shikimate pathway, which is the major source of aromatic compounds in bacteria, fungi, algae, higher plants and apicomplexan parasites (125-127). The reaction consists of the reversible transfer of the *enol*pyruvyl moiety from PEP to shikimate 3-phosphate, to yield 5-*enol*pyruvylshikimate-3-phosphate and inorganic phosphate (128). EPSPS was identified as a target for inhibitors, like the herbicide glyphosate (*N*-phosphonomethylglycine) (128;129). As the shikimate pathway is essential for survival of the apicomplexan parasites *Plasmodium falciparum*, *Toxoplasma gondii* and *Cryptosporidium parvum*, while being absent in mammals, EPSPS is a promising therapeutic target for developing new antiparasitic drugs.

MurA and EPSPS share a common enzymatic reaction mechanism and a unique three-dimensional topology. In absence of substrate, MurA exhibits an "open" conformation. Upon substrate binding, the conformation changes to the more tightly packed "closed" form, following an induced fit mechanism. Thereby, the substrates are properly

positioned for catalysis (130-132). In the "closed" form, MurA shows a significant increase in proteolytic stability (133).

The NikO enzyme from *S. tendae* was shown to catalyse the transfer of an *enol*pyruvyl group from PEP to the 3´-OH group of UMP, generating 3´-*enol*pyruvyl-UMP (3´-EPUMP). This reaction constitutes the first step towards the biosynthesis of the aminohexuronic acid moiety of nikkomycins (98).
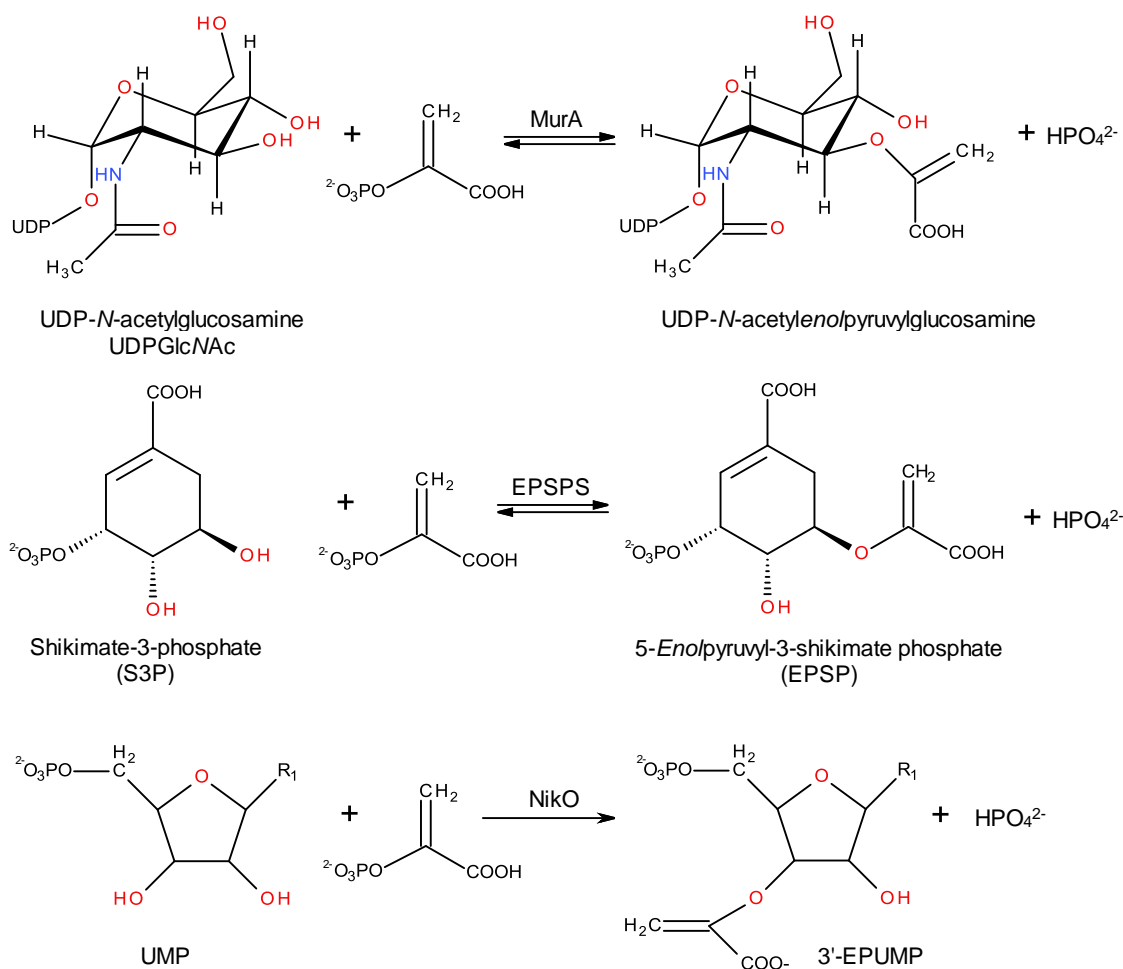
Scheme 10: Reactions catalysed by the *enol*pyruvyl transferases UDP-*N*-acetylglucosamine *enol*pyruvyltransferase (MurA), 5-*enol*pyruvylshikimate-3-phosphate synthase (EPSPS), and *S. tendae* NikO (R_1= uracil or 4-formyl-4-imidazoline-2-one).

NikO and MurA show striking similarities in their active sites. The cysteine residue, which has been shown to be susceptible to alkylation by fosfomycin in the "closed" conformation of MurA (124;134), is conserved in NikO. This cysteine residue is found in an extended loop region in MurA. Upon formation of the "closed" conformation, it

moves towards the active site cleft. The rate of inactivation of MurA by fosfomycin is considerably increased in the presence of its substrate, UDP-*N*-acetylglucosamine, which is also due to the conformational change the enzyme undergoes upon substrate binding (134;135). NikO, however, was discovered to react with fosfomycin in the absence of its substrate (120). This can either be explained by its permanent existence in a closed form, where C130, which is equivalent to C115 in MurA, is permanently activated, or by the presence of UMP bound to NikO in the enzyme preparation.

2.1.2 The role of *St*NikO in nikkomycin biosynthesis

Originally, it was hypothesized that the nucleoside moiety of nikkomycins is generated by the addition of an *enol*pyruvyl group from PEP to the 5´-position of ribose of either uridine or its 4-formyl-4-imidazoline-2-one analog. This step is then followed by speculative modifications to yield aminohexuronic acid (136).

With 3´-EPUMP as the reaction product of NikO, significant modifications of the previous models of nikkomycin biosynthesis are required. It is a challenging task to find the explanation how nikkomycin structures, which unvariably exhibit a branching point at the 5´- rather than the 3´-position, are generated from 3´-EPUMP.

2.2 Materials and Methods

2.2.1 Reagents

All chemicals were of highest grade commercially available and purchased from Sigma−Aldrich (St. Louis, MO, USA), Fluka (Buchs, Switzerland), or Merck (Darmstadt, Germany). Nickel−nitrilotriacetic acid agarose (Ni−NTA) was from Qiagen (Hilden, Germany), Sephadex resin from Pharmacia Biotech AB (Uppsala, Sweden).

2.2.2 Expression in *Escherichia coli*

Chemically competent *E. coli* BL21(DE3) cells were transformed with the expression plasmid pET21d(*nikO*), which was generated by Christian Ginj. The gene is designed in a way that allows expression of NikO with a C-terminal hexahistidine tag. Expression of NikO was achieved by growing a 10 mL preculture in Luria-Bertani (LB) medium containing 100 µg/mL ampicillin over night at 37 °C. The preculture was used to inoculate 750 mL LB medium containing 100 µg/mL ampicillin for plasmid selection. The culture was incubated at 37 °C until an OD600 of 0.5 and IPTG was added to a

final concentration of 0.1 mM. The culture was incubated for 3 h at 37 °C and cells were harvested by centrifugation. The pellet was washed with 0.9 % NaCl solution and stored at -20 °C.

2.2.3 Generation of a NikO D82A/E83A/K325A variant by site-specific mutagenesis

Site directed mutagenesis was carried out in two steps according to the QuikChange® XL Site-Directed Mutagenesis Kit from Stratagene (Santa Clara, CA, USA). The pET21d(*nikO*) plasmid served as template in the first step to introduce the mutations that led to substitution of the amino acids at positions 82 and 83. The resulting plasmid served as a template to additionally introduce the mutation that led to the K325A variant. The following primers and their complementary counterparts were used: 5'- G CAC TAC GAG GCG GCG GCG ACG TTC ACC GTC G -3' for the D82A/E83A mutations and 5'- CAC CCG CTG ACG GCG CCG TTG CGG CCC GTG -3' for the K325A mutation. The underlined nucleotides denote the mutated codons. After each step of mutagenesis, the sequence of the transformation construct was verified by DNA-sequence analysis. Transformation and expression was carried out as described for wild type NikO.

2.2.4 Cell disruption and purification

The pellet was thawed and resuspended in lysis buffer (100 mM Tris-HCl buffer at pH 8.0, containing 300 mM NaCl and 10 mM imidazole), using 2 mL buffer per gram of wet cells. Cells were disrupted by 30 min incubation with lysozyme and 0.5 s sonication pulses for 10 min while cooling on ice. The cell debris was removed by centrifugation at 18 000 g for 30 min at 4 °C.

The hexahistidine-tagged NikO was purified by Ni-NTA affinity chromatography, loading the supernatant onto a Ni-NTA column (Qiagen), previously equilibrated with lysis buffer. After loading of the filtered lysate, the column was washed with 10 column volumes of wash buffer (100 mM Tris-HCl, 300 mM NaCl, 20 mM imidazole, pH 8.0) and bound protein was recovered with elution buffer (100 mM Tris-HCl, 300 mM NaCl, 150 mM imidazole, pH 8.0). The purity of the eluted 3 mL fractions was determined using SDS-polyacrylamide gel electrophoresis. Fractions containing NikO were pooled and concentrated using Amicon® Ultra Centrifugal Filter Units (Millipore, Billerica, MA, USA). The buffer was exchanged to 100 mM Tris buffer (pH 7.5) using a PD-10 column (GE Healthcare, Uppsala, Sweden) and the solution of NikO protein was stored

at -20 °C. For crystallization trials, the protein was further purified by gel filtration chromatography, using a Hi Load™ 16/70 Superdex 75 prep grade column (Pharmacia Biotech AB, Uppsala, Sweden) which was mounted on a fast protein liquid chromatography (FPLC) system (ÄKTA Explorer, Pharmacia Biotech AB, Uppsala, Sweden). The column was equilibrated with 20 mM Tris-HCl buffer at pH 7.5.

2.2.5   Generation and purification of 3'-*enol*pyruvyl-UMP (3'-EPUMP)

Enzymatic reactions were set up by incubating 1 mM PEP, 1 mM UMP and 10 μM NikO in 100 mM Tris-HCl at pH 7.5 and 30 °C for one hour. 3'-EPUMP was further purified by RP-HPLC, using an Atlantis dC18 column (Waters, Dublin, Ireland), mounted on an UltiMate 3000 HPLC system (Dionex, Germering, Germany). The elution was carried out by applying a linear gradient of 0.05% trifluoroacetic acid to acetonitrile in 25 min, using a flow rate of 1 mL/min. The purified product was lyophilized.

2.3   Results and Discussion

NikO and the surface engineered variant NikO D82A/E83A/K325A were mainly expressed and purified to perform crystallization trials and to elucidate the structure of the protein alone and in the presence of 3'-EPUMP and its inhibitor fosfomycin. The results of crystallization are described and discussed by Gustav Oberdorfer in his doctoral thesis (119).

As the NikO reaction constitutes the first step towards the biosynthesis of the aminohexuronic acid moiety of nikkomycins, the product of the reaction, 3'-EPUMP is supposed to serve as a substrate for the next enzyme in the biosynthetic pathway. Enough 3'-EPUMP could be produced to test each of the enzymes cotranscribed with NikO for its ability to convert 3'-EPUMP to the next intermediate of aminohexuronic acidbiosynthesis.

CHAPTER 3

3 Expression and characterization of NikK

Information and results regarding the NikK enzyme is summarized in the following manuscript, which was submitted to FEBS Journal in July 2011. My contribution to that work consisted in all the steps involving the cloning, expression, purification and biochemical characterization of the enzyme.

Characterization of the PLP-dependent aminotransferase NikK from *Streptomyces tendae* and its putative role in nikkomycin biosynthesis

Alexandra Binter[1], Gustav Oberdorfer[2], Sebastian Hofzumahaus[1], Stefanie Nerstheimer[1], Georg Altenbacher[1], Karl Gruber[2], and Peter Macheroux[1*]

From [1]Graz University of Technology, Institute of Biochemistry, Graz, Austria, and [2]University of Graz, Institute of Molecular Biosciences, Graz, Austria

Address correspondence to:

Prof. Dr. Peter Macheroux, Institute of Biochemistry, Graz University of Technology, Petersgasse 12, A-8010 Graz, Austria; Email: peter.macheroux@tugraz.at, Tel.: +43-316-873 6450, FAX: +43-316-873 6952

or

Prof. Dr. Karl Gruber, Institute of Molecular Biosciences, University of Graz, Humboldtstr. 50/3, A-8010 Graz, Austria; Email: karl.gruber@uni-graz.at, Tel.: +43-316-380 5483, FAX: +43-316-380 9897

Running title: NikK, an aminotransferase in nikkomycin biosynthesis

Abbreviations

AspAT, aspartate:2-oxoglutarate aminotransferase; DNPH, 2,4-dinitrophenyl hydrazine; 3'-EPUMP, 3'-enolpyruvyl uridine monophosphate; HEPES, 4-(2-hydroxyethyl)-1-piperazineethanesulfonic acid; HisC, histidinol phosphate aminotransferase; HPHT, hydroxypyridylhomothreonine; MME, monomethyl ether; Mops, 3-(N-morpholino)propanesulfonic acid; PDB, protein databank; PEG, polyethylene glycol; PEP, phosphoenolpyruvate; PLP, pyridoxal 5'-phosphate; PMP, pyridoxamine 5'-phosphate; Tris, tris(hydroxymethyl)aminomethane ; UMP, uridine monophosphate

Abstract

As inhibitors of chitin synthase, nikkomycins have attracted interest as potential antibiotics. The biosynthetic pathway to these peptide nucleosides in *Streptomyces tendae* is only partially known. In order to elucidate the last step of the biosynthesis of the aminohexuronic building block, we have heterologously expressed a predicted aminotransferase encoded by the gene *nikK* from *S. tendae* in *Escherichia coli*. The purified protein, which is essential for nikkomycin biosynthesis, has a pyridoxal-5-phosphate cofactor bound as a Schiff base to lysine 221. The enzyme possesses aminotransferase activity and uses several standard amino acids as amino group donors with a preference for glutamate (Glu > Phe > Trp > Ala > His > Met > Leu). Therefore, we propose that NikK catalyzes the introduction of the amino group into the ketohexuronic acid precursor of nikkomycins. At neutral pH, the UV-Vis absorbance spectrum of NikK has two absorbance maxima at 357 and 425 nm indicative of the presence of the deprotonated and protonated aldimine with an estimated pK_a of 8.3. The rate of donor substrate deamination is faster at higher pH, indicating that an alkaline environment favors the deamination reaction.

A variety of structurally related peptide nucleosides termed nikkomycins have been isolated from the culture filtrates of *Streptomyces tendae* and *ansochromogenes* (1;2). Nikkomycins show structural similarity to the chitin synthase substrate UDP-N-acetylglucosamine and hence inhibit chitin biosynthesis in fungi and insects (3). Owing to this inhibition nikkomycins have potential as potent fungicidal, insecticidal, and acaricidal compounds. As they are non-toxic to mammals and easily degradable in nature, they are recognized as ideal fungicides for human therapy and insecticides for agriculture (4;5).

In 1970, the first producing strain for nikkomycins, *S. tendae* Tü901, was isolated from a soil sample near Nikko, Japan, as part of a program to discover novel fungicides and insecticides for agricultural use (5;6). Nikkomycins are composed of a peptidyl and a nucleoside moiety, which are synthesized separately and then linked by a peptide bond (7). The peptidyl moiety consists of hydroxypyridylhomothreonine (HPHT, nikkomycin D) which is derived from L-lysine and 2-oxo-butyrate (8;9). 5-aminohexuronic acid, which is bound N-glycosidically either to uracil or to 4-formyl-4-imidazoline-2-one, forms the nucleoside moiety of nikkomycins Z and X, respectively (2). Nikkomycin X and Z are the main components of nikkomycins in S. tendae and ansochromogenes, and also the most active compounds. The corresponding nucleoside moieties are designated as nikkomycin C_X and C_Z (10).

The nikkomycin biosynthetic gene cluster in *S. tendae* consists of 22 structural genes, organized in three polycistronic operons and a monocistronically transcribed regulatory gene. Although functions have been assigned to many of those genes by sequence comparisons and gene knock-out experiments (11), the biosynthesis of nikkomycins is so far only partially understood. The biosynthesis of the peptidyl moiety commences with the deamination of L-lysine to the corresponding α-keto acid, catalysed by the aminotransferase NikC (12). After spontaneous cyclization and dehydration of the α-keto acid, the resulting piperideine-2-carboxylate is oxidized by the FAD containing enzyme NikD to form picolinic acid (13). Picolinic acid is activated and loaded to coenzyme A by the ATP-dependent picolinate-CoA ligase NikE, and the resulting CoA-thioester is reduced to picolinaldehyde by the dehydrogenase NikA (9;14;15). An aldol condensation between picolinaldehyde and 2-oxobutyrate is catalysed by the aldolase NikB, generating 4-(2'-pyridinyl)-2-oxo-4-hydroxyisovalerate (POHIV) which is aminated by NikT to 4-(2'-pyridinyl)-homothreonine (PHT). Hydroxylation of PHT by

NikG and NikF at the pyridinyl moiety then yields the final peptide residue for nikkomycin biosynthesis (8;16;17).

Nikkomycins of the X series comprise a 4-formyl-4-imidazolin-2-one base, which originates from L-histidine. After L-histidine is activated and transferred to the carrier protein NikP1, it is hydroxylated by NikQ. NikP2 is necessary for the hydrolytic release of β-OH-His from NikP1 (2). Further transformations lead to the imidazolone base which is possibly transferred to 5'-phosphoribosyl-1-pyrophosphate by NikR, an enzyme with significant sequence similarity to uracil phosphoribosyl transferases (11).

The enolpyruvyl transferase NikO has been demonstrated to catalyse the formation of 3'-enolpyruvyl uridine monophosphate (3'-EPUMP) out of uridine monophosphate and phosphoenolpyruvate (18). This is totally different from the previously proposed pathway for the biosynthesis of the nucleoside moiety, where the enolpyruvyl moiety is attached to the 5'-position of uridine (19). It can be expected that NikO also catalyses the analogous reaction with 5'-phosphoribofuranosyl-4-formyl-4-imidazolin-2-one instead of UMP, because nikO inactivated mutants produced neither the nikkomycins I, J, X and Z nor the nucleoside moieties C_X and C_Z, but accumulated the novel nucleoside ribofuranosyl-4-formyl-4-imidazolone in the culture filtrate (19). Considering the introduction of the enolpyruvyl group at the 3'-position of UMP, a rearrangement of the carbon skeleton, catalysed by the enzymes which are cotranscribed with NikO, was postulated (18). Structural genes for the biosynthesis of the aminohexuronic acid moiety are encoded on the nikIJKLMNO operon, and nikL, nikK and nikM disruption mutants accumulated bicyclic nikkomycins S_X and S_Z in the fermentation medium (11). The characterization of the encoded enzymes will shed light on the reactions that lead to aminohexuronic acid. Here, we report the heterologous expression and biochemical characterization of NikK. Our studies show that the enzyme is a pyridoxal-5'-phosphate dependent aminotransferase with L-glutamate as the preferred amino group donor. We propose that NikK catalyses the introduction of the amino group into the nucleoside moiety of nikkomycin antibiotics as shown in Scheme 1.

Materials and Methods

Reagents

All chemicals were of highest grade commercially available and purchased from Sigma−Aldrich (St. Louis, MO, USA), Fluka (Buchs, Switzerland), or Merck (Darmstadt, Germany). Nickel−nitrilotriacetic acid agarose (Ni−NTA) was from Qiagen (Hilden, Germany), Sephadex resin from Pharmacia Biotech AB (Uppsala, Sweden). The chaperone plasmid set was from Takara (Shiga, Japan).

Determination of the nikK gene sequence

Genomic DNA was isolated from *Streptomyces tendae* Tü901/8c, using the illustra™ bacteria genomicPrep Mini Spin Kit from GE Healthcare (Buckinghamshire, UK). The *nikK* gene region was amplified by PCR and several clones of the PCR product were analyzed by DNA-sequencing (Eurofins DNA; Ebersberg, Germany).

Cloning and expression in Escherichia coli

The synthetic gene in *E. coli* codon usage, encoding for the *S. tendae* NikK, was ordered from DNA 2.0. It contained an *NdeI* restriction site at the 5'-end and a *XhoI* restriction site at the 3'-end, and was cloned into the *NdeI/XhoI* restriction sites of the pET21a vector (Novagen), generating the expression plasmid pET21a(*nik*K). The gene was designed without a stop codon, which allows expression of the protein with a C-terminal hexahistidine tag. The *nikK* sequence on the expression plasmid was verified by DNA-sequencing (Eurofins DNA).

Chemically competent *E. coli* BL21(DE3) cells were transformed with the chaperone plasmid pG-KJE8 (Takara Bio Inc.), these transformants were made competent and transformed with pET21a(*nik*K).

Expression of NikK with the help of co-expressed chaperones (dnaK, dnaJ, grpE, groES, groEL) was achieved by growing a 10 mL preculture in Luria-Bertani (LB) medium containing 50 µg/mL ampicillin and 20 µg/mL chloramphenicol over night at 37 °C. The preculture was used to inoculate 750 mL LB medium containing 50 µg/mL ampicillin and 20 µg/mL chloramphenicol for plasmid selection, 1 mM pyridoxine for cofactor integration and 0.5 mg/mL L-arabinose and 1 ng/mL tetracycline for chaperone induction. The culture was incubated at 37 °C until an OD600 of 0.5 and IPTG was added to a final concentration of 0.1 mM. The culture was

incubated over night at 20 °C and cells were harvested by centrifugation. The pellet was washed with 0.9 % NaCl solution and stored at -20 °C.

Generation of NikK K221M and E265A/E266A/Q267A variants by site-specific mutagenesis

Site directed mutagenesis was carried out according to the QuikChange® XL Site-Directed Mutagenesis Kit from Stratagene (Santa Clara, CA, USA). The pET21a(nikK) plasmid served as template. The following primers and their complementary counterparts were used: 5'-C CAC GTA GTT CGT GTG AAT ACC TTC TCT <u>ATG</u> AGC TAC GGC CTG TCT GG -3' for the NikK K221M variant and 5'- GT CGC TCC CTG <u>GCG</u> <u>GCG</u> <u>GCG</u> GCT GTT TTC ACT GCG ATT TG -3' for the NikK E265A/E266A/Q267A variant. The underlined nucleotides denote the mutated codons. After mutagenesis, the sequence of the transformation construct was verified by DNA-sequence analysis. Transformation and expression was carried out as described for wild type NikK.

Cell disruption and purification

The pellet was thawed and resuspended in lysis buffer (50 mM phosphate buffer at pH 8.0, containing 300 mM NaCl and 10 mM imidazole), using 2 mL buffer per gram of wet cells. After adding a few milligrams of pyridoxal 5'-phosphate, cells were disrupted by 30 min incubation with lysozyme and 0.5 s sonication pulses for 10 min while cooling on ice. The cell debris was removed by centrifugation at 18 000 g for 30 min at 4 °C.

The hexahistidine-tagged NikK was purified by Ni-NTA affinity chromatography, loading the supernatant onto a Ni-NTA column (Qiagen), previously equilibrated with lysis buffer. After loading of the filtered lysate, the column was washed with 10 column volumes of wash buffer (50 mM sodium phosphate, 300 mM NaCl, 20 mM imidazole, pH 8.0) and bound protein was recovered with elution buffer (50 mM sodium phosphate, 300 mM NaCl, 150 mM imidazole, pH 8.0). The purity of the eluted 3 mL fractions was determined using SDS-polyacrylamide gel electrophoresis. Fractions containing NikK were pooled and concentrated using Centripreps (Millipore). The buffer was exchanged to 50 mM potassium phosphate containing 150 mM NaCl (pH 7.5) using a PD-10 column (GE Healthcare) and the deeply yellow solution of NikK protein was stored at 4 °C.

Native molecular mass determination

The molecular mass of the purified protein was determined by gel filtration chromatography in order to assess the oligomerization state of native NikK. The analytical column, a Superdex 200 10/300 GL (Pharmacia Biotech AB) was mounted on a fast protein liquid chromatography (FPLC) system (ÄKTA Explorer, Pharmacia Biotech AB). The column was equilibrated with 100 mM Tris-HCl buffer containing 150 mM NaCl at pH 7.5. A 100 µL sample containing 200 µg of NikK was applied to the column, and the elution volume was determined by monitoring the absorbance at 280 and 430 nm. The column was calibrated using a high-molecular-mass gel-filtration calibration kit (Amersham Biosciences; α-chymotrypsinogen A, 25 kDa; ovalbumin, 43 kDa; bovine serum albumin, 67 kDa; aldolase, 158 kDa; catalase, 232 kDa; and ferritin, 440 kDa).

Spectrophotometric measurements and determination of protein concentration

UV-vis absorbance spectra were recorded with a Specord 205 spectrophotometer (Analytik Jena, Germany), and fluorescence emission spectra with a Hitachi U-3210 fluorescence spectrophotometer (Tokyo, Japan). The protein solution contained 50 mM potassium phosphate buffer at pH 7.5. To measure protein solutions at various pH values, either 200 mM Tris (pH 8-10), or Mops (pH 6-7.9) buffers were used. Enzyme concentrations were measured using the Pierce BCA^{TM} Protein Assay Kit from Thermo Scientific. Spectra of the NikK wild type, NikK K221M and free PLP were taken in 100 mM potassium phosphate buffer, at pH 8.0.

Aminotransferase activity assay

The transfer of amino groups from L-alanine to α-ketoglutarate was assayed according to the procedure established by Reitman and Frankel (20), also described by Vedavathi et al. (21). In our activity test, 2,4-dinitrophenyl hydrazine (DNPH) was added after a reaction time of 30 min.

Amino donor specificity and rapid reaction kinetics

The decrease of the absorbance bands at 425 nm and 357 nm, and the increase at 330 nm were followed spectrophotometrically, in order to assess the transfer reaction of the amino group from the donor amino acid to the PLP-cofactor (22). All experiments were carried out at 25 ºC. The enzyme solution containing 100 μM NikK and 200 mM Tris-HCl was mixed with an equal volume of amino acid solution of varying concentrations in the same buffer and the absorbance decrease was measured immediately after mixing. The experiment was carried out at various pH, using stopped flow equipment (SF-61DX2, Hi-Tech Scientific) and measuring time-dependent changes of the absorbance spectrum (300 to 700 nm) with a diode array detector or at single wavelengths (330 nm, 357 nm, 425 nm) with a photomultiplier.

Crystallization

After affinity and gel-filtration purification, native hexahistidine-tagged NikK and the K221M variant of NikK were extensively dialyzed over night against 10 mM Tris-HCl at pH 7.5. The purified triple variant, NikK E265A/E266A/Q267A was dialyzed against 10 mM HEPES buffer pH 7.5. The dialyzed samples were concentrated using Centripreps (Millipore) to a variety of final concentrations ranging from 4.4 mg/ml to 12 mg/ml for native NikK, to ~5 mg/ml for the active site lysine variant K221M and to 5, 10, 20 and 40 mg/ml for the triple variant. Several commercially available crystallization screens (Hampton Research Index Screen, Hampton Research Crystal Screen I+II, Hampton Research PEG/Ion Screen, Hampton Research Silver Bullet Screen, Hampton Research Additive Screen, Hampton Research Detergent Screen, Quiagen Classic II Suite, Quiagen PEG-Suite, Molecular Dimensions Morpheus Screen) were set up by using either microbatch or sitting-drop vapor diffusion methods, employing an Oryx 7 crystallization robot. For all concentrations the crystallization setups were done by mixing equal amounts of protein and precipitant solution with final drop volumes of 1, 2, 3 or 4 μl. Crystallization setups were incubated at 293 K and 289 K respectively. Crystals were obtained under various conditions (e.g. 0.1 M Tris pH 8.5, 0.3 M magnesium formate, 0.2 M sodium chloride; 0.1 M Tris pH 8.5, 25% w/v polyethylene glycol (PEG) 3350, 0.02 M magnesium chloride; 0.1 M HEPES pH 7.5, 22% w/v polyacrylic acid 5100; 0.2 M ammonium fluoride, 20% w/v PEG 3350, pH 6.2; 0.1 M HEPES pH 7.5, 25 % (w/v) PEG 2000 MME; 0.2 M magnesium acetate, 20 %(w/v) PEG 3350; 0.2 M magnesium sulphate, 20 % (w/v) PEG 3350; 0.2 M di-sodium

tartrate, 20 % (w/v) PEG 3350; 0.2 M tri-sodium citrate, 20 % (w/v) PEG 3350) and grew to full size within one day.

Molecular modelling

The homology model of dimeric NikK was built using YASARA (23;24). The structure of HisC from *E. coli* (PDB accession code 1fg3) (25) which shares 25% sequence identity with NikK was manually selected as the template for modelling. In order to get a good plasticity of the NikK active site, a gem-diamine complex between PLP, histidinol-phosphate and the active site lysine residue, present in the template structure, was kept during modelling. This model was further refined using secondary structure predictions (HHpred, http://toolkit.tuebingen.mpg.de/hhpred) (26;27) for previously unaligned regions using the program MODELLER v9.8 (28). Optimization of the model was facilitated using a protocol described by Krieger et al (29). Briefly, a short molecular dynamics simulation was carried out under constant pressure and temperature conditions. The homology model was solvated in a water box, sodium ions were used to neutralize charges on the protein and the modelled ligand intermediate was parameterized automatically. The solvation box was 7.5 Å bigger than the protein in each direction. The whole system was optimized by a steepest descent energy minimization using the AMBER 03 force field (30;31). Long range electrostatic interactions were treated using the Particle-Mesh-Ewald method (32). A trajectory was run for a total of 500 ps with snapshots taken every 25 ps. Every snapshot structure was minimized by a simulated annealing run and the energies were tabulated. The lowest energy snapshot was taken as the best optimized structure and analysed using YASARA (www.yasara.org) and PyMOL (www.pymol.org).

For docking calculations the structures of ligands (external aldimines of glutamic acid, leucine, cysteine and the ketohexuronic acid) were built in Maestro (http://www.schrodinger.com) and geometry optimized using the OPLS force field (33;34). Partial charges for the ligands were computed with the Antechamber program of Amber 11 using the semiempirical AM1-bcc method (35). The refined homology model was prepared according to requirements of AutoDock v4.2 (addition of polar hydrogen atoms, addition of partial charges, assignment of atom types). The modelled ligand-intermediate was deleted from the model prior to docking and the simulations were performed with AutoDock v4.2 (36) using the implemented Lamarckian genetic algorithm with a population size of 350 individuals, and an average number of

generations of about 900. The cubic energy grid was centered on the Nε atom of K221 and had an extension of 22.5 Å in each direction. While all ligand structures were treated as fully flexible to ensure a maximum degree of freedom during the simulations, all protein residues were kept rigid. For each ligand structure, 50 independent docking runs were performed and the resulting binding modes were clustered based on an r.m.s.-deviation cut-off of 2.0 Å. The obtained structures were further subjected to geometry optimization in YASARA.

Every protein-ligand complex was analyzed individually to see, whether it meets the criteria for a mechanistically reasonable binding mode (angle between N□ of K221, C4A and C4 of PLP at around 90°, distance of N1 from PLP to the carboxyl group of D190 within 4 Å, salt bridge between the α-carboxyl group of the ligand and R343, superposition with the PLP-cofactor).

Results

Genomic sequencing of the nikK gene

The *nikK* gene region was sequenced six times to confirm the DNA sequence deposited in the UniProt database (GenBank: CAC80909.1). In all cases we detected two deviations from the deposited sequence: the codon for the amino acid in position 348 specified asparagine instead of aspartate, and the codon for position 349 specified aspartate instead of histidine (see supplementary Figure S1). Accordingly, these alterations were taken into account for the generation of the synthetic gene used for heterologous expression of *nikK*.

NikK expression and native molecular weight determination

Several attempts to heterologously express the PCR-amplified *nikK* gene in *Escherichia coli* and *Pichia pastoris* were unsuccessful. Hence, a synthetic gene in *E. coli* codon usage was employed to express the protein. In addition, the soluble protein yield could be doubled to 5 mg/L medium by concomitant expression of the chaperone genes *dnaK, dnaJ, grpE, groEL* and *groES*. The C-terminally hexahistidine-tagged protein was purified to near homogeneity by a one-step Ni-NTA-affinity chromatography, yielding about 0.6 mg of NikK per gram of wet biomass.

Size exclusion chromatography generated a single peak with an elution volume corresponding to a molecular mass of 79 kDa. Since the calculated molecular mass of the protein is 39.5 kDa, the native molecular mass determination indicates that NikK forms a dimer in solution.

UV-vis absorbance properties of NikK

The UV-Vis absorbance spectrum of purified NikK indicated the presence of a PLP cofactor (Figure 1). The features of the absorbance spectrum strongly depend on the pH (Figure 1). At high pH, the spectrum is dominated by an absorbance maximum at 357 nm while at low pH the maximum absorbance shifts to longer wavelength (425 nm). The pH-dependent spectral changes were used to calculate a pK_a value of 8.3 for the internal aldimine species that typically forms between the PLP cofactor and the side chain of a lysine residue (Figure 1, insert) (22). At low pH, an additional peak at 330 nm appeared which is characteristic for the presence of pyridoxamine-5´-phosphate. PLP-dependent aminotransferases like *E. coli* tryptophanase or tryptophan indole-lyase

from *Proteus vulgaris*, show a characteristic band at 340 nm which corresponds to the enolimine form of the cofactor (37). This species exhibits a fluorescence emission maximum at around 500 nm on excitation at 340 nm (38). However, no fluorescence emission was observed with purified NikK, indicating that the absorbance in this region can be assigned solely to the deprotonated form of the PLP Schiff base and the PMP form of the cofactor.
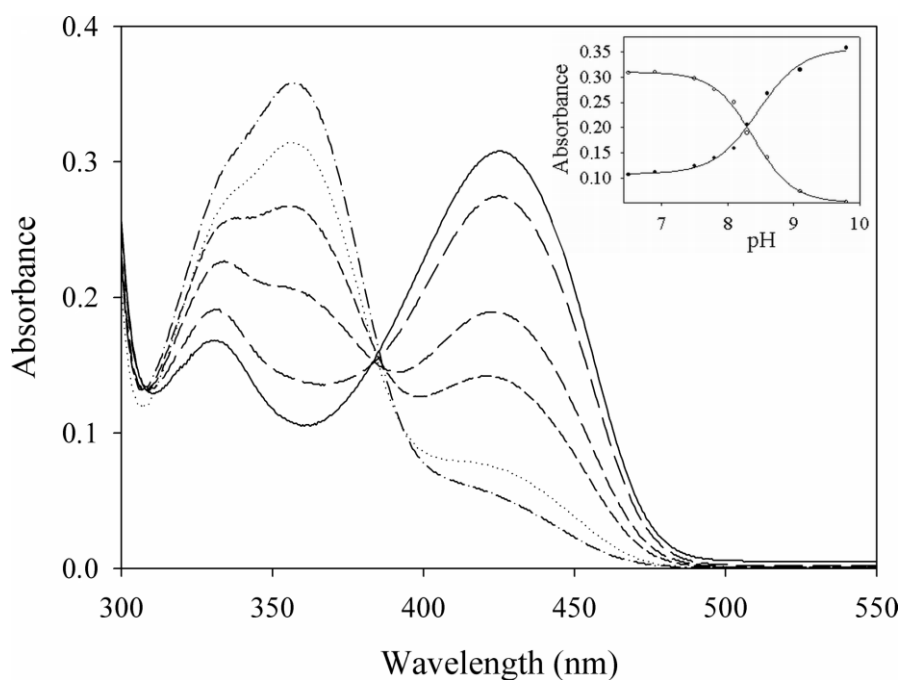
Figure 1

Absorbance spectra of NikK at various pH values (6.5: solid line; 7.8: long dashed, 8.1: medium dashed; 8.6: short dashed; 9.1: dotted; 9.8: dash-dotted line). The arrows indicate the direction of change with increasing pH. The insert shows the pH dependence of the absorbance at 357 nm (●) and 425 nm (○).

Demonstration of aminotransferase activity

The deamination of L-alanine in the presence of α-ketoglutarate was observed by measuring the absorbance of the coloured complex formed by pyruvate and DNPH at 540 nm. The colour change in the presence of NikK enzyme clearly showed that L-alanine had been converted to pyruvate. No colour change is seen in the absence of α-ketoglutarate, which serves as an amino acceptor. Thus, it is evident that NikK comprises aminotransferase activity.

Amino donor specificity: screening of amino acids

The first amino transfer reaction has been followed with various amino acids at pH 8.0 and 9.0 (Table 1). The most active amino group donor is L-glutamate. Based on the spectral changes occurring in the presence of L-glutamate, shown in Figure 2, v_{max} and K_D values of the NikK catalysed deamination of L-glutamate were determined (Figure 3 and Table 2). Other amino acids (Phe, Trp, Ala, His, Met, Leu) also show significant amino group donor activity. The spectral changes were negligible in the presence of Gly, Ile, Thr, and Pro. The rapid reaction observed with L-cysteine is probably due to the formation of a stable thiazolidine ring between L-cysteine and PLP and not to amino group transfer (39;40).
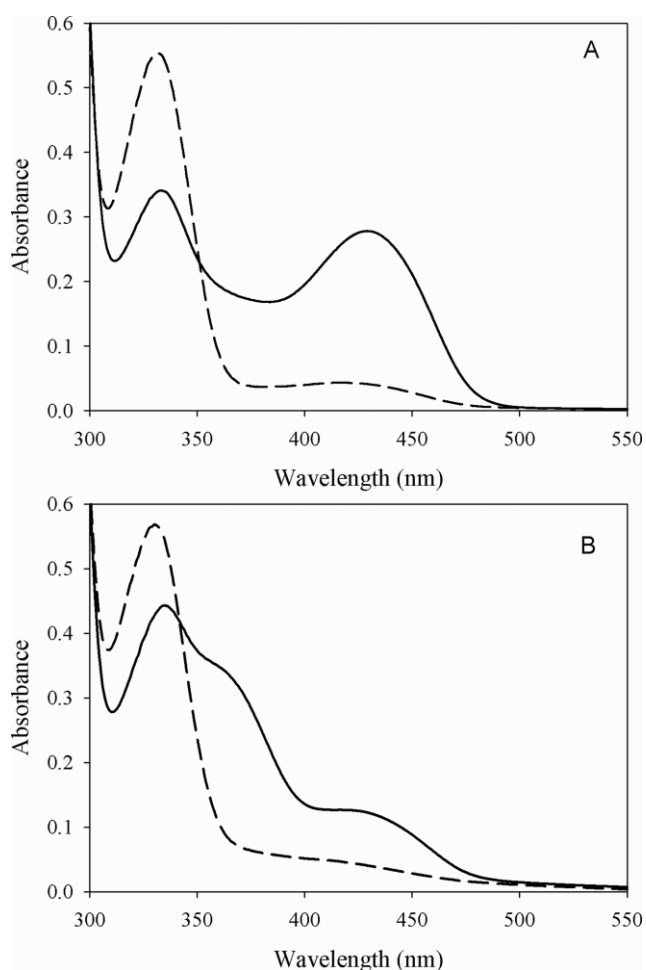
Figure 2

Spectral changes in the presence of 5 mM L-glutamate at pH 8.0 (A) and pH 9.0 (B) The solid lines show spectra of a NikK solution in the absence of glutamate, the dashed lines are spectra taken after 5 min incubation with glutamate.
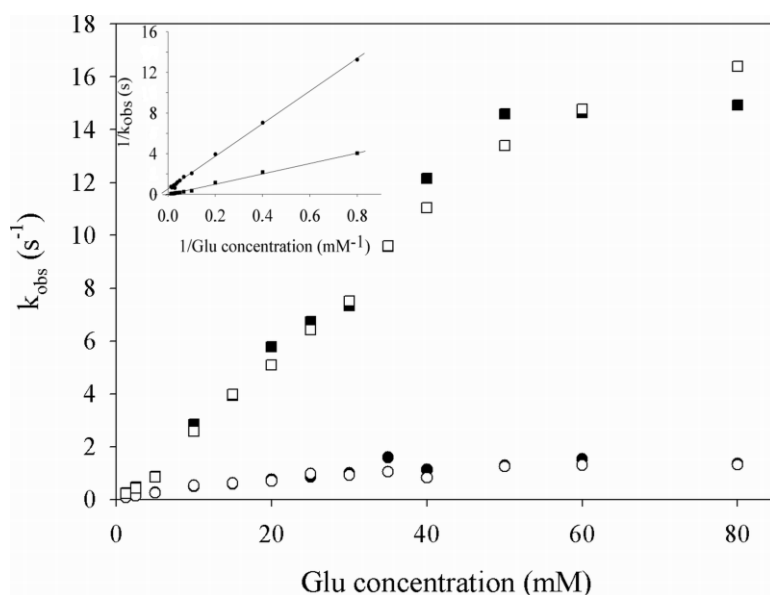
Figure 3

Observed absorbance change in the presence of glutamate. ● 330 nm, pH 8; ○ 425 nm, pH 8; ■ 330 nm, pH 9; □ 357 nm, pH 9. The insert shows a Lineweaver Burk linearization to determine the v_{max} and K_D values by following the absorbance decrease at 330 nm at pH 8 (●) and pH 9 (○).

Table 2
v_{max} and K_D values of the transamination reactions of NikK with L-glutamate

	v_{max} (s^{-1})	K_D (mM)
pH 8.0	2.0 ± 0.18	32.4 ± 5.5
pH 9.0	32 ± 22	128 ± 38

Rapid reaction kinetics

Following time-dependent spectral changes after mixing NikK with the respective amino acid in a stopped-flow device, it was observed that the reactions proceed in a monophasic manner, except in the case of cysteine as substrate (see above). The k_{obs} values for several substrate concentrations were determined by monitoring the absorbance increase at 330 nm and the absorbance decrease at 425 nm at pH 8 or at 357 nm at pH 9 (Table 1). At a fixed amino acid concentration, the observed rate was independent of the wavelength used to monitor the reaction.

pH-Dependence of amino group transfer

To assess the pH dependence of amino group transfer, L-alanine was used as amino group donor at different pH values. As shown in Figure 4, the decrease at 430 nm is ca. 10 times faster at pH 9 than at pH 7. The pH-dependence of the reaction rate correlates with the pH-dependent spectral changes described above (Figure 1 and insert). Accordingly, the inflection point of the pH-dependency shown in Figure 4 is close to the determined pK_a of the aldimine species (= 8.3). This supports the view that the deprotonated Schiff base represents the active form of the enzyme-bound PLP cofactor.
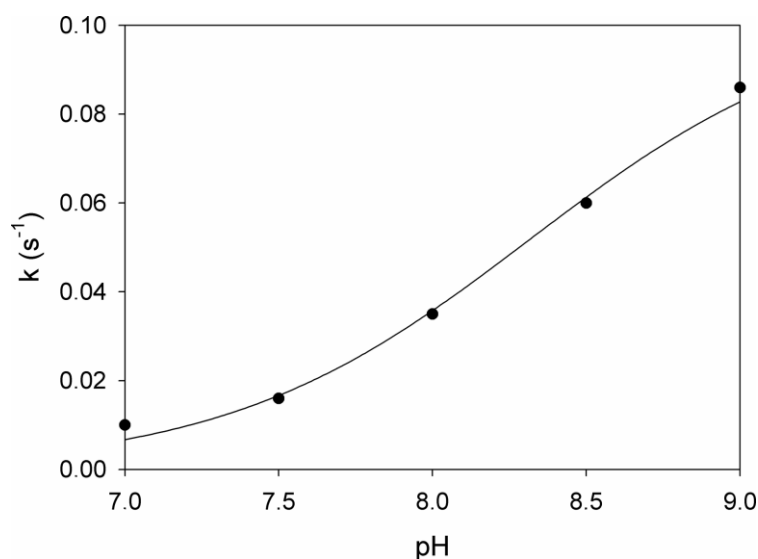
Figure 4

Rate of the absorbance decrease during the first amino transfer reaction with 7.5 mM L-alanine as amino group donor, plotted against the pH. The sigmoidal function shows an inflection point at pH 8.3, the pKa of the Lys221-PLP Schiff base. The reaction rate increases with the pH, indicating that the deprotonated Schiff base is the active form.

Crystallization

Initial crystallization screens with native hexahistidine-tagged NikK yielded very thin plate-like crystals in various conditions. Several of these initial conditions could be optimized to a certain extent, showing slightly enhanced growth in the third dimension, but the crystals always remained plate like. Even the optimized crystals gave only weak and highly anisotropic diffraction patterns which could not be processed.

In an attempt to improve crystallization, we used the surface entropy reduction prediction (SERp) server (41;42) and our model (see below) to predict amino acid

replacements which could enhance crystal growth. Thus, a triple variant, NikK E265A/E266A/Q267A, was generated, however, we were unable to obtain crystals. Similarly, the K221M variant did not yield crystals, neither under the conditions optimized for the wild type enzyme, nor under other conditions covered in several commercially available screens.

Homology model

Blast searches against a nonredundant set of protein sequences (NCBI) showed that close homologues to NikK, with sequence identities of more than 50%, only occur in other *Streptomyces* followed by a few sequences of histidinol phosphate aminotransferases from various organisms, exhibiting around 30% sequence identity. A blast search against the protein databank (PDB) identified the structure of HisC from *E. coli* in complex with histidinol phosphate (PDB code: 1fg3, 25% sequence identity) as the most suitable template. NikK was modelled as a dimer, because dimer formation was found to be essential for many aminotransferases in order to build up functional active sites (25;43;44) and because size exclusion chromatography indicated the occurrence of NikK dimers in solution.

The modelled NikK structure exhibits the same three domains into which structures of aminotransferases can usually be divided, namely N-terminal arm, small domain and PLP-binding domain (25;43) (Figure 5). The model, however, shows very different loop conformations in the small domain (residues 33-40) as well as in the PLP-binding domain (residues 49-65). Compared to the sequence of HisC from *E. coli*, NikK is 12 residues longer, which results in the difference between the two aforementioned regions. Interestingly, the different loop conformations of residues 33-40 introduce three completely new interaction possibilities for substrates in the active site, by shifting the corresponding loop towards the PLP cofactor. Concomitant with the shape alteration in this loop region, residues 49-65, which are predicted to form a small helix in NikK rather than an extended loop as in HisC, are affected as they are close in space. Furthermore, a tyrosine residue from one protomer, that in analogous aminotransferase structures, is pointing towards the active site of the vice versa protomer (25;43;45-48) (Y55 in HisC corresponding to Y61 in NikK) is part of the affected residue range (Figure 6). Other essential active site residues (Asp190, Tyr193, Ser220, Lys221 and Arg330) (25;49), however, are very well conserved in sequence and structure.
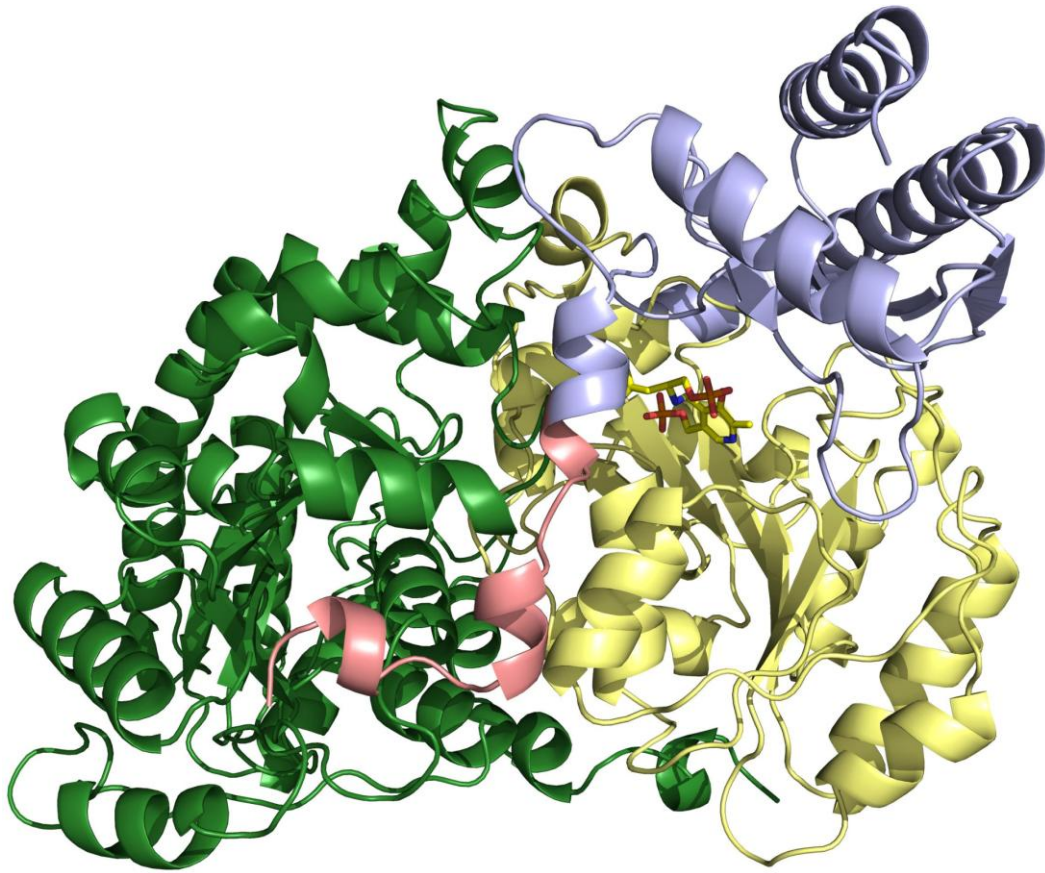
Figure 5

Overall structure of the NikK homology model. The enzyme was modelled as a dimer. One protomer is shown in green (left) whereas the other protomer is color coded for the three domains typical for aminotransferases: N-terminal arm (salmon), small domain (light blue) and PLP-binding domain (pale yellow). The PLP histidinol-phosphate adduct, which was kept during modelling to assure a maximum in plasticity of the active site is shown in a stick representation and colored in yellow. The figure was created with PyMol (www.pymol.org).
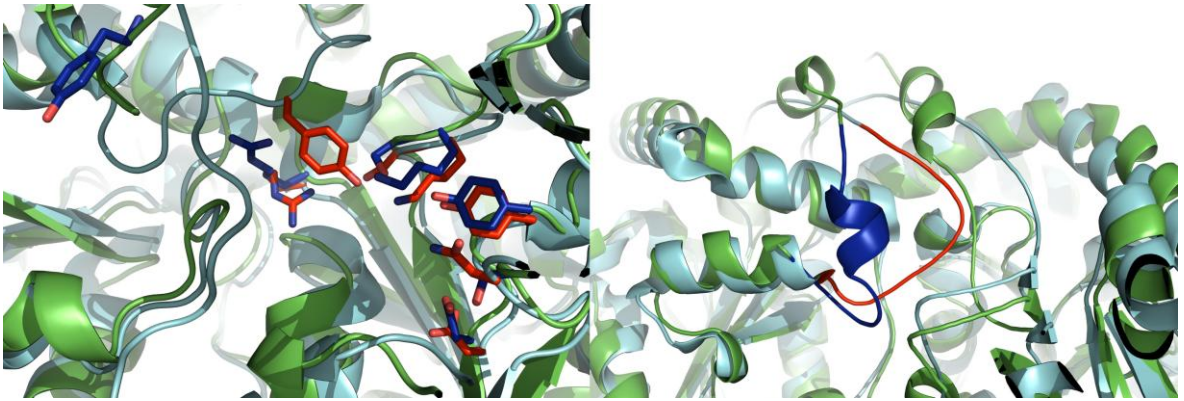
Figure 6

Comparison of the homology model of NikK with HisC from *E. coli*.

Left: superposition of the NikK homology model and the experimentally determined structure of HisC (PDB accession code 1fg3). Residues corresponding to NikK are coloured in dark blue whereas HisC is shown in red. Right: a color-coded (NikK: dark blue, HisC: red) cartoon representation of the region that in contrast to HisC is predicted as a helix in NikK and therefore adopts a completely different conformation, which results in a differently shaped binding pocket.

The role of K221 in Schiff base formation

Our homology model of NikK suggests that K221 is potentially involved in the formation of the internal Schiff base with the PLP cofactor. To test this hypothesis, we generated a NikK variant where K221 is replaced by methionine (K221M). The isolated K221M variant displays a deep yellow colour, however the UV-vis spectrum shows remarkable differences to the spectrum obtained with wild type protein (Figure 7). In contrast to wild type protein, the absorbance maximum of the K221M variant is shifted to lower wavelength (400 nm) resembling the absorbance spectrum of free PLP rather than the enzyme-bound Schiff base (see Figure 7). The addition of glutamic acid (10 mM final concentration) to the K221M variant results in a shift of the absorbance maximum to around 410 nm, indicating that an external aldimine can be formed between non-covalently bound PLP and the amino acid without prior binding of the cofactor to K221. However, formation of the external aldimine in the K221M variant

does not lead to deamination of the substrate as the active site lysine is essential for the conversion of the cofactor to the PMP form.
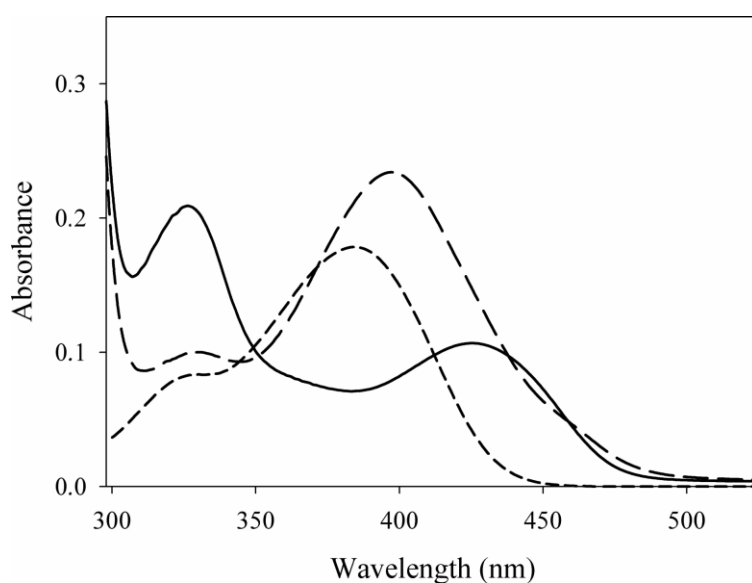
Figure 7

UV-vis absorbance spectra of NikK wild type (solid line), NikK (K221M) (long dashed line) and free PLP (short dashed line). The spectra were taken at pH 8.0 at an enzyme or PLP concentration of 25 μM.

Substrate docking

We docked three possible amino group donors and the proposed keto-acid substrate in their external aldimine form into the active site of NikK and obtained mechanistically reasonable binding modes for all of them. Characteristic interactions of the docked ligands were H-bonding of pyridine N1 to D190, stacking interactions of the PLP-pyridine ring with F112, salt bridge formation between the α-carboxylate of the ligands with R343/R330 and PLP-phosphate group stabilization by H-bonding to the main chain NH and side chain OH of S88.

Compared to structures of other aminotransferases (e.g. HisC from *E. coli* and aspartate aminotransferases from various organisms), additional interactions (Figure 8A-D) of the ligands with the enzyme, are provided by the altered loop region (residues 33 to 35) above the active site (Figure 8). Within this loop especially K33 was found to form an additional salt-bridge with the α-carboxylate of the docked ligands. Apart from that, further interactions of the amino acid substrate side chains were facilitated by a salt

bridge between the δ-carboxyl group and R229 (glutamate, Figure 8B), hydrophobic interactions of the leucine *sec*-butyl group with F19 (Figure 8D) and a possible disulfide bridge formation of cysteine with C35 (Figure 8C).
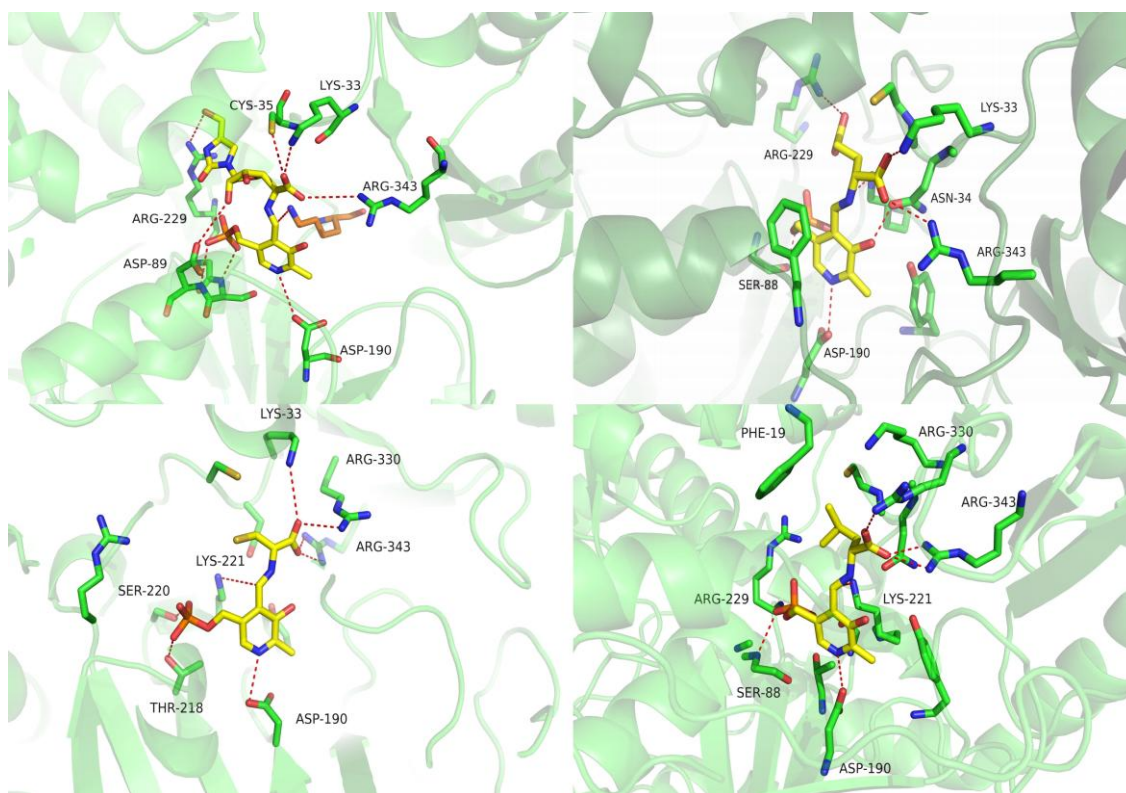
Figure 8

Docked and energy minimized complex structures of the NikK homology model and three representative amino group donors as well as the ketohexuronic acid moiety built as external aldimines. (a) Ketohexuronic acid linked via a Schiff base to PMP building an external aldimine. Active site residues are shown as sticks and interactions between protein residues and substrate are indicated by the red dashed lines. The active site lysine K221 is coloured in orange. (b) Docked complex of NikK and glutamic acid external aldimine. Residues from a loop region above the active site are forming additional interactions with the δ-carboxyl group of the substrate. In addition, stacking interactions of a phenylalanine residue with the pyridine ring of PLP can be seen. (c) Docked external aldimine form of cysteine. It can be seen that there is another cysteine side chain close enough to form a disulfide bridge. (d) Leucine docked as external aldimine to the active site of NikK. Even though there are multiple polar interaction possibilities, the hydrophobic side chain of leucine gets accommodated, making hydrophobic interactions with an adjacent phenylalanine residue. All residues are labelled according to NikK amino acid numbering.

Docking of our proposed substrate for NikK, ketohexuronic acid, into the active site gave a reasonably looking binding mode as well. Here, additional ligand side chain interactions with the enzyme are hydrogen bonding between D89 and the OH-groups of the sugar moiety as well as the interaction of the 4-formyl-4-imidazoline-2-one with the conserved R229 (Figure 8A). Moreover, the obtained docking pose also made evident how important the additional space in the active site of NikK is in order to accommodate this large substrate.

To compare the plasticity of the active sites of our NikK homology model with its template, HisC from *E.coli*, we superimposed the obtained docking pose of the ketohexuronic acid onto the HisC active site, by fitting the two PLP cofactors to each other. This resulted in clashes with side chain and main chain atoms of HisC residues 54-58. These residues however, correspond to residues 60-64 in NikK, which are part of one altered loop region (Figure 9).
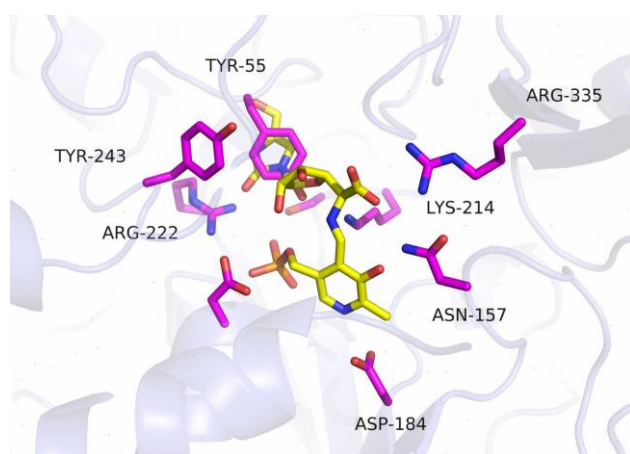
Figure 9

Superposition of the binding mode obtained for the ketohexuronic acid docked as an external aldimine to NikK, with the active site structure of HisC. The orientation of the loop region (residues 54 to 58) in HisC would introduce clashes with the sugar moiety of the substrate. This is further evidence that the different structure of this loop region is essential for binding of ketohexuronic acid.

Discussion

Several structurally related peptide nucleosides termed nikkomycins are produced by *Streptomyces tendae* and *ansochromogenes* (6). One characteristic feature of the biosynthesis is the modular set up where a dipeptide comprised of two non-standard amino acids and an aminohexuronic acid moiety are synthesized separately and then condensed to the desired product (with various nucleobases N-glycosidically linked to the sugar). Several steps of the dipeptide biosynthesis were studied (50;51) but so far only the initial reaction step towards the biosynthesis of aminohexuronic acid was reported. In this first reaction, NikO, a member of the *enol*pyruvyl transferases catalyzes the transfer of an *enol*pyruvyl group to the 3' position of UMP, yielding 3'-*enol*pyruvyl-UMP (18). A series of unknown enzymatic reactions then leads to the conversion to aminohexuronic acid. In *S. tendae*, a set of genes (*nikI, nikJ, nikK, nikL, nikM*) were identified that encode enzymes catalyzing the required chemical steps (19). In order to gain further insight into the biosynthetic pathway, we have expressed *nikK* to demonstrate its role as an aminotransferase involved in the last step of the biosynthesis of aminohexuronic acid from ketohexuronic acid (Scheme 1).
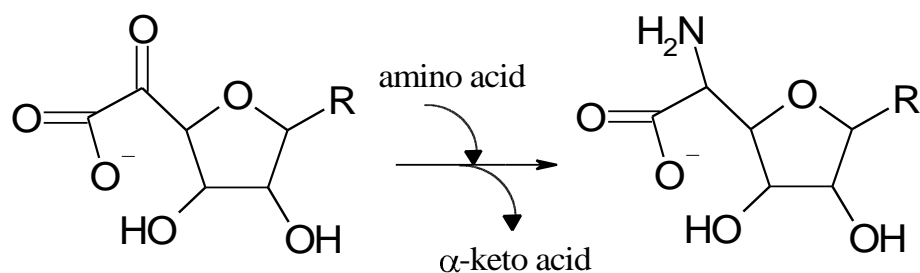
Scheme 1

Proposed final step in the biosynthesis of the aminohexuronic building block of nikkomycins catalyzed by NikK. NikK plays an essential part in the biosynthetic pathway of nikkomycin antibiotics. It is assumed that the NikK enzyme catalyzes the introduction of the amino group into the aminohexuronic acid moiety of nikkomycins.

The *nikK* gene encodes a 39.5 kDa protein which shows sequence similarities to several pyridoxal-5'-phosphate containing histidinol phosphate aminotransferases, e. g. 44% similarity and 25% identity to the histidinol phosphate aminotransferase HisC from *Escherichia coli*. Using a synthetic *nikK* gene optimized for *E. coli* codon usage, a sizable amount of soluble protein was produced. The yellow colour of the protein solution and the UV-vis absorbance properties of the protein indicated the presence of pyridoxal-5'-phosphate. NikK was shown to form a dimer in solution, like many other PLP-dependent enzymes, with each protomer having a mass of approximately 40 kDa as judged from SDS-PAGE. For many PLP-dependent enzymes, dimer formation seems to be essential for forming a functional active site (25).

The PLP cofactor features distinct peaks in the UV-vis absorbance spectrum. The peak at 425 nm, which is prominent at lower pH values, represents the protonated form of the nitrogen in the Schiff base formed between the aldehyde group of the cofactor and the side chain amino group of an active site lysine residue. On the other hand, the peak at 357 nm observed at high pH shows the deprotonated form of the Schiff base nitrogen. The absorbance spectra intersect in a single isosbestic point at 380 nm. From the pH-dependence of the Uv-Vis absorbance spectra, a pK_a of 8.3 was determined. This value is significantly higher than the value of 6.6 and 6.8 determined for histidinol phosphate aminotransferase (EC 2.6.1.9) and aspartate aminotransferase (EC 2.6.1.1), respectively. Apparently, in those enzymes the pK_a increases successively during catalysis. In AspAT, the pK_a is expected to increase to 8.8 in the Michaelis complex that is formed with the substrate amino acid and to above 10 in the external aldimine. The low pKa value of the unliganded enzyme is explained by the strain on the imine-pyridine torsion angle of the Schiff base, which is also crucial for the successive increase of the pKa (52;53). On binding of the substrate amino acid, the pKa increases and a proton is transferred from the protonated amino group of the substrate to the Schiff base nitrogen. The free amino group then nucleophilically attacks the imine, which has an increased electrophilicity due to protonation. In this so-called transaldimination step, the PLP-substrate Schiff base is formed (53). However, the imine nitrogen of another member of subfamily I aminotransferases, glutamine:phenylpyruvate aminotransferase from *Thermus thermophilus*, shows a comparingly high pK_a value of 9.3 (54).

The protonated Schiff base can also form an enolimine with an absorbance at 340 nm. We have observed an additional peak at 330 nm in the UV-vis absorbance spectrum of the purified NikK enzyme. However, the enolimine exhibits a typical fluorescence emission centered at around 500 nm which could not be detected in the case of NikK (22). Therefore, we conclude that the absorbance at 330 nm is not due to the enolimine but rather from the PMP form of the cofactor, which might be formed during cell disruption and purification, when the protein is in contact with molecules that function as amino group donors.

Our homology model predicted K221 as a potential candidate for Schiff base formation with the PLP cofactor. In order to confirm this assignment we have exchanged K221 with leucine by site-directed mutagenesis of the nikK gene. The resulting K221M variant shows significant changes in the UV-Vis spectrum with an absorbance maximum at 400 nm (Figure 7). The absorbance spectrum of the K221M variant resembles that of free PLP suggesting that the variant is still capable of PLP binding, however, unable to form the internal Schiff base. Although the addition of a potential amino group donor yields the external aldimine, further conversion to pyridoxamine-5-phosphate is not observed, clearly demonstrating that K221 is the catalytic lysine in the active site of NikK. In pyridoxal-5'-phosphate-dependent aminotransferases, the transfer of the amino group between two amino acids proceeds in two steps, summarized in the following equations:

PLP-enzyme + amino acid A ↔ PMP-enzyme + keto acid A   (1)

PMP-enzyme + keto acid B ↔ PLP-enzyme + amino acid B   (2)

In amino transfer reactions catalysed by pyridoxal-5'-phosphate dependent enzymes the first reaction step is always a transaldimination reaction, which starts by conversion of the internal aldimine formed by the PLP cofactor and the ε-amino group of the lysine residue in the active site into an external aldimine intermediate by replacing the lysine residue with the amino acid substrate (46). Most likely, the mechanism is comparable to that of serine- glyoxylate aminotransferase, which was described by Karsten *et al*: The amino acid substrate binds with its α-amine protonated, and an enzymatic base accepts a

proton from the amino group of the substrate. The resulting free amino group attacks the PLP cofactor at C4', leading to a *gem*-diamine intermediate, which then collapses to form the external aldimine. In the external aldimine, the α-proton is abstracted from the amino acid substrate by the ε-amino group of the lysine residue, resulting in the quinonoid intermediate. The most important function of PLP is the stabilization of carbanions generated by the loss of the proton at Cα of the substrate. The negative charge is delocalized by resonance into the π-electron system of the quinonoid intermediate. These properties of a suitable electron sink are further enhanced by a close interaction of the pyridinium nitrogen with an aspartate residue (55). According to our homology model, this role is fulfilled by D190 in the active site of NikK. Proton transfer from the ε-amino group of the lysine to C4' of the quinonoid intermediate leads to the ketamine which is finally hydrolysed to the keto acid corresponding to the substrate and the PMP form of the enzyme (56;57).

We have characterized the deamination step spectroscopically with several amino acids by observing the absorbance change at 330 nm, 357 nm and 425 nm. The reaction rate was negligible with Ser, Gly, Ile, Thr, and Pro as amino group donors while other amino acids, like Phe, Trp, Ala or His, showed significant amino donor activity (Table 1). Glutamate turned out to be the most active amino-donor (Table 1). Interestingly, glutamate was also found to be the amino group donor for the structurally related histidinol phosphate aminotransferases. For example, HisC from *E. coli* catalyzes the seventh step in the histidine biosynthetic pathway, the transfer of the amino group from glutamate to imidazoleacetol phosphate (25). Hence, Glu is a likely candidate as an amino group donor for the in vivo biosynthesis of the aminohexuronic acid in *Streptomyces*. The transamination reaction with glutamate is pH dependent, with rates increasing at higher pH (see Figures 2 and 3, and Table 2). The pH-dependency of the rate exhibits the same pKa as protonation/deprotonation equilibrium of the Schiff base nitrogen indicating that the deprotonated form of the Schiff base is the active form of the enzyme.

Very rapid spectral changes in the NikK spectrum are observed in the reaction with cysteine. However, the reaction does not proceed in a monophasic manner as it is observed with the other amino acids, but seems to consist of a rapid and a slow phase (for rates see Table 1). We suppose that these observations are due to a side reaction,

and not to amino group transfer. Cysteine reacts with PLP, resulting in the formation of a stable thiazolidine ring, a species that absorbs at 330 nm (39;40).

Table 1
Reactivity of NikK with various amino acids. Reaction rates (k_{obs}) were measured at a concentration of 10 mM of the respective amino acid at pH 8.0 and pH 9.0 by monitoring the absorbance decrease at 425 nm or 357 nm and the absorbance increase at 330 nm.

	pH 8.0 k (s^{-1})		pH 9.0 k (s^{-1})	
	425 nm	330 nm	357 nm	330 nm
Glu	0.560	0.586	3.396	3.687
Phe	0.103	0.116	0.200	0.212
Trp	0.070	0.069	1.204	1.406
Ala	0.056	0.058	0.171	0.163
His	0.052	0.055	0.092	0.097
Met	0.050	0.050	0.109	0.113
Leu	0.045	0.052	0.110	0.117
Asp	0.031	0.031	0.128	0.114
Gln	0.020	0.022	0.037	0.045
Arg	0.013	0.016	0.009	0.010
Lys	0.011	0.011	0.040	0.044
Val	0.003	0.003	0.006	n.d.
Cys	4.2/0.003	3.4/0.003	n.d.	n.d.
Ser	0.002	0.003	n.d.	n.d.
Gly	0.000	0.000	n.d.	n.d.
Ile	0.000	0.000	n.d.	n.d.
Thr	0.000	0.000	n.d.	n.d.
Pro	0.000	0.000	n.d.	n.d.

Our results demonstrate that NikK is an active transaminase with a preference for glutamate as amino group donor (equation 1). The enzyme may then transfer the amino group to ketohexuronic acid (keto acid B in equation 2) to complete the synthesis of aminohexuronic acid used as a building block for nikkomycins (see Scheme 1). How the ketohexuronic acid is synthesized by the gene products of *nikI, nikJ, nikL*, and *nikM*

from the first metabolite 3'-enolpyruvyl-UMP is currently subject of further investigations in our laboratory.

To gain deeper insight into the structure of NikK and the amino acids directly involved in the transamination reaction, we attempted to crystallize the protein. Several initial crystallization conditions were found that gave rise to thin, plate-like crystals, however, none of these crystals could be improved to give satisfactory diffraction sufficient to obtain high-resolution data. Interestingly, NikK seems to favour crystal growth in two dimensions and therefore several approaches to enhance crystal growth in the third dimension (e.g. covering of the reservoir solution with different mixtures of oil (58), addition of organic solvents to the crystallization droplets, different protein concentrations, macro-seeding) were conducted, but were unsuccessful.

Therefore, we built a homology model of NikK using the structure of histidinol-phosphate aminotransferase from *E. coli* as a template. Despite the low sequence identity (25%), NikK displays conservation of many essential active site residues such as D190, Y193, S220, K221 and R330). Looking at the subtle differences between our model and other aminotransferase structures, including its template, two loop regions (residues 33-40 and 49-65) occur in a different conformation. These new conformations, not only introduce additional interaction partners for a bound substrate in the active site of NikK, but also have a major influence on the size and plasticity of NikKs binding pocket (Figure 8). The change in loop conformations accompanied by the gain in active site space is in agreement with the increased spatial requirements of the ketohexuronic acid sustrate compared to the amino group acceptor of HisC.

Apart from that, we obtained very intriguing results for docking of the ketohexuronic acid too. The slightly changed shape of the binding pocket in NikK enabled the accommodation of our big substrate in the active site. Thus we propose that this change in shape is necessary to enable the amination of the ketohexuronic acid substrate to the aminohexuronic acid product. Further evidence for this shape alterations being essential for NikK to act as an aminotransferase on such a big substrate is, that by superposing the docking pose of the ketohexuronic acid onto the PLP cofactor in the HisC structure, clashes with side- and main chain atoms of residues 54-58, from the second protomer, are found (Figure 9).

Furthermore, we docked three different amino acids (Glu, Leu and Cys) and the proposed substrate, ketohexuronic acid, in their external aldimine form into the active site of the homology model, to get a better understanding of the aminotransferase activity of NikK and to see if its active site could accommodate our proposed substrates. This enabled us to identify the active site residues, which provide important interactions with the ligands. As a result we can now give a better rationalisation for the highest measured reactivity of glutamate as amino group donor, since the polar, charged side chain gets accommodated very well by forming a salt bridge between R229 and the δ-carboxyl group of the amino acid. Moreover, we also found an explanation for the lower reactivity for leucine through the docking calculations. In the model, the environment of the active site is aligned by more polar than apolar residues and the only hydrophobic interaction for the sec-butyl side chain of leucine is that with F19. Thus, the negatively charged glutamic acid is clearly preferred over hydrophobic substrates such as leucine in our model.

A different situation can be imagined for cysteine. As there is a cysteine residue presented by the loop above the active site, very close to the external aldimine SH group in the obtained docking pose, disulfide bridge formation between the two side chains would abolish transaldimination. This observation can serve as an additional explanation for the non-acceptance of cysteine as an amino group donor (Figure 9).

Acknowledgments

Supplementary Figure S1

DNA- and amino acid sequence of NikK. Changes to the sequence in the data bank are in bold face and underlined (N348 instead of D and D349 instead of H). The DNA-sequence in the database for these two amino acids is AAG CAC.

```
   1 ATGCCAGCTCGTGAAGGTGCAGACTCTCCGTTCCTGCGTGAATCTGCTGGTCGTTTTCGT
   1 M   P   A   R   E   G   A   D   S   P   F   L   R   E   S   A   G   R   F   R
  61 AACCGCCGCGTTCGTGTTCCGGATGAAATCAATCTGAAAAATTGTGGTCTGCTGGACAGC
  21 N   R   R   V   R   V   P   D   E   I   N   L   K   N   C   G   L   L   D   S
 121 CGCGCTGCGGCAGTTCATCGTGCGACCCTGGCAGAATTCGATCCAAATGATGTTCTGACC
  41 R   A   A   A   V   H   R   A   T   L   A   E   F   D   P   N   D   V   L   T
 181 TATCCGATCCTGCAGCCGGTTTACGGTATGCTGGCTGACCGTTTCGGTGTGGACACCGAT
  61 Y   P   I   L   Q   P   V   Y   G   M   L   A   D   R   F   G   V   D   T   D
 241 TCCCTGGTGCTGACCGCTGGTTCTGACCCTGGTCTGAACCTGCTGACCCGTGCGTTCCCG
  81 S   L   V   L   T   A   G   S   D   P   G   L   N   L   L   T   R   A   F   P
 301 GAAGTGTCCCGTATTGTTCTGCACCAGCCGAACTTCGACGGTTGGGCAAAATTCGCAGCC
 101 E   V   S   R   I   V   L   H   Q   P   N   F   D   G   W   A   K   F   A   A
 361 ATCTCTGGCTGCGTTCTGGATCCGGTTGCTCCTGATCCAGAAACCGGCCTGTTTGACCTG
 121 I   S   G   C   V   L   D   P   V   A   P   D   P   E   T   G   L   F   D   L
 421 CGCGATCTGGCACGTCGTCTGCGTGCAGGTGCACCGGCGTTCGTGGTGGTTACCACTCCG
 141 R   D   L   A   R   R   L   R   A   G   A   P   A   F   V   V   V   T   T   P
 481 CACTCCTTTACTGGCCAGGTACACGGTCGTGAAGAGCTGGCTGAACTGGCTGACGCCGTT
 161 H   S   F   T   G   Q   V   H   G   R   E   E   L   A   E   L   A   D   A   V
 541 GCCGAGCATGGCTCCCTGCTGGTGGTTGATACTGCTTACCTGGCTTTTACTGAAGGTGGT
 181 A   E   H   G   S   L   L   V   V   D   T   A   Y   L   A   F   T   E   G   G
 601 GAAGAACTGGTACGTGGTCTGGCTGGTCTGCGCCACGTAGTTCGTGTGAATACCTTCTCT
 201 E   E   L   V   R   G   L   A   G   L   R   H   V   V   R   V   N   T   F   S
 661 AAGAGCTACGGCCTGTCTGGCGCCCGTATTGCTGTGACCGTAGCACACCCGGCTACCGCG
 221 K   S   Y   G   L   S   G   A   R   I   A   V   T   V   A   H   P   A   T   A
 721 CGTCACCTGTTCGACCTGGACCCAGAAGGCTCTGTGTCCGCACCGGCAGTTGCCCTGCTG
 241 R   H   L   F   D   L   D   P   E   G   S   V   S   A   P   A   V   A   L   L
 781 CGTCGCTCCCTGGAGGAGCAGGCTGTTTTCACTGCGATTTGGGCGGACGTGCGCCGTCTG
 261 R   R   S   L   E   E   Q   A   V   F   T   A   I   W   A   D   V   R   R   L
 841 CGCGAACGTTTTGCCGCCGAGGTGGAACGCGCCGTCCCGGGTTGGCACGCGCGTCCGTCT
 281 R   E   R   F   A   A   E   V   E   R   A   V   P   G   W   H   A   R   P   S
 901 GGCGGTAACTTCGTCACCTGGGACGTTCCGGGCCCTGCTGACGCGGGTGCAGCTTCTCGC
 301 G   G   N   F   V   T   W   D   V   P   G   P   A   D   A   G   A   A   S   R
 961 CACCTGCTGGGTCGTGGCATCGTTGTTCGTGATCTGTCTGGTGCGCCGGGTCTGCCTGCT
 321 H   L   L   G   R   G   I   V   V   R   D   L   S   G   A   P   G   L   P   A
1021 GCTGTCCGTATTGCGGTAGCC**AACGAC**GCAGTAGTGCGTCAAGTCGTTGCCGCGCTGGGT
 341 A   V   R   I   A   V   A   **N**   **D**   A   V   V   R   Q   V   V   A   A   L   G
1081 GACCGTTACCGTGAAGGTGTTGCC
 361 D   R   Y   R   E   G   V   A
```

Supplementary figure S2
Alignment of the amino acid sequences of NikK from *Streptomyces tendae*, histidinol phosphate aminotransferase HisC from *Escherichia coli*, aspartate aminotransferase (AAT) from *E. coli,* and SanB from *S. ansochromogenes.* Important conserved residues are marked with an asterisk: K221, the lysine residue which forms the Schiff base with the PLP cofactor, and D190, the aspartate which interacts with the pyridinium nitrogen of PLP to maintain it in the protonated form, thereby enhancing the electron sink nature of the cofactor.

```
NikK S.tendae        1   -MPAREGADS PFLRESAGRF RNRRVRVPDE INLKNCGLLD SR---AAAVH RATLAEFDPN   56
HisC E.coli          1   -------MST VTITDLAREN VRNLTPYQSA RRLGGNGDVW LN---ANEYP TAVEFQLTQQ   50
AAT E.coli           1   MFENITAAPA DPILGLADLF RADERPGKIN LGIGVYKDET GKTPVLTSVK KAEQYLLENE   60
SanB S.ansochromogenes  1   -MPAREGAGS PFLRESAGRF RNRRVRVPDE INLKNCGLLD SR---AAAVH RATLAEFDPD   56

NikK S.tendae        57  DVLTYP---- -----ILQP- -VYGMLADRF GVDTDSLVLT ASDPGLNLL TRAFPEVSR-  104
HisC E.coli          51  TLNRYP---- -----ECQPK AVIENYAQYA GVKPEQVLVS RCADEGIELL IRAFCEPGKD  101
AAT E.coli           61  TTKNYLGIDG IPEFGRCTQE LLFGKGSALI NDKRARTAQT PGGTGALRIA ADFLAKNTSV  120
SanB S.ansochromogenes  57  DVLTYP---- -----ILQP- -VYGMLADRF GVDTDSLVLT ASDPGLNLL TRAFPEVSR-  104

NikK S.tendae        105 IVLHQPN--- FDGWAKFAAI SGCVLDPVAP DPETGLFDLR DLARRLRAGA PAFVVVTT--  159
HisC E.coli          102 AILYCPP--- TYGMYSVSAE TIGVECRTVP TLDNWQLDLQ GISDKLDG-- VKVVYVCS--  154
AAT E.coli           121 KRVWVSNPSW PNHKSVFNSA DLEVREYAYY DAENHTLDFD ALINSLNEAQ AGDVVLFHGC  180
SanB S.ansochromogenes  105 IVLHQPN--- FDGWAKFAAI SGCVLDPVAP DPETGLFDLR DLARRLRAGA PAFVVVTT--  159
                                                           *

NikK S.tendae        160 PHSFTQVHG REELAELADA VAEHGSLLVV DTAYLAFTE- ---GGEELVR GLAGLRHVVR  215
HisC E.coli          155 PNNPTQLIN PQDFRTLLEL TRGK-AIVVA DEAYIEFCP- ---QAS-LAG WLAEYPHLAI  208
AAT E.coli           181 CHNPTIDPT LEQWQTLAQL SVEKGWLPLF DFAYQGFARG LEEDAEGLRA FAAMHKELIV  240
SanB S.ansochromogenes  160 PHSFTQVHG REELAELADA VAEHGSLLVV DTAYLAFTE- ---GGEELVR GLAGLRHVVR  215
                                                           *

NikK S.tendae        216 VNTFSKSYGL SGAR---IAV TVAHPATAR- --HLFDLDPE GSVSAP---A VALLRRSLEE  266
HisC E.coli          209 LRTLSKAFAL AGLR---CGF TLANEEVIN- --LLMKVIAP YPLSTP---V ADIAAQALSP  259
AAT E.coli           241 ASSYSKNFGL YNERVGACTL VAADSETVDR AFSQMKAAIR ANYSNPPAHG ASVVATILSN  300
SanB S.ansochromogenes  216 VNTFSKSYGL SGAR---IAV TVAHPATAR- --HLFDLDPE GSVSAP---A VALLRRSLEE  266

NikK S.tendae        267 QAVFTAIWAD VRRLRER-FA AEVERAVPGW HARPSGGNFV TWDVPGPADA GAASRHLLGR  325
HisC E.coli          260 QGIVAMRERV AQIIAEREYL IAALKEIP-- CVEQVFDSET NYILARFKAS SAVFKSLWDQ  317
AAT E.coli           301 DALRAIWEQE LTDMRQR--- IQRMRQLFVN TLQEKGANRD FSFIIKQNGM FSFSGLTKEQ  357
SanB S.ansochromogenes  267 QAVFTAIWAD VRRLRER-FA AEVERAVPGW HARPSGGNFV TWDVPDPADA GAASRHLLGR  325

NikK S.tendae        326 GIVVRDLSGA PGLP-AAVRI AVANDAVVRQ VVAALGDRYR --------EG VAX-------  369
HisC E.coli          318 GIILRDQNKQ PSLS-GCLRI TVGTREESQR VIDALRAEQV X--------- ----------  357
AAT E.coli           358 VLRLREEFGV YAVASGRVNV AGMTPDNMAP LCEAIVAVL- ---------- ----------  396
SanB S.ansochromogenes  326 GIVVRDLSGA PGLP-AAVRI RSRNETVVRR VVAALGDRYR YLRRGLLVRG PAPSPETAPA  384

NikK S.tendae        369 ---------- ---------- ---------- ---------- ---------- ----------  369
HisC E.coli          357 ---------- ---------- ---------- ---------- ---------- ----------  357
AAT E.coli           396 ---------- ---------- ---------- ---------- ---------- ----------  396
SanB S.ansochromogenes  385 LGGLGIRTVV DLRLEEERRQ YRGPEYTGAT VLSRPVAGDM SRIRGNVRPR PSDYLANYRD  444

NikK S.tendae        369 ---------- ---------- ---------- ---------- ---------- ----------  369
HisC E.coli          357 ---------- ---------- ---------- ---------- ---------- ----------  357
AAT E.coli           396 ---------- ---------- ---------- ---------- ---------- ----------  396
SanB S.ansochromogenes  445 MLTRAAPVAA EIVDLLAEGA EVPVYICCAM GKDRTGVVSA LVLRALGVRT ADVARDYALT  504

NikK S.tendae        369 ---------- ---------- ---------- ---------- ---------- ----------  369
HisC E.coli          357 ---------- ---------- ---------- ---------- ---------- ----------  357
AAT E.coli           396 ---------- ---------- ---------- ---------- ---------- ----------  396
SanB S.ansochromogenes  505 ARAYRALRSA DARPNWTRED TLAQLRLRTS TPAATMRSLI AGIEAEHGSV ARMLTLHGLR  564

NikK S.tendae        369 ---------- -------- 369
HisC E.coli          357 ---------- -------- 357
AAT E.coli           396 ---------- -------- 396
SanB S.ansochromogenes  565 EETRLRTVVG AFTHPAHL 582
```

62

Supplementary figure S3: Gel filtration chromatogram of NikK. The elution volume of 60 mL corresponds to a molecular weight of 80.6 kDa, indicating that NikK occurs as a dimer in solution.
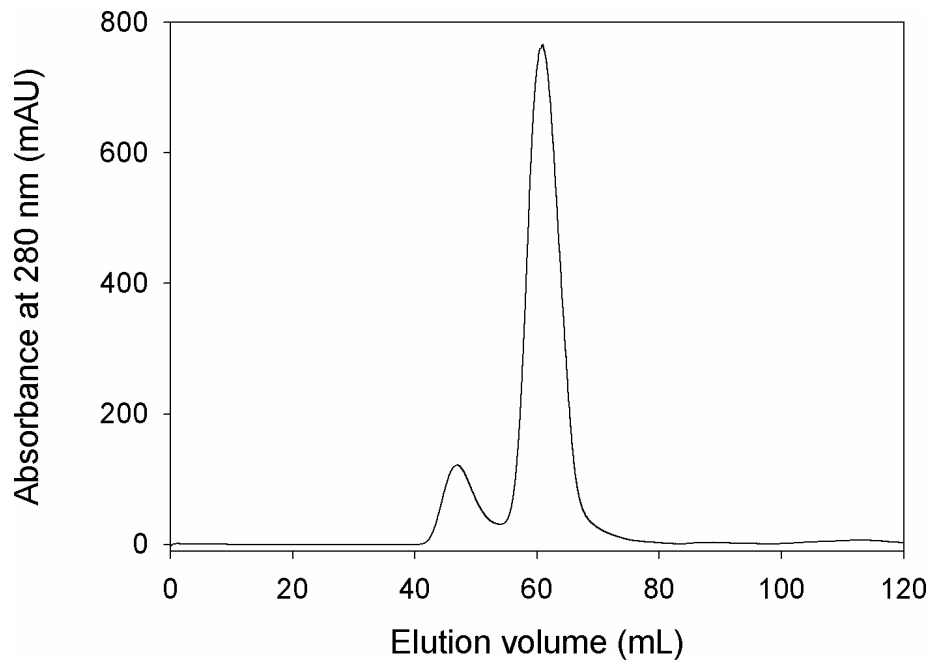
Supplementary figure S4: SDS-Gel of NikK. Lane 1 shows the Low-Molecular-Weight Standard, Lane 2 shows NikK after purification by gel filtration chromatography.
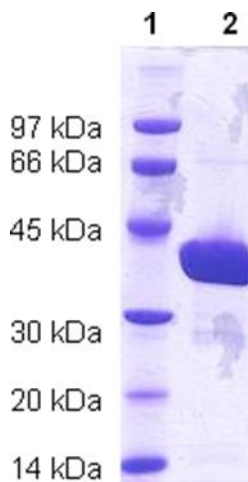
References

1.   Bormann, C., Mattern, S., Schrempf, H., Fiedler, H. P., and Zähner, H. (1989) Isolation of *Streptomyces tendae* mutants with an altered nikkomycin spectrum, J. Antibiot. (Tokyo) 42, 913-918.

2.   Chen, H., Hubbard, B. K., O'Connor, S. E., and Walsh, C. T. (2002) Formation of beta-hydroxy histidine in the biosynthesis of nikkomycin antibiotics, Chem. Biol. 9, 103-112.

3.   Kim, M. K., Park, H. S., Kim, C. H., Park, H. M., and Choi, W. (2002) Inhibitory effect of nikkomycin Z on chitin synthases in *Candida albicans*, Yeast 19, 341-349.

4.   Brillinger, G. U. (1979) Metabolic products of microorganisms. 181. Chitin synthase from fungi, a test model for substances with insecticidal properties, Arch. Microbiol. 121, 71-74.

5.   Hector, R. F. (1993) Compounds active against cell walls of medically important fungi, Clin. Microbiol. Rev. 6, 1-21.

6.   Dähn, U., Hagenmaier, H., Höhne, H., König, W. A., Wolf, G., and Zähner, H. (1976) Stoffwechselprodukte von Mikroorganismen. 154. Mitteilung. Nikkomycin, ein neuer Hemmstoff der Chitinsynthese bei Pilzen, Arch. Microbiol. 107, 143-160.

7.   Decker, H., Zähner, H., Heitsch, H., König, W. A., and Fiedler, H. P. (1991) Structure-activity relationships of the nikkomycins, J. Gen. Microbiol. 137, 1805-1813.

8.   Bruntner, C., Lauer, B., Schwarz, W., Möhrle, V., and Bormann, C. (1999) Molecular characterization of co-transcribed genes from *Streptomyces tendae* Tü901 involved in the biosynthesis of the peptidyl moiety of the peptidyl nucleoside antibiotic nikkomycin, Mol. Gen. Genet. 262, 102-114.

9.   Niu, G., Liu, G., Tian, Y., and Tan, H. (2006) SanJ, an ATP-dependent picolinate-CoA ligase, catalyzes the conversion of picolinate to picolinate-CoA during nikkomycin biosynthesis in *Streptomyces ansochromogenes*, Metab. Eng. 8, 183-195.

10.   Liao, G., Li, J., Li, L., Yang, H., Tian, Y., and Tan, H. (2009) Selectively improving nikkomycin Z production by blocking the imidazolone biosynthetic pathway of nikkomycin X and uracil feeding in *Streptomyces ansochromogenes*, Microb. Cell Fact. 8, 61.

11.   Bormann, C. (2002) Biosynthesis of the peptidyl nucleoside antibiotic nikkomycin in *Streptomyces tendae* Tü901 deduced from the analysis of the gene cluster and mutational studies, in Microbial Secondary Metabolites: Biosynthesis, Genetics and Regulation (Fierro, F. and Martin J.F., Eds.) pp 43-61.

12.   Bruntner, C. and Bormann, C. (1998) The *Streptomyces tendae* Tu901 L-lysine 2-aminotransferase catalyzes the initial reaction in nikkomycin D biosynthesis, Eur. J. Biochem. 254, 347-355.

13.   Bruckner, R. C., Zhao, G., Venci, D., and Jorns, M. S. (2004) Nikkomycin biosynthesis: formation of a 4-electron oxidation product during turnover of NikD with its physiological substrate, Biochemistry 43, 9160-9167.

14.   Ling, H., Wang, G., Tian, Y., Liu, G., and Tan, H. (2007) SanM catalyzes the formation of 4-pyridyl-2-oxo-4-hydroxyisovalerate in nikkomycin biosynthesis by interacting with SanN, Biochem. Biophys. Res. Commun. 361, 196-201.

15.   Ling, H. B., Wang, G. J., Li, J. E., and Tan, H. R. (2008) sanN encoding a dehydrogenase is essential for Nikkomycin biosynthesis in *Streptomyces ansochromogenes*, J. Microbiol. Biotechnol. 18, 397-403.

16.   Jia, L., Tian, Y., and Tan, H. (2007) SanT, a bidomain protein, is essential for nikkomycin biosynthesis of *Streptomyces ansochromogenes*, Biochem. Biophys. Res. Commun. 362, 1031-1036.

17.   Li, Y., Ling, H., Li, W., and Tan, H. (2005) Improvement of nikkomycin production by enhanced copy of sanU and sanV in *Streptomyces ansochromogenes* and

characterization of a novel glutamate mutase encoded by sanU and sanV, Metab. Eng. 7, 165-173.

18.   Ginj, C., Ruegger, H., Amrhein, N., and Macheroux, P. (2005) 3'-Enolpyruvyl-UMP, a novel and unexpected metabolite in nikkomycin biosynthesis, Chembiochem 6, 1974-1976.

19.   Lauer, B., Süssmuth, R., Kaiser, D., Jung, G., and Bormann, C. (2000) A putative enolpyruvyl transferase gene involved in nikkomycin biosynthesis, J. Antibiot. (Tokyo) 53, 385-392.

20.   Reitman, S. and Frankel, S. (1957) A colorimetric method for the determination of serum glutamic oxalacetic and glutamic pyruvic transaminases, Am. J. Clin. Pathol. 28, 56-63.

21.   Vedavathi, M., Girish, K. S., and Kumar, M. K. (2004) Isolation and characterization of cytosolic alanine aminotransferase isoforms from starved rat liver, Mol. Cell Biochem. 267, 13-23.

22.   Dolzan, M., Johansson, K., Roig-Zamboni, V., Campanacci, V., Tegoni, M., Schneider, G., and Cambillau, C. (2004) Crystal structure and reactivity of YbdL from *Escherichia coli* identify a methionine aminotransferase function, FEBS Lett. 571, 141-146.

23.   Krieger, E., Darden, T., Nabuurs, S. B., Finkelstein, A., and Vriend, G. (2004) Making optimal use of empirical energy functions: force-field parameterization in crystal space, Proteins 57, 678-683.

24.   Krieger, E., Joo, K., Lee, J., Lee, J., Raman, S., Thompson, J., Tyka, M., Baker, D., and Karplus, K. (2009) Improving physical realism, stereochemistry, and side-chain accuracy in homology modeling: Four approaches that performed well in CASP8, Proteins-Structure Function and Bioinformatics 77, 114-122.

25.   Sivaraman, J., Li, Y., Larocque, R., Schrag, J. D., Cygler, M., and Matte, A. (2001) Crystal structure of histidinol phosphate aminotransferase (HisC) from *Escherichia coli*, and its covalent complex with pyridoxal-5'-phosphate and l-histidinol phosphate, J. Mol. Biol. 311, 761-776.

26.   Söding, J., Biegert, A., and Lupas, A. N. (2005) The HHpred interactive server for protein homology detection and structure prediction, Nucleic Acids Res. 33, W244-W248.

27.   Söding, J. (2005) Protein homology detection by HMM-HMM comparison, Bioinformatics 21, 951-960.

28.   Sali, A. and Blundell, T. L. (1993) Comparative protein modelling by satisfaction of spatial restraints, J. Mol. Biol. 234, 779-815.

29.   Krieger, E. and Vriend, G. (2002) Models@Home: distributed computing in bioinformatics using a screensaver based approach, Bioinformatics 18, 315-318.

30.   Duan, Y., Wu, C., Chowdhury, S., Lee, M. C., Xiong, G. M., Zhang, W., Yang, R., Cieplak, P., Luo, R., Lee, T., Caldwell, J., Wang, J. M., and Kollman, P. (2003) A point-charge force field for molecular mechanics simulations of proteins based on condensed-phase quantum mechanical calculations, J. Comput. Chem. 24, 1999-2012.

31.   Wang, J., Wolf, R. M., Caldwell, J. W., Kollman, P. A., and Case, D. A. (2004) Development and testing of a general amber force field, J. Comput. Chem. 25, 1157-1174.

32.   Essmann, U., Perera, L., Berkowitz, M. L., Darden, T., Lee, H., and Pedersen, L. G. (1995) A Smooth Particle Mesh Ewald Method, J. Chem. Phys. 103, 8577-8593.

33.   Jorgensen, W. L. and Tirado-Rives, J. (1988) The OPLS Force Field for Proteins. Energy Minimizations for Crystals of Cyclic Peptides and Crambin., J. Am. Chem. Soc. 110, 1657-1666.

34.   Jorgensen, W. L., Maxwell, D. S., and Tirado-Rives, J. (1996) Development and Testing of the OPLS All-Atom Force Field on Conformational Energetics and Properties of Organic Liquids., J. Am. Chem. Soc. 118, 11225-12236.

35.   D. A. Case, T. A. Darden, III., C. L. Simmerling, J. Wang, R. E. Duke, R. Luo, K. M.R. C. Walker, W. Zhang, Merz, D. A. Pearlman, M. Crowley, B. Wang, S. Hayik, A. Roitberg, G. Seabra, K. F. Wong, F. Paesani, X. Wu, S. Brozell, V. Tsui, H. Gohlke, L. Yang, C. Tan, J. Mongan, V. Hornak, G. Cui, P. Beroza, D. H. Mathews,

C. Schafmeister, W. S. Ross, P. A. Kollman (2010) University of California, San Francisco, AMBER 11.

36.   Morris, G. M., Goodsell, D. S., Halliday, R. S., Huey, R., Hart, W. E., Belew, R. K., and Olson, A. J. (1998) Automated Docking Using a Lamarckian Genetic Algorithm and and Empirical Binding Free Energy Function, J. Comput. Chem. 1639-1662.

37.   Zakomirdina, L. N., Kulikova, V. V., Gogoleva, O. I., Dementieva, I. S., Faleev, N. G., and Demidkina, T. V. (2002) Tryptophan indole-lyase from *Proteus vulgaris*: kinetic and spectral properties, Biochemistry (Mosc.) 67, 1189-1196.

38.   Mizuguchi, H., Hayashi, H., Miyahara, I., Hirotsu, K., and Kagamiyama, H. (2003) Characterization of histidinol phosphate aminotransferase from *Escherichia coli*, Biochim. Biophys. Acta 1647, 321-324.

39.   Johnson, G. F., Tu, J. I., Bartlett, M. L., and Graves, D. J. (1970) Physical-chemical studies on the pyridoxal phosphate binding site in sodium borohydride-reduced and native phosphorylase, J. Biol. Chem. 245, 5560-5568.

40.   Schonbeck, N. D., Skalski, M., and Shafer, J. A. (1975) Reactions of pyridoxal 5'-phosphate, 6-aminocaproic acid, cysteine, and penicillamine. Models for reactions of Schiff base linkages in pyridoxal 5'-phosphate-requiring enymes, J. Biol. Chem. 250, 5343-5351.

41.   Derewenda, Z. S. (2004) Rational protein crystallization by mutational surface engineering, Structure 12, 529-535.

42.   Goldschmidt, L., Cooper, D. R., Derewenda, Z. S., and Eisenberg, D. (2007) Toward rational protein crystallization: A Web server for the design of crystallizable protein variants, Protein Sci. 16, 1569-1576.

43.   Haruyama, K., Nakai, T., Miyahara, I., Hirotsu, K., Mizuguchi, H., Hayashi, H., and Kagamiyama, H. (2001) Structures of *Escherichia coli* histidinol-phosphate aminotransferase and its complexes with histidinol-phosphate and N-(5'-phosphopyridoxyl)-L-glutamate: double substrate recognition of the enzyme, Biochemistry 40, 4633-4644.

44.   Jensen, R. A. and Gu, W. (1996) Evolutionary Recruitment of Biochemically Specialized Subdivisions of Family I within the Protein Superfamily of Aminotransferases, J. Bacteriol. 2161.

45.   Cheong, C. G., Escalante-Semerena, J. C., and Rayment, I. (2002) Structural studies of the L-threonine-O-3-phosphate decarboxylase (CobD) enzyme from *Salmonella enterica*: the apo, substrate, and product-aldimine complexes, Biochemistry 41, 9079-9089.

46.   Kirsch, J. F., Eichele, G., Ford, G. C., Vincent, M. G., Jansonius, J. N., Gehring, H., and Christen, P. (1984) Mechanism of action of aspartate aminotransferase proposed on the basis of its spatial structure, J. Mol. Biol. 174, 497-525.

47.   Smith, D. L., Almo, S. C., Toney, M. D., and Ringe, D. (1989) 2.8-A-resolution crystal structure of an active-site mutant of aspartate aminotransferase from *Escherichia coli*, Biochemistry 28, 8161-8167.

48.   Ura, H., Nakai, T., Kawaguchi, S. I., Miyahara, I., Hirotsu, K., and Kuramitsu, S. (2001) Substrate recognition mechanism of thermophilic dual-substrate enzyme, J. Biochem. 130, 89-98.

49.   Mehta, P. K. and Christen, P. (2000) The molecular evolution of pyridoxal-5'-phosphate-dependent enzymes, Adv. Enzymol. Relat. Areas Mol. Biol. 74, 129-184.

50.   Lauer, B., Russwurm, R., and Bormann, C. (2000) Molecular characterization of two genes from *Streptomyces tendae* Tu901 required for the formation of the 4-formyl-4-imidazolin-2-one-containing nucleoside moiety of the peptidyl nucleoside antibiotic nikkomycin, Eur. J. Biochem. 267, 1698-1706.

51.   Venci, D., Zhao, G., and Jorns, M. S. (2002) Molecular characterization of NikD, a new flavoenzyme important in the biosynthesis of nikkomycin antibiotics, Biochemistry 41, 15795-15802.

52.   Hayashi, H., Mizuguchi, H., and Kagamiyama, H. (1998) The imine-pyridine torsion of the pyridoxal 5'-phosphate Schiff base of aspartate aminotransferase lowers its pKa in the unliganded enzyme and is crucial for the successive increase in the pKa during catalysis, Biochemistry 37, 15076-15085.

53.   Mizuguchi, H., Hayashi, H., Okada, K., Miyahara, I., Hirotsu, K., and Kagamiyama, H. (2001) Strain is more important than electrostatic interaction in controlling the pKa of the catalytic group in aspartate aminotransferase, Biochemistry 40, 353-360.

54.   Hosono, A., Mizuguchi, H., Hayashi, H., Goto, M., Miyahara, I., Hirotsu, K., and Kagamiyama, H. (2003) Glutamine:phenylpyruvate aminotransferase from an extremely thermophilic bacterium, *Thermus thermophilus* HB8, J. Biochem. 134, 843-851.

55.   Eliot, A. C. and Kirsch, J. F. (2004) Pyridoxal phosphate enzymes: mechanistic, structural, and evolutionary considerations, Annu. Rev. Biochem. 73, 383-415.

56.   Karsten, W. E., Ohshiro, T., Izumi, Y., and Cook, P. F. (2001) Initial velocity, spectral, and pH studies of the serine-glyoxylate aminotransferase from *Hyphomicrobium methylovorum*, Arch. Biochem. Biophys. 388, 267-275.

57.   Karsten, W. E., Ohshiro, T., Izumi, Y., and Cook, P. F. (2005) Reaction of serine-glyoxylate aminotransferase with the alternative substrate ketomalonate indicates rate-limiting protonation of a quinonoid intermediate, Biochemistry 44, 15930-15936.

58.   Chayen, N. E. (1997) A novel technique to control the rate of vapour diffusion, giving larger protein crystals, J. Appl. Cryst. 30, 198.

CHAPTER 4

4   Expression and characterization of NikL

4.1 Introduction

4.1.1 Protein tyrosine phosphatases

Protein tyrosine phosphatases (PTPs) catalyse the removal of phosphate groups attached to tyrosine residues on proteins via a cysteinyl-phosphate enzyme intermediate. The phosphorylation of protein tyrosine is a common post-translational modification which can create novel recognition motifs for protein interactions and cellular localization. Furthermore, it affects protein stability and regulates enzyme activity. As maintaining an appropriate level of protein tyrosine phosphorylation is essential for many cellular functions, PTPs are key enzymes in signal transduction pathways and cell cycle control and have great importance for the control of cell growth, proliferation, differentiation and transformation (137;138). The hallmark for the superfamily of protein tyrosine phosphatases is the active site sequence C(X)5R, also known as the PTP signature motif (138).

4.1.2 *St*NikL

The NikL enzyme from *Streptomyces tendae* shows sequence similarities to protein tyrosine/serine phosphatases and its sequence contains the C(X)5R motif. In *S. tendae*, NikK and NikL are encoded on two adjacent open reading frames (ORFs). In the *sanB* gene of S. *ansochromogenes*, there is no stop codon between the sequences analogous to the *nikK* and *nikL* genes of *S. ansochromogenes*. SanB is a 63 kDa protein which possesses a putative histidinol-phosphate aminotransferase subunit with 97% sequence identity to NikK (39 kDa) and a putative phosphatase subunit with 94% sequence identity to NikL (26 kDa). Due to the similarity to protein tyrosine phosphatases, it was speculated that NikL catalyses a dephosphorylation reaction, possibly the dephosphorylation of the nikkomycin intermediate 3'-EPUMP to 3'-EP-uridine. To elucidate the role of NikL in the biosynthesis of nikkomycins, attempts were made to express and characterize the enzyme.

4.2 Materials and Methods

4.2.1 Reagents

All chemicals were of highest grade commercially available and purchased from Sigma−Aldrich (St. Louis, MO, USA), Fluka (Buchs, Switzerland), or Merck (Darmstadt, Germany). Alkaline phosphatase from bovine intestinal mucosa was from Sigma-Aldrich (St. Louis, MO, USA). Nickel−nitrilotriacetic acid agarose (Ni−NTA) was from Qiagen (Hilden, Germany), amylose resin from New England Biolabs (Ipswich, MA, USA), Sephadex resin from Pharmacia Biotech AB (Uppsala, Sweden). The rabbit His-probe antibody was from Santa Cruz Biotechnology (Santa Cruz, CA, USA), and the anti-rabbit antibody from Sigma-Aldrich (St. Louis, MO, USA). The enterokinase and the *E. coli* ER2509 strain were from New England Biolabs (Ipswich, MA, USA).

4.2.2 Cloning and expression in *Escherichia coli*

The pJ201 plasmid containing a synthetic gene in *E. coli* codon usage, encoding for a fusion protein of the *S. tendae* NikK and NikL, was ordered from DNA 2.0 (Menlo Park, CA, USA). It was designed according to the corresponding DNA sequence in the database but without a Stop codon after NikK, and with NdeI and XhoI restriction sites for cloning into the pET21a vector. The vector pET21a(*nikK-nikL)* was transformed into *E. coli* BL21(DE3) cells and expression and purification was performed as described for NikK or NikM (6.2.2). The NikK-NikL fusion protein was observed to form aggregates and could not be purified properly, so it was decided to express NikL as a fusion protein with the maltose binding protein (MBP). The described pJ201 plasmid with the *nikK-nikL* fusion gene was used as a template for amplification of the *nikL* gene by PCR, in order to express NikL or create the fusion protein of NikL with MBP. The Phusion™ High Fidelity DNA Polymerase was purchased from Finnzymes (Espoo, Finland), both primers contained a KpnI restriction site and the 5'-primer contained the sequence for an additional hexahistidine tag (5´- ATG GTC CCA GGC CTG CCG AAC GTG C -3´ and 5´- TTA GTG ATG ATG GTG ATG ATG CAG ACG CAC TGG ATG AGT GAA AGC ACC TAC TAC GGT G -3´). The PCR product was cloned into the KpnI restriction site of the pMAL-c4E vector from New England Biolabs (Ipswich, MA, USA). The sequence of the expression plasmid pMAL(*nikL*) was verified by DNA-sequencing (Eurofins DNA, Ebersbach, Germany). This plasmid allows the expression of NikL as a fusion protein with maltose binding protein (MBP)

73

at the N-terminus and with an additional C-terminal hexahistidine tag. A further construct for expression without the hexahistidine tag was generated by site specific mutagenesis, using the QuikChange® XL Site-Directed Mutagenesis Kit from Stratagene (Santa Clara, CA, USA). The mutagenesis primers were designed in a way to substitute the codon for the first histidine residue with a stop codon. Chemically competent *E. coli* ER2508 cells were transformed with the expression plasmid pMAL(*nikL*). Expression of NikL was achieved by growing a 10 mL preculture in Luria-Bertani (LB) medium containing 100 µg/mL ampicillin over night at 37 °C. The preculture was used to inoculate 750 mL LB medium containing 100 µg/mL ampicillin for plasmid selection. The culture was incubated at 37 °C until an OD600 of 0.5 and IPTG was added to a final concentration of 0.1 mM. The culture was incubated for 3 h at 37 °C and cells were harvested by centrifugation. The pellet was washed with 0.9 % NaCl solution and stored at -20 °C.

MBP-NikL was also expressed under concomitant co-overexpression of chaperone proteins. Chemically competent *E. coli* ER2508 cells were transformed with the pG-kJE8 plasmid from Takara (Japan). These cells were made competent and transformed with pMAL(*nikL*). Fermentation was carried out as described for NikK.

4.2.3 Cell disruption and purification

Several strategies for purification of the MBP-NikL fusion protein and the NikL-product of its cleavage by enterokinase were tried: Ni-NTA affinity chromatography, affinity chromatography using an amylose column, and gel filtration as well as combinations of the purification methods.

For purification by Ni-NTA affinity chromatography, the pellet was thawed and resuspended in lysis buffer (100 mM Tris-HCl buffer at pH 8.0, containing 300 mM NaCl and 10 mM imidazole), using 2 mL buffer per gram of wet cells. Cells were disrupted by 30 min incubation with lysozyme and 0.5 s sonication pulses for 10 min while cooling on ice. The cell debris was removed by centrifugation at 18 000 g for 30 min at 4 °C. The supernatant was loaded onto a Ni-NTA column (Qiagen), previously equilibrated with lysis buffer. After loading of the filtered lysate, the column was washed with 10 column volumes of wash buffer (100 mM Tris-HCl, 300 mM NaCl, 20 mM imidazole) and bound protein was recovered with elution buffer (100 mM Tris-HCl, 300 mM NaCl, 150 mM imidazole, pH 8.0). The purity of the eluted 3 mL fractions was determined using SDS-polyacrylamide gel electrophoresis. Fractions

containing the MBP-NikL fusion protein were pooled and concentrated using Amicon® Ultra Centrifugal Filter Units (Millipore, Billerica, MA, USA). The buffer was exchanged to storage buffer (20 mM Tris-HCl, 50 mM NaCl, pH 8.0) using a PD-10 column (GE Healthcare) and the protein solution was stored at 4 °C.

Purification using the affinity of the MBP to the amylose column was performed at 4 °C. The cell pellet was thawed and resuspended in column buffer (20 mM Tris-HCl, 200 mM NaCl, 1 mM EDTA, pH 7.4), using 7.5 mL buffer per gram of wet cells. Cells were disrupted by 30 min incubation with lysozyme and 0.5 s sonication pulses for 10 min while cooling on ice. The cell debris was removed by centrifugation at 18 000 g for 30 min at 4 °C, and the filtered lysate was loaded to the amylose column, which was previously equilibrated with 8 bed volumes of column buffer. The column was washed with 12 bed volumes of column buffer, and the fusion protein was eluted with 3 bed volumes of elution buffer (20 mM Tris-HCl, 200 mM NaCl, 1 mM EDTA, 10 mM maltose, pH 7.4). The purity of the eluted 3 mL fractions was determined using SDS-polyacrylamide gel electrophoresis. Fractions containing the MBP-NikL fusion protein were pooled and concentrated using Amicon® Ultra Centrifugal Filter Units (Millipore, Billerica, MA, USA). The buffer was exchanged to storage buffer (20 mM Tris-HCl, 50 mM NaCl, pH 8.0) using a PD-10 column (GE Healthcare) and the protein solution was stored at 4 °C.

To combine both purification methods, the protein solution resulting after Ni-NTA affinity chromatography was diluted with an excess of column buffer (20 mM Tris-HCl, 200 mM NaCl, 1 mM EDTA, pH 7.4) and applied to the amylose column, or, the protein solution resulting from purification by the amylose column was diluted with an excess of lysis buffer (100 mM Tris-HCl buffer at pH 8.0, containing 300 mM NaCl and 10 mM imidazole) and applied to the Ni-NTA column. Further steps of washing and elution were carried out as described for the respective column. To verify the presence of the intact MBP-NikL fusion protein, MALDI-time of flight MS measurements with a Micro MX (Waters, Milford, MA, USA) instrument and Western Blots using antibodies against the hexahistidine tag were performed.

After affinity chromatography, the fusion protein was further purified by gel filtration chromatography, using a HiLoad 16/60 Superdex™ 200 prep grade column (Pharmacia Biotech AB, Uppsala, Sweden) which was mounted on a fast protein liquid

chromatography (FPLC) system (ÄKTA Explorer, Pharmacia Biotech AB). The column was equilibrated with 20 mM Tris-HCl buffer at pH 8.0, containing 50 mM NaCl.

4.2.4 Cleavage of the fusion protein

To assess the best conditions for enzymatic cleavage of MBP-NikL by enterokinase, several tests were performed, following the instruction manual for the pMAL™ Protein Fusion and Purification System from New England Biolabs. The reaction mix contained about 1 mg/mL fusion protein in 20 mM Tris-HCl at pH 8.0, 50 mM NaCl, 2 mM $CaCl_2$, 0.2 ng/L enterokinase and varying concentrations of SDS (0-0.05%) and was incubated for varying time periods (1h to overnight) at room temperature. Cleavage was monitored by SDS-PAGE and Western Blot using antibodies against the hexahistidine tag. After cleavage, the reaction mix was applied to the amylose column to remove MBP contents.

4.2.5 Testing 3'-EPUMP as a potential substrate for NikL

Solutions of the MBP-NikL fusion protein after purification by each of the methods described above and of the fusion protein after treatment with enterokinase were incubated for varying time periods (30 min to overnight) with varying concentrations of 3'-EPUMP (0.1 mM to 5 mM) under various conditions (pH 6.5 to 8.5; 20 to 30 °C; presence of 0-10 mM $MgCl_2$ and 0-10 mM $CaCl_2$). The samples were diluted with 0.05% trifluoroacetic acid and analysed by RP-HPLC, using an Atlantis dC18 column (Waters, Dublin, Ireland), mounted on an UltiMate 3000 HPLC system (Dionex, Germering, Germany). The elution was carried out by applying a linear gradient of 0.05% trifluoroacetic acid to acetonitrile in 25 min, using a flow rate of 1 mL/min.

Furthermore, we tried to test the MBP-NikL fusion protein for phosphatase activity, using *p*-nitrophenylphosphate as model substrate. The assay contained 1 mM *p*-nitrophenylphosphate, 50 mM $MgCl_2$ and 2 μM enzyme in 100 mM Tris-HCl (pH 8.0). After incubation for 60 min and 165 min, 0.1 M NaOH was added and the absorbance at 405 nm was measured. A reference without enzyme was also prepared and measured.

4.2.6 Dephosphorylation of 3'-EPUMP by alkaline phosphatase

The reaction mix contained 5 mM 3'-EPUMP, 0.2 mg/mL alkaline phosphatase and 100 mM Tris-HCl, pH 9.0. After incubation for 2 h at 20 °C, HPLC measurements were carried out as described above.

4.3 Results

Expression of a NikK-NikL fusion protein was successful but resulted in aggregates which could not be purified. The MBP-NikL fusion protein could be expressed in *E. coli* and its cleavage by enterokinase worked, as could be observed on SDS-gels. The expression of the whole *nikL* gene sequence with C-terminal hexahistidine tag was confirmed by Western Blots, using anti-His$_6$ antibodies. Gel filtration experiments resulted in a molecular weight of over 200 kDa, the whole protein eluted within the exclusion volume of the column. The protein preparation could not be separated from an unidentified protein of about 60 kDa, not even after enterokinase cleavage. Expression and purification of the variant of MBP-NikL without hexahistidine tag also resulted in soluble aggregates, and co-overexpression of chaperones did not alter these results.
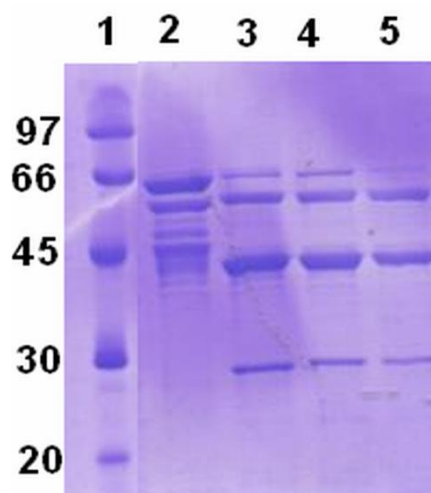
Figure 8: SDS Gel of MPB-NikL and enterokinase cuts. The molecular weight of NikL is 26 kDa, of MBP it is 42 kDa. Lane 1: LMW Standards, molecular weights are given in kDa; lane 2: MBP-NikL after elution from the amylose column; lanes 3-5: MBP-NikL solution after treatment with enterokinase, in the presence of 0.005, 0.01, and 0.02% SDS.

3´-EPUMP was not converted by amylose-column purified MBP-NikL, neither with nor without treatment with enterokinase. Incubation of 3´-EPUMP with MBP-NikL purified by Ni-NTA affinity chromatography resulted in a change in the HPLC elution profile. The new peak had the same retention time as the peak that emerges after treatment of 3´-EPUMP with alkaline phosphatase. The observed reaction was very slow and conversion was not completed after 15 hours.

Incubation of 3'-EPUMP with alkaline phosphatase led to conversion to 3'-EP-uridine (see Figure 9).

Phosphatase activity of the enzyme preparations using *p*-nitrophenylphosphate as model substrate was not observed.
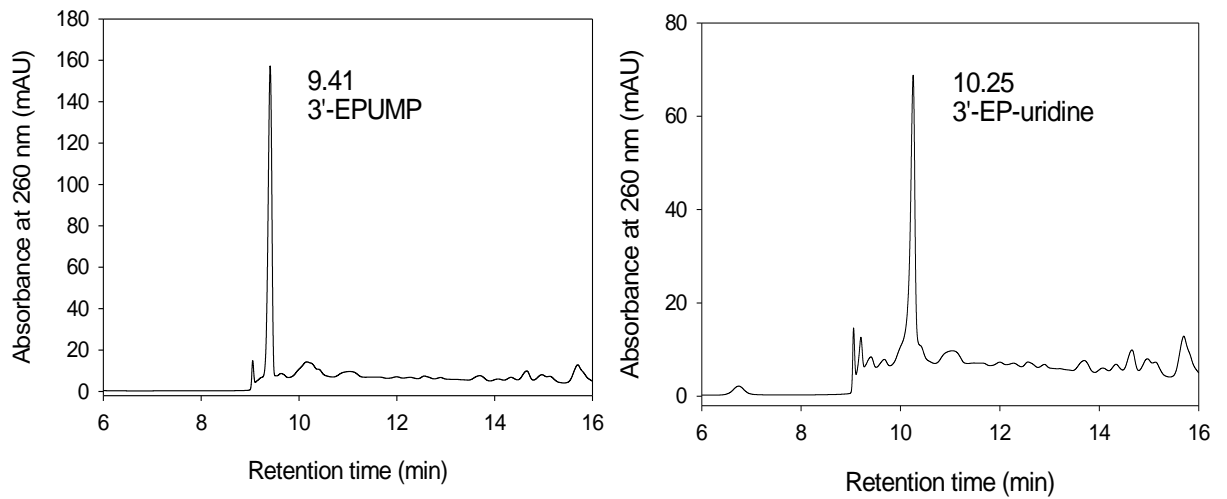
Figure 9: HPLC elution profiles of 3'-EPUMP before (left) and after 2 h of incubation with alkaline phosphatase (right panel).

4.4 Discussion

The enzyme encoded by the *nikL* gene shows sequence similarity to protein tyrosine phosphatases. Therefore it is expected to catalyze a dephosphorylation reaction. If the phosphate group in 5´-position is released by a phosphatase acting downstream to NikO, there is still the question whether this phosphate cleavage would occur before or after skeleton rearrangement. If the former is the case, 3´-EPUMP might be the substrate of NikL.
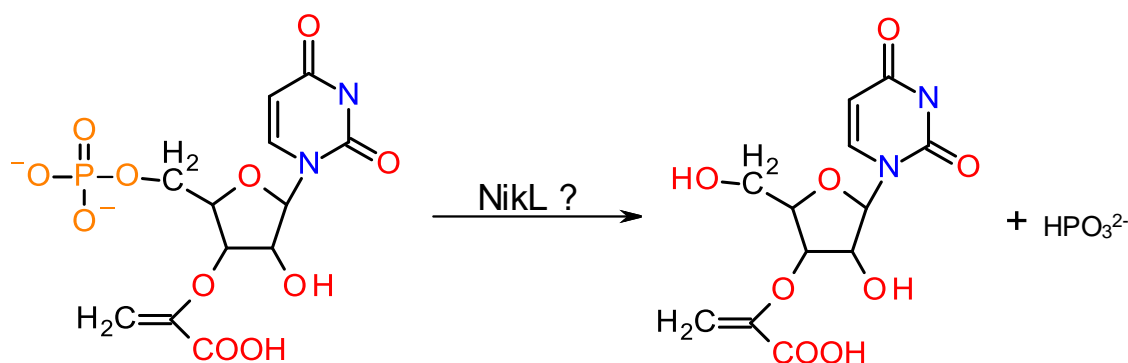
Scheme 11: Hypothetic role of NikL in nikkomycin biosynthesis: the dephosphorylation of 3'-EPUMP.

As previous attempts to express the *nikL* gene heterologously in *Escherichia coli* and *Pichia pastoris* failed, we tried expression of hexahistidine tagged NikL as a fusion protein with the maltose binding protein (MBP). A construct of the gene encoding for MBP and *nikL* in *E. coli* codon usage could be expressed but purification turned out to be difficult. The fusion protein was observed to form aggregates which included an unidentified protein. NikL, after cleavage with enterokinase, could not be separated from those aggregates, and expression without the hexahistidine tag did not make a difference in the formation of aggregates. Hoping that at least a small amount of active NikL might be present in the enzyme preparation, we carried out several experiments, testing 3´-EPUMP as substrate. No conversion was observed using MBP-NikL purified with an amylose column, not even after cleavage with enterokinase. Neither did the enzyme show phosphatase activity with the model substrate *p*-nitrophenylphosphate. The enzyme preparation resulting from the purification by Ni-NTA affinity chromatography was shown to slowly dephosphorylate 3´-EPUMP. As this purification method results in a solution that is significantly contaminated by *E. coli* proteins, we assume that the observed phosphatase activity derives from other enzymes than NikL.

Apparently, 3´-EPUMP is readily dephosphorylated by ubiquitous phosphatases in the cytoplasm. This raises the question whether dephosphorylation of 3´-EPUMP is catalyzed by enzymes present in the *S. tendae* cell which are not encoded within the *nik* gene cluster. This would be rather unusual, as in *Streptomyces* spp. transcription and translation of enzymes involved in the biosynthesis of secondary metabolites are tightly coupled and the clustering of genes is important for proper timing of expression (77;78).

The sequence of the SanB enzyme of *S. ansochromogenes* is highly identical to a NikK-NikL fusion protein. Considering this, it might also be possible that NikL plays a part in regulation or stabilization of NikK and does not directly catalyze a step in the biosynthetic pathway. Conclusively, it has to be stated that the role of NikL in the nikkomycin biosynthetic pathway remains completely undissolved.

CHAPTER 5

5   Expression and characterization of the iron-sulfur protein NikJ

5.1 Introduction

5.1.1 Iron-sulfur proteins: properties and structures of iron-sulfur clusters

Presumably, iron-sulfur proteins were among the first catalysts in nature. In the days of anaerobic life at high temperature in volcanic vents, iron and sulphur must have been of great importance, as they belong to the chemically most versatile elements. Due to their versatility, their ready assembly, and their function as compact redox catalysts in the range of low potentials, they still show a unique usefulness (139).

Iron-sulfur proteins, which are present in all three domains of life, are characterized by the presence of iron-sulfur clusters, which contain sulfide-linked di-, tri-, and tetrairon centers which occur in variable oxidation states (140). The simplest polymetallic system is the $[Fe_2S_2]$ cluster, which is constituted by two iron ions bridged by two sulphide ions. It can be coordinated by four cysteinyl ligands or by two cysteines and two histidines, and exists in two oxidation states, $(Fe^{III})_2$ and $Fe^{III}Fe^{II}$. The $[Fe_4S_4]$ cluster, which is the most frequently encountered cluster, features four iron ions and four sulphide ions which are placed at the vertices of a cubane-type structure (Figure 10). Cysteinyl ligands usually further coordinate its Fe centers. The $[Fe_3S_4]$ cluster, which is found more rarely in nature, is a variant of the $[Fe_4S_4]$ cluster. Each of three sulphide ions bridges two iron ions, while three iron ions are bridged by a fourth sulphide bridge. In a number of iron-sulfur proteins, the $[Fe_4S_4]$ cluster can be reversible converted to the $[Fe_3S_4]$ cluster by oxidation and loss of Fe (139).
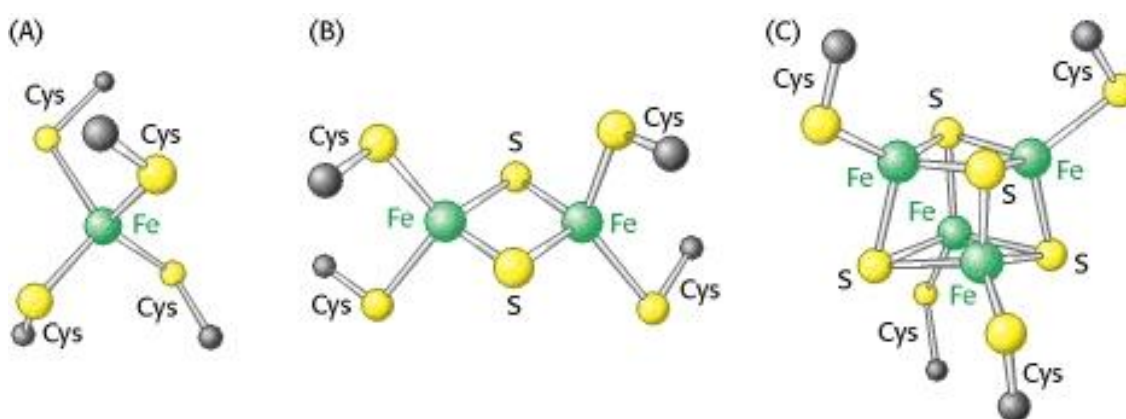
Figure 10: Iron-sulfur clusters. (A) A single iron ion bound by four cysteine residues. (B) 2Fe-2S cluster with iron ions bridged by sulfide ions. (C) 4Fe-4S cluster. (Figure taken from http://www.ncbi.nlm.nih.gov/books/NBK22505/)

More complex iron-sulfur clusters are also common. In some cases, a $[Fe_4S_3]$ fragment serves as a building block for more complicated clusters. A famous example is the MoFe cluster of nitrogenase, where two $[Me_4S_3]$ fragments are linked by sulphides, and the P-cluster of the same enzyme, where two $[Fe_4S_3]$ modules are linked by cysteines (141). In Fe-only hydrogenases, several clusters are involved which are placed along a protein scaffold to provide a pathway for electron transfer (142).

5.1.2   Functions of iron-sulfur clusters

Electron transfer is the most obvious function of iron-sulfur clusters, considering that the redox potentials of Fe-S proteins span a remarkable range. In the mitochondrial electron-transfer chain there are altogether more than ten Fe-S clusters. One of the biggest multi-Fe-S proteins known is mammalian NADH dehydrogenase, and the electron carrier before ubiquinone always is a Fe-S flavoprotein (139).

Fe-S enzymes also play important roles in redox and nonredox catalysis. For instance, the unliganded iron of the $[Fe_4S_4]$ cluster in the active site of aconitase serves as a Lewis acid in catalyzing the abstraction of hydroxyl and a proton from the substrate. These are reattached with their positions inverted (143). This is how the citric acid cycle enzyme aconitase catalyses the stereospecific isomerisation of citrate to isocitrate, via *cis*-aconitate (144).

$[Fe_4S_4]$ clusters are also widely used as primary electron donors in the initiation of reactions that occur by a free radical mechanism, involving S-adenosylmethionine (145). The so-called radical SAM superfamily is described in section 5.1.4.

Fe-S clusters can assume different oxidation states and are vulnerable toward oxidative destruction, which allows their use by nature in sensing and signalling reactions (139). In the SoxR/SoxS system of *E. coli*, for example, the oxidation state of the $[Fe_2S_2]$ cluster serves as a trigger to the response to the O_2^- radical. In the 1+ state of the cluster, SoxR is inactive. In the presence of O_2^-, it becomes oxidized to the 2+ state, triggering a complex stress response, resulting in the biosynthesis of protective proteins (146). In some cases, the Fe-S clusters are destroyed in the sensing act to produce the signal for response. For example, cytoplasmic aconitase acquires the ability to bind so-called iron-responsive elements on RNA only upon loss of the cluster (147;148).

5.1.3 Iron-sulfur cluster biosynthesis

The cellular process of iron-sulfur cluster biosynthesis depends on complex protein machineries (149;150). It is essential to almost all forms of life and is remarkably conserved in prokaryotes and eukaryotes. In bacteria, three distinct types of iron-sulfur cluster machinery have been established, the NIF, ISC and SUF systems (Figure 11). In each case the overall mechanism involves the assembly of transient clusters on scaffold proteins, mediated by cysteine desulfurase (NifS, IscS, SufS), and the subsequent transfer of the clusters to the apoproteins.
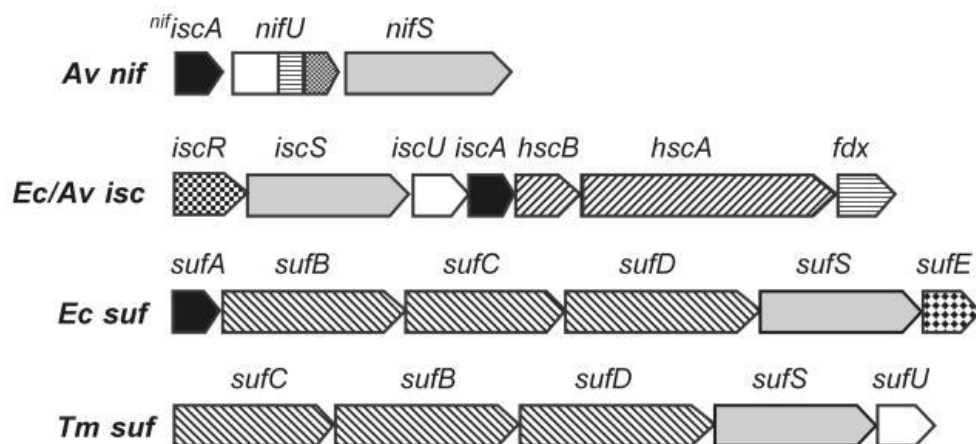
Figure 11: Organization of genes in selected bacterial nif, isc, and suf operons (*Av,Azotobacter vinelandii; Ec, Escherichia coli; Tm, Thermotoga maritima*). Figure taken from Bandyopadhyay *et al* (149).

The ISC system is the primary system for Fe-S biosynthesis in bacteria (151;152). With a few additional components, the ISC systems constitutes the Fe-S biosynthetic machinery in the mitochondria of eukaryotic cells, which supports the hypothesis that the mitochondrial ISC system was inherited from the bacterial endosymbiotic ancestor of the organelle (153;154).

The NIF system is specific for iron-sulfur cluster assembly in nitrogen fixing organisms such as *Azotobacter vinelandii* (152).

The SUF system plays a similar general role in many bacteria as the ISC system, but works only under conditions of iron starvation or oxidative stress (150;155). The bacterial SUF system also forms the basis for the iron-sulfur cluster assembly machinery in plant chloroplasts (153) and apparently is the sole system for Fe-S cluster biogenesis in archea and cyanobacteria.

All three Fe-S cluster assembly systems involve a cysteine desulfurase (NifS, IscS, SufS), which is a homodimeric, pyridoxal phosphate-dependent enzyme that catalyzes the conversion of L-cysteine to L-alanine and an enzyme-bound cysteine persulfide (156) which can transfer S^0 directly, or via the SufE sulphur transferase (150) to the active site of scaffold proteins (157;158). At least one type of potential scaffold protein (NifU, IscU, SufU, ^{Nif}IscA, IscA, SufA) capable of assembling both $[Fe_2S_2]^{2+}$ and $[Fe_4S_4]^{2+}$ clusters forms part of each machinery (159-162). It is not fully known which is the immediate iron donor for cluster assembly, but frataxin and its bacterial homolog CyaY were discussed to play the role as iron donors for U-type scaffold proteins (154;163). After cysteine desulfurase-mediated assembly of transient $[Fe_2S_2]^{2+}$ and $[Fe_4S_4]^{2+}$ clusters on scaffold proteins, preformed clusters are transferred to the apo froms of acceptor proteins (159;162). In addition to sulphur donor, sulphur transfer and scaffold proteins, other proteins encoded in the ISC, NIF, and SUF systems play roles in transcriptional regulation and energy production (150).

5.1.4   The radical SAM superfamily

Enzymes of the radical SAM superfamily function by a mechanism in which S-adenosylmethionine (SAM) serves as an oxidizing agent in DNA repair and the biosynthesis of vitamins, coenzymes and antibiotics. Radical SAM superfamily members are involved in highly diverse biochemical processes in animals, plants and microbes. They contain the cysteine motif CxxxCxxC, which nucleates a $[Fe_4S_4]$ cluster. By the use of a strong reducing agent, namely the low potential $[Fe_4S_4]^{1+}$ cluster, a powerful oxidizing agent is generated from SAM: the 5´-deoxyadenosyl radical (145). The $[Fe_4S_4]$ clusters in the group of radical SAM enzymes are unique in that they are formed with three cysteinyl ligands to iron while the ligands to the fourth iron originate with SAM (164-170). The radical SAM enzymes are mechanistically related to the family of adenosylcobalamine-dependent enzymes, but they use SAM as a source of the 5´-deoxyadenosyl radical and are much more numerous and diverse in function. Controlled cleavage of unreactive C-H bonds in alkyl groups represents one of the most chemically difficult reactions in enzymology. The reactions of radical SAM enzymes are chemically diverse but their mechanisms all involve the reductive cleavage of SAM to the deoxyadenosyl radical (145).

5.1.5 The chemical diversity of radical SAM enzymes and the role of SAM

The first radical enzymes described was lysine-2,3-aminomutase (LAM) (Figure 12a), which converts L-lysine to L-β-lysine in antibiotic biosynthesis (171). In LAM and spore photoproduct lyase (Figure 12b), an enzyme which is involved in bacterial DNA repair, SAM serves as a reversible source of the 5´-deoxyadenosyl radical. After mediating hydrogen transfer, the 5´-deoxyadenosyl radical is regenerated and reverts to SAM. In these enzymes, SAM works as a coenzyme and is not consumed (145).

In other enzymes, SAM does not function catalytically, but as a substrate that undergoes reductive cleavage to methionine and 5-deoxyadenosine, generating a stable glycyl radical at in the active site of the enzyme. This is the case for pyruvate formate lyase (PFL) activase (Figure 12c), an enzyme that stimulates the reaction of PFL (pyruvate + CoA $\rightarrow$ formate + acetyl-CoA) (172), and for ribonucleoside triphosphate reductase (ARR) (Figure 12d), whose activase subunit generates a glycyl radical in the catalytic subunit (173;174).

The last step of biotin synthesis, as well as of lipoic acid biosynthesis, consists of the insertion of sulphur into unactivated C-H bonds. To generate the thiophane ring of biotin, a sulphur atom is inserted into two C-H bonds by biotin synthase (BioB) in a SAM-dependent reaction (Figure 12e) that leads to the production of methionine and 5´-deoxyadenosine (173;174). Lipoic acid results from the insertion of two sulphur atoms into C-H bonds of its precursor, which is catalysed by LipA (Figure 12f) (173;174). BioB and LipA also use SAM as an oxidizing substrate and source of the 5´-deoxyadenosyl radical, but, unlike PFL and ARR activases, they do not generate stable radicals (145).
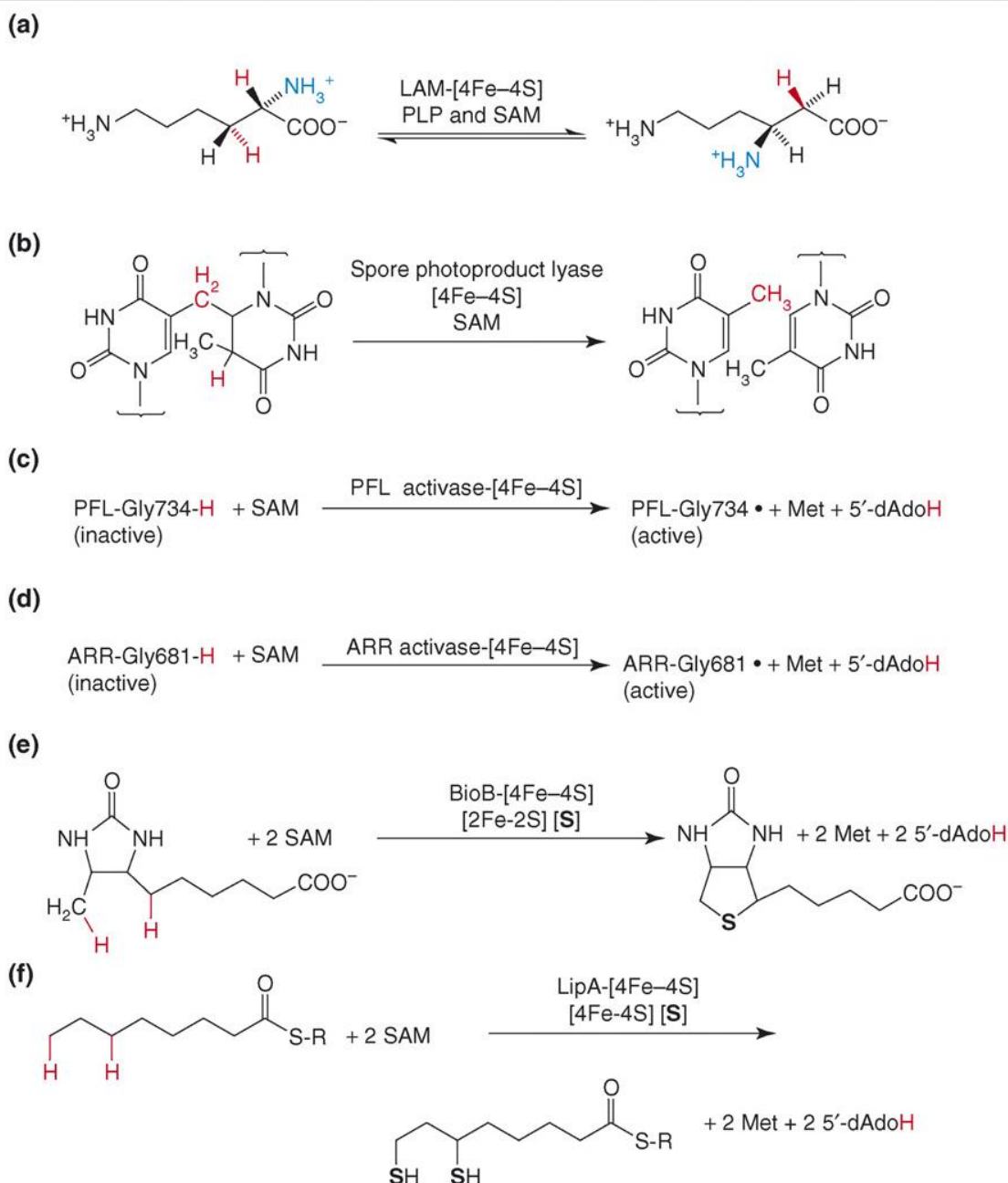
Figure 12: Reactions catalyzed by several well studied radical SAM enzymes. (a) lysine-2,3-aminomutase, (b) spore photoproduct lyase, (c) pyruvate formate-lyase activase, (d) ribonucleoside triphosphate reductase activase, (e) biotin synthase, (f) lipoyl synthase. Figure adapted from Wang and Frey, 2007 (145).

5.2 Materials and Methods

5.2.1 Reagents

All chemicals were of highest grade commercially available and purchased from Sigma−Aldrich (St. Louis, MO, USA), Fluka (Buchs, Switzerland), or Merck (Darmstadt, Germany). Nickel−nitrilotriacetic acid agarose (Ni−NTA) was from Qiagen (Hilden, Germany), *Strep*-Tactin® resin from IBA BioTAGnology (Göttingen, Germany), Sephadex, Q Sepharose and phenylsepharose resin from Pharmacia Biotech AB/GE Healthcare (Uppsala, Sweden).

5.2.2 Cloning and expression in *Escherichia coli*

Streptomyces tendae Tü901/8c was grown in 250 mL LB-Medium at 30 °C for six days. Genomic DNA was isolated using the Illustra™ bacteria genomic Prep Mini Spin Kit from GE Healthcare (Buckinghamshire, UK) and used as a template for PCR using Phusion™ High Fidelity DNA Polymerase from Finnzymes (Espoo, Finland). The PCR products contained an *NdeI* restriction site at the 5'-end and a *XhoI* restriction site at the 3'-end, and were cloned into the *NdeI/XhoI* restriction sites of the pET21a vector (Novagen), generating the expression plasmid pET21a(*nikJ*). The *nikJ* gene was designed without a stop codon, which allows expression of the protein with a C-terminal hexahistidine tag. To express NikJ with a *Strep* tag, the expression plasmid pET21a(*nikJ*^Strep^) was generated, using pET21a(*nikJ*) as a template. The 5'-primer encoded the *Strep* tag (5´ -ccg ctc gag cgg tca ttt ttc gaa ctg cgg gtg gct cca agc gct tgc cgg gcg cag ggc c- 3´). The PCR products also contained an *NdeI* restriction site at the 5'-end and an *XhoI* restriction site at the 3'-end, and were cloned into the *NdeI/XhoI* restriction sites of the pET21a vector. The sequence on each expression plasmid was verified by DNA-sequencing (Eurofins DNA, Ebersbach, Germany).

Chemically competent *E. coli* BL21(DE3) cells were transformed with a plasmid containing the *isc* cluster from *E. coli* and a gene for chloramphenicol resistance, which we obtained from Tobias Gräwert from TU Munich (175). These transformants were made competent and transformed with pET21a(*nikJ*) and pET21a(*nikJ*^Strep^). Expression of NikJ with either a hexahistidine, or a *Strep* tag, was achieved by growing a 10 mL preculture in Luria-Bertani (LB) medium containing 100 µg/mL ampicillin and 25 µg/mL chloramphenicol over night at 37 °C. The preculture was used to inoculate 500 mL TB medium (12 g/L peptone, 24 g/L yeast extract, 2.3 g/L KH_2PO_4, 12.5 g/L

K$_2$HPO$_4$, 4 mL/L glycerol, 1 mM L-cysteine, 30 mg/L ammonium iron(III)citrate), containing 100 μg/mL ampicillin and 25 μg/mL chloramphenicol for plasmid selection. The culture was incubated at 37 °C for 2 h, and IPTG was added to a final concentration of 1 mM. The culture was incubated overnight at 30 °C and cells were harvested by centrifugation. The pellet was washed with 0.9 % NaCl solution and stored at -20 °C.

5.2.3   Cell disruption and centrifugation

The cell pellet containing His-tagged NikJ was thawed and resuspended in lysis buffer (100 mM Tris-HCl buffer at pH 8.0, 300 mM NaCl and 10 mM imidazole), the pellet after expression of *Strep*-tagged NikJ (NikJ^{Strep}) was thawed and resuspended in buffer W (100 mM Tris-HCl, pH 8.0, 150 mM NaCl) using 2 mL buffer per gram of wet cells. Cells were disrupted by 30 min incubation with lysozyme and 0.5 s sonication pulses for 10 min while cooling on ice. The cell debris was removed by centrifugation at 18,000 g for 30 min at 4 °C. In several attempts to purify NikJ^{Strep} under the exclusion of oxygen, the suspension of pellet in buffer W was prepared in a glove box filled with N$_2$, 0.5 mg/mL lysozyme and 1 mM PMSF were added, and the mixture underwent freezing at -20°C and thawing at room temperature in a tightly closed Oak Ridge Centrifuge Tube (Nalgene, Rochester, NY, USA). Triton X-100 was added to a final concentration of 0.5% and after 30 min shaking at room temperature, it was centrifugated at 18 000 g for 30 min at 4 °C and transferred back into the glove box for purification.

5.2.4   Purification by Ni-NTA affinity chromatography

The hexahistidine-tagged NikJ enzyme was purified by Ni-NTA affinity chromatography, loading the respective supernatant onto a Ni-NTA column (Qiagen), previously equilibrated with lysis buffer. After loading of the filtered lysate, the column was washed with 10 column volumes of wash buffer (100 mM Tris-HCl, 300 mM NaCl, 20 mM imidazole, pH 8.0 and bound protein was recovered with elution buffer (100 mM Tris-HCl, 300 mM NaCl, 150 mM imidazole, pH 8.0). The purity of the eluted 3 mL fractions was determined using SDS-polyacrylamide gel electrophoresis. Fractions containing NikJ were pooled and concentrated using Amicon$^®$ Ultra Centrifugal Filter Units (Millipore, Billerica, MA, USA).

After purification, the buffer was exchanged to 100 mM Tris buffer (pH 7.5) using a PD-10 column (GE Healthcare) and the solution of the protein was stored at -20 °C. When intended for crystallization, NikJ was further purified by gel filtration

chromatography, using a Hi Load™ 16/60 Superdex 200 prep grade column (Pharmacia Biotech AB) which was mounted on a fast protein liquid chromatography (FPLC) system (ÄKTA Explorer, Pharmacia Biotech AB, Uppsala, Sweden). The column was equilibrated with 50 mM Tris-HCl buffer at pH 7.5.

5.2.5   Purification by the *Strep*-tag purification system

Several attempts were made to purify NikJ using the *Strep*-tag® Purification Protocol (IBA BioTAGnology, Göttingen, Germany). The purification and buffer exchange was initially performed without oxygen exclusion, then with the use of an AtmosBag™ (Sigma-Aldrich) which was filled with N_2, and finally under anoxic conditions in a glove box. With the help of the Strep-Tactin® Column Evaluation Set from IBA BioTAGnology (Göttingen, Germany), a Strep-Tactin® Superflow® Gravity flow column (5 mL) was chosen for purification of NikJ. All chromatographic steps were performed according to the *Strep*-tag® Purification Protocol from IBA BioTAGnology, using buffers without EDTA. The purity of the eluted protein was checked by SDS-PAGE. After purification, the buffer was exchanged to 100 mM Tris buffer (pH 7.5) using a PD-10 column (GE Healthcare).

5.2.6   Determination of the oligomerization state by gel filtration and Native PAGE

NikJ, which was purified by Ni-NTA affinity chromatography, was loaded onto a Hi Load™ 16/60 Superdex 200 prep grade column (Pharmacia Biotech AB) which was mounted on a fast protein liquid chromatography (FPLC) system (ÄKTA Explorer, Pharmacia Biotech AB). The column was equilibrated with 50 mM Tris-HCl buffer at pH 7.5. Elution of the protein was monitored by measuring the absorbance at 280 and 450 nm.

Native PAGE was performed according to the Mini-PROTEAN®3 Cell (Bio-Rad, Hercules, CA, USA) instruction manual for SDS-PAGE, without the addition of SDS. A 12.5% separating gel was used, and the buffer for the 5% stacking gel had a pH of 8.8. 30 µg of protein were applied to each lane, and the gels were run at 90 V and 4 °C for three hours.

5.2.7   Expression and purification of NifS

The plasmid encoding the scaffold protein for iron-sulfur cluster biosynthesis from *Azotobacter vinelandii*, NifS, was a gift from Dennis Dean (Virginia Polytech Institute,

USA). It was transformed into chemically competent *E. coli* BL31(DE3) cells. Expression of NifS was achieved by growing a 10 mL preculture in Luria-Bertani (LB) medium containing 100 µg/mL ampicillin over night at 37 °C. The preculture was used to inoculate 500 mL LB medium containing 100 µg/mL ampicillin for plasmid selection and 1 mM pyridoxine for incorporation of the PLP cofactor. The culture was incubated at 37 °C until an OD600 of 0.5 was reached and lactose was added to a final concentration of 10 g/L. The culture was further incubated for 3 h at 30 °C and cells were harvested by centrifugation. The pellet was washed with 0.9 % NaCl solution and stored at -20 °C.

The pellet was thawed and resuspended in 100 mM Tris-HCl buffer (pH 7.5) using 3 mL buffer per gram of wet cells. Cells were disrupted by 0.5 s sonication pulses for 10 min while cooling on ice. The cell debris was removed by centrifugation at 18,000 g for 30 min at 4 °C. The supernatant was subjected to 25-45% ammonium sulphate cuts. After precipitation, the protein pellet was dissolved in 100 mM Tris-HCl buffer (pH 7.5) and applied to a HiLoad™ 16/10 Q Sepharose$^®$ High Performance column (GE Healthcare, Uppsala, Sweden), previously equilibrated with 20 mM Tris-HCl (pH 7.5). Bound NifS was eluted using a gradient (0-0.6 M NaCl in 30 min, at a flow rate of 3 mL/min). Fractions containing NifS were pooled, concentrated using Amicon$^®$ Ultra Centrifugal Filter Units (Millipore, Billerica, MA, USA) and applied to a Phenyl Sepharose6$^®$ Fast Flow XK26/20 column (GE Healthcare, Uppsala, Sweden), previously equilibrated with 20 mM Tris-HCl (pH 7.5), containing 0.5 M $(NH_4)_2SO_4$. Bound NifS was eluted using a gradient (0.5-0 M $(NH_4)_2SO_4$ in 30 min, at a flow rate of 3 mL/min). Fractions containing NifS were pooled, concentrated using Amicon$^®$ Ultra Centrifugal Filter Units (Millipore, Billerica, MA, USA), and stored at -20 °C.

5.2.8   Purification in the presence of S-adenosylhomocysteine

In an attempt to stabilize Fe-S clusters during purification by Ni-NTA affinity chromatography as well as purification by the *Strep*-tag$^®$ system, chromatography was performed with supplying S-adenosylhomocysteine to all buffers involved in purification (1 mM end concentration).

5.2.9   Fe-S cluster reconstitution

Reconstitution of Fe-S clusters of NikJ was performed in the N_2 atmosphere of a glove box, using a method described in the literature (176;177). Stock solutions of all components of the reaction mixture were made oxygen-free by flushing with N_2. The

reaction mixture, which was prepared in 50 mM Tris-HCl buffer at pH 7.6, contained 0.2 mM $(NH_4)_2Fe(SO_4)_2$, 1 mM L-cysteine, 2.5 mM DTT, 50 mM KCl, 0.4 μM NifS and 40 μM NikJ[Strep] (freshly purified under anoxic conditions). To monitor the progress of reconstitution, the reaction mix was filled in a quartz cuvette which was tightly closed with a plug and parafilm and UV-vis spectra were taken with a Specord 205 spectrophotometer (Analytic Jena, Germany). After reconstitution and incubation for 30 min, 2.5 mL of the reaction mix were applied onto a PD-10 desalting column (GE Healthcare, Uppsala, Sweden) to provide freshly reconstituted NikJ in Tris-HCl buffer (pH 7.5).

5.2.10 Determination of the Fe content of NikJ

The protein concentration of the samples was determined according to the Bio Rad Protein Assay previous to iron analysis. Two samples of NikJ which was purified by Ni-NTA affinity chromatography and gel filtration were sent to a facility specialized in chemical analysis (Spurenanalytisches Labor Dr. Baumann, Pirkensee, Germany) for determination of their iron content. Later, we analysed NikJ samples for iron in our own lab, using the method described by W.W. Fish (178). Several samples of NikJ solution in 100 mM Tris-HCl (pH 7.5), containing 0.1-0.3 mg Protein, were dried in a SpeedVac. Standards for calibration containing iron(II)ethylenediammonium sulphate were prepared in the same buffer and also dried in the SpeedVac.
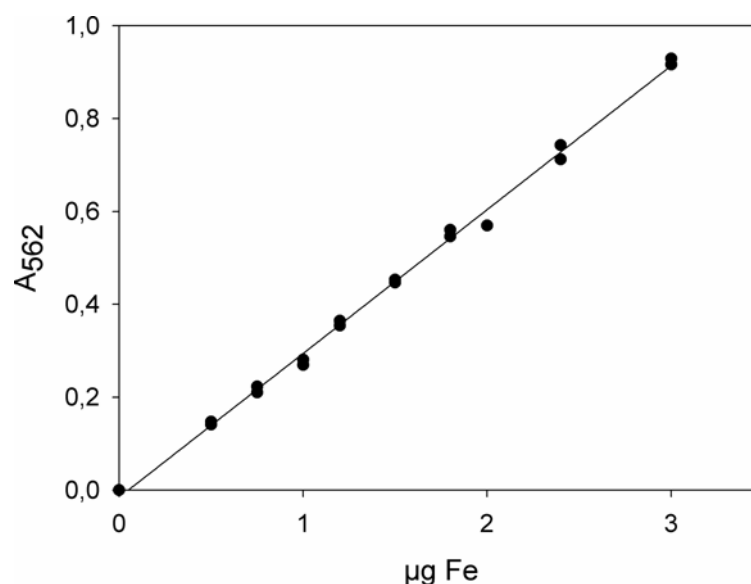
Figure 13: Calibration for the determination of the Fe content of biological samples. $A_{562}=-0.0156(\pm0.0070)+[0.3098(\pm0.0042)]*m_{Fe}$

To each sample and standard, 0.5 mL of Reagent A (142 mM $KMnO_4$ solution in 0.6 N HCl) was added and the mixture was incubated at 60 ºC for 2 h. 0.1 mL of Reagent B (6.5 mM ferrozine (disodium 3-(2-pyridyl)-5,6-bis(4-phenyl sulfonate)-1,2,4-triazine), 13.1 mM neocuproine (2,9-dimethyl-1,10-phenantroline), 2 M ascorbic acid, 5 M ammonium acetate) was added and, after incubation for 1 h at 20 ºC, the mixture was centrifuged for 5 min to remove particles and the absorbance of the supernatant at 562 nm was measured with a Specord 205 spectrophotometer (Analytic Jena, Germany).

5.2.11 Reductive cleavage of SAM

The reduction of SAM was assayed applying a method used by Rubach *et al* (179) for HydE and HydG iron-only hydrogenase. The reaction mixture contained 100 mM Tris-HCl (pH 8.0), NikJ (in concentrations between 18 and 40 μM, freshly purified with or without addition of S-adenosylhomocysteine, or reconstituted), 50 mM KCl, 1 mM SAM, 3 mM sodium dithionite and 5 mM DTT. Controls were prepared without addition of NikJ. The reactions were incubated at 37 ºC or 25 ºC and after 1 h or 15 h they were analysed by reverse-phase HPLC, using an Atlantis dC18 column (Waters, Dublin, Ireland) mounted on an UltiMate 3000 HPLC system (Dionex, Germering, Germany). A gradient of 0.1% TFA to 0.1% TFA:28% acetonitrile was applied and absorbance was monitored at 280 nm.

5.3 Results

5.3.1 Expression and purification of NikJ

The NikJ enzyme can be expressed in *E. coli* in significant amounts (approx. 1.7 mg/L TB medium). Freshly purified protein shows the dark brown colour which is typical for Fe-S proteins. After further purification by gel filtration, a loss of intensity in colour is observed.
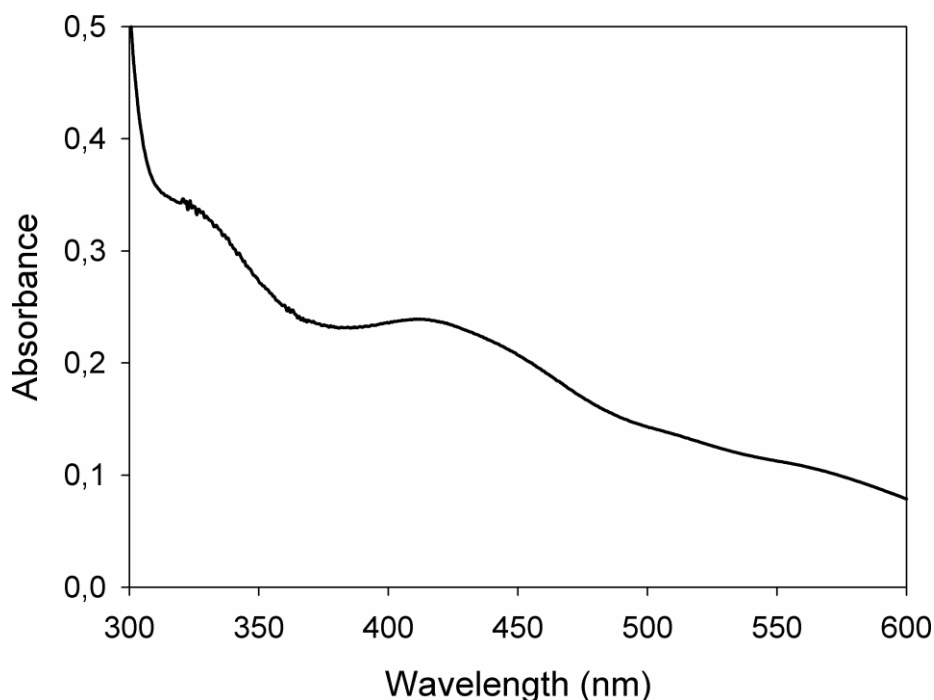
Figure 14: UV-vis absorbance spectrum of *Strep*-tagged NikJ, after purification in the AtmosBag® fro Sigma-Aldrich.

5.3.2 Fe-S cluster reconstitution

Changes in the UV-vis spectra indicate that iron-sulfur clusters could indeed be reconstituted by the applied method to some extent, as the peak at 420 nm increases. The exclusion of oxygen was observed to be important to prevent the immediate formation of a black precipitate. The black precipitate (probably FeS), which shifts the whole UV-vis spectrum to higher absorbance values due to turbidity, is always observed after some time of incubation, but at an earlier timepoint when NikJ is absent.
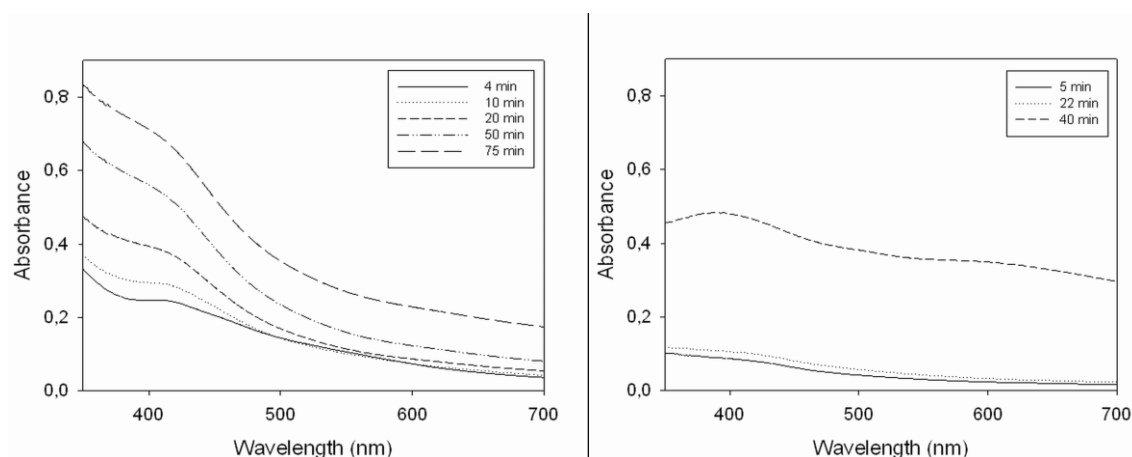
Figure 15: Spectra taken of the reconstitution mixture after various time points. The left panel shows the mixture including NikJ, the panel on the right side is the control without NikJ. Preciptitation of FeS leads to turbidity after longer incubation periods in both reaction mixtures.

5.3.3   The iron content of NikJ

The two samples of His-tagged NikJ purified without exclusion of oxygen, which were sent to the analytical laboratory of Dr. Baumann, were determined to have bound 0.5 mol and 1 mol Fe per mol NikJ, respectively.

The iron content of several enzyme preparations determined by the colorimetric method varied between 2.0 and 3.5 mol Fe/mol NikJ. After reconstitution trials, the iron content of NikJ was not determined, due to the lack of a method to remove the reagent $(NH_4)_2Fe(SO_4)_2$ without exposing the Fe-S clusters to oxygen.

5.3.4   Molecular weight and oligomerization state of NikJ

To determine the oligomerization state of NikJ, gel filtration and Native PAGE experiments were performed. Gel filtration of NikJ, which was prepared by Ni-NTA affinity chromatography resulted in three peaks, merging into each other. When the elution volumes of the two peak maxima that lie within the separation range of the column are taken to calculate the molecular weight, this results in a pentamer and a di- or trimer of NikJ. Native PAGE showed two bands with smear between them. When NaCl is present during electrophoresis, the band of the faster migrating oligomer is less pronounced. A certain proportion of protein apparently forms aggregates which elute outside the separating range of the column (at around 70 mL) and do not enter the electrophoresis gel.
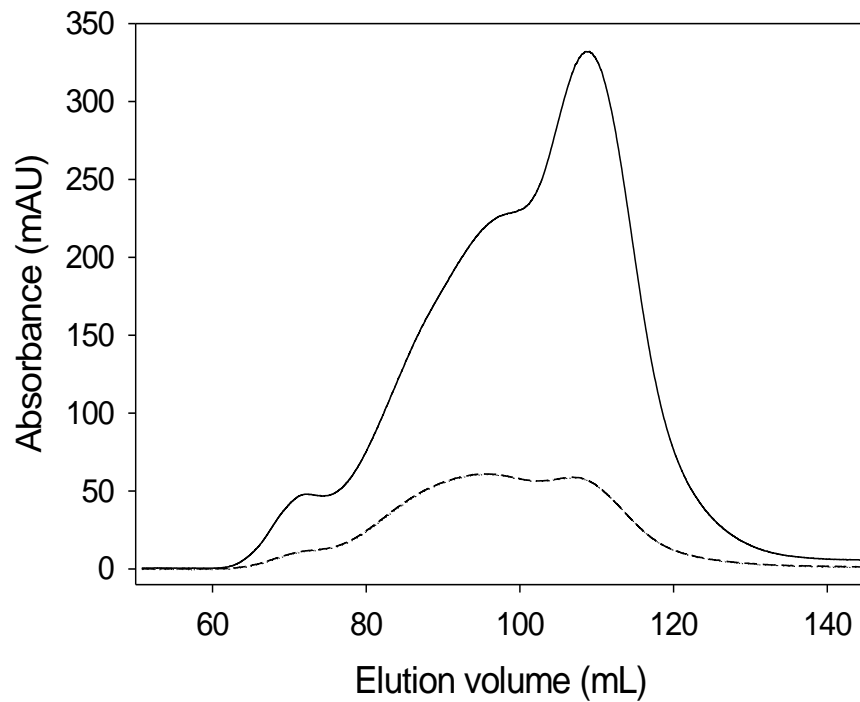
Figure 16: Elution profile of the gel filtration chromatography of NikJ after purification by Ni-NTA chromatography. The absorbance was monitored at 280 nm (solid line) and 450 nm (dashed line).
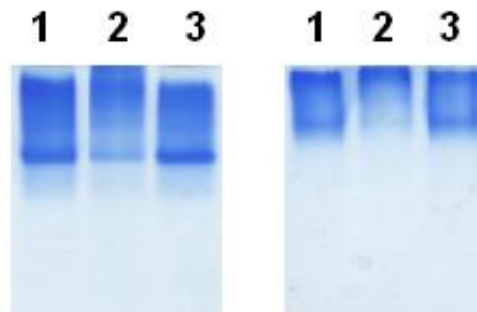
Figure 17: Native PAGE gels. The gel on the left was run without NaCl addition, the gel on the right hand side had 300 mM NaCl in the running buffer. Lanes 1: NikJ purified by Ni-NTA chromatography, lanes 2: NikJ from the gel filtration fraction of an elution volume of 94-96 mL, lanes 3: NikJ from the gel filtration fraction of an elution volume of 112-114 mL.

5.3.5 Reductive cleavage of SAM

In order to determine if NikJ belongs to the radical-SAM superfamily, it was assayed for the ability to reductively cleave SAM, by anaerobic incubation of the reconstituted protein with an excess of SAM and dithionite. The reductive cleavage should be monitored by the formation of 5´-deoxyadenosine. The HPLC elution profiles of the reaction mixture incubated with or without NikJ did not reveal any ongoing reaction. The SAM peak was unaltered, and no new peak resulting from 5´-deoxyadenosine could be observed.

5.4 Discussion

Although NikJ is readily expressed and can be purified in significant amounts, its iron-sulfur clusters provide a challenge in handling the protein. The clusters are decomposed when oxygen is present and it might be assumed that their stability is low even under anoxic conditions. Most purification steps we performed in a glove box, and the *Strep*-tag® purification system leads to a very pure enzyme solution, which permits to avoid a further gel filtration step. We were not able to completely exclude oxygen during cell disruption and centrifugation with our equipment. Concentrating protein solutions after elution was also not possible under anoxic conditions.

NikJ is expected to contain a $[Fe_4S_4]$ cluster, as it is related to radical SAM enzymes. Iron determination always resulted in less than 4 Fe atoms per NikJ monomer, indicating that Fe has been lost upon degradation of the clusters. Of course, the accuracy of the colorimetric method is questionable, and determination of the protein concentration by the Bio-Rad assay contributes to a potential error in quantitation. (A more accurate method for the determination of protein concentration was not available, as the contribution of the Fe-S cluster to the extinction coefficient at 280 nm is unknown and the BCA reaction, which was successfully applied for NikK, is affected by Fe.) Still, the results indicate that iron is lost, probably from $[Fe_4S_4]$ clusters.

NikJ was observed to be present in different oligomerization states. The peaks of gel filtration chromatography merge into each other and Native PAGE shows a smear. It seems that a smaller and a larger oligomer (maybe a di-or trimer and a tetra- or hexamer) exist in equilibrium, which shifts to the larger species when NaCl is present.

NikJ could not be shown to reductively cleave SAM, so we could not ascertain that NikJ indeed belongs to the radical SAM superfamily. The reason for the lack of activity is unclear. NikJ might be inactive due to inappropriate reaction conditions or the oxidative destruction of its Fe-S clusters. However, also NikJ that underwent reconstitution by NifS did not cleave SAM. Crystallization trials (performed by Gustav Oberdorfer; 119) were unsuccessful so far. The complete exclusion of oxygen during all steps of cell disruption, purification and crystallization would be an appropriate means to further characterize the enzyme.

The most important question regarding NikJ is the role it plays in nikkomycin biosynthesis. The enzyme shows sequence similarities to radical SAM proteins and Fe-S oxidoreductases. Therefore, NikJ might catalyze an oxidation reaction. Schüz *et al* found the bicyclic nikkomycins S_x and S_z in the culture broth of *Streptomyces tendae* Tü901/S 2566 and showed that when Fe is added to the production medium, the production of S_x and S_z decreases, with a concomitant increase in the production of nikkomycins X and Z (99). From this observation it can be concluded that either, S_x and S_z are intermediates of the biosynthetic pathway of the aminohexuronic acid moiety, which are converted to the biologically active nikkomycins X and Z in an iron-dependent manner, or they are side products of the biosynthetic pathway, whose formation is promoted by a lack of iron. According to our hypothesis, the bicyclic nikkomycins S_x and S_z are intermediates of the biosynthetic pathway and represent the substrates for the iron-sulfur enzyme NikJ. An attempt to produce S_x and S_z in *Streptomyces tendae* Tü901/S 2566 and test them as substrates for NikJ is described in (8.2.7).

CHAPTER 6

6   Expression and characterization of NikI and NikM

6.1 Introduction

6.1.1 NikI and NikM show similarity to prolyl-4-hydroxylases

The NikI (24.5 kDa) and NikM (24 kDa) enzymes, whose function in nikkomycin biosynthesis is unclear, share about 45% sequence similarity. As they show similarity to the α-subunit of bacterial prolyl-4-hydroxylases, they might be involved in the hydroxylation of an intermediate of the nikkomycin biosynthetic pathway.

6.1.2 The role of prolyl 4-hydroxylases

Prolyl-4-hydroxylases (EC 1.14.11.2) catalyze the hydroxylation of proline residues in X-Pro-Gly sequences, leading to the formation of 4-hydroxyproline in collagens (180). This irreversible reaction is the most common posttranslational modification in humans (181). The presence of 4-hydroxyproline is required for the stability of collagen, the major component of connective tissue, at physiological temperature (182). Stabilization of the collagen triple helix is the best known role for 4-hydroxyproline, and it is also found in proteins with collagen-like domains and elastin. However, prolyl-4-hydroxylases are not unique to animals, but they are found in plants and microorganisms as well (181). Hydroxyproline-rich glycoproteins are a major component of the cell wall of higher plants and green algae and play a role in plant growth and cellular interaction (183). Hydroxyproline is also found in bacterial antibiotic peptides. These non-ribosomal peptides often contain non-natural and modified amino acids. In bacteria, animals and plants, sterospecific hydroxylation occurs at the $4R$ position of proline (184). Other isomers of hydroxyproline and other proline modifications occur only in bacteria. Free proline is the precursor to all the forms of hydroxyproline in bacteria (185).

6.1.3 Catalysis of 4-hydroxyproline formation

Prolyl 4-hydroxylase is a member of the non-heme iron (II), α-ketoglutarate-dependent dioxygenase family. The hydroxylation of proline requires Fe^{2+}, α-ketoglutarate, molecular oxygen and ascorbate (Scheme 12). It involves oxidative decarboxylation of α-ketoglutarate, and succinate and CO_2 are produced (186). During most catalytic cycles, ascorbate is not consumed, but the enzyme also catalyzes decarboxylation of α-ketoglutarate without hydroxylation, leading to an uncoupling of co-substrate turnover (187). The inactivation of the enzyme by uncoupling can be overcome by ascorbate, which reduces Fe^{3+} to Fe^{2+} (188).

a) prolyl-procollagen+ α-ketoglutarate + O_2 $\xrightarrow{Fe^{2+}}$ 4-hydroxyprolyl-procollagen + succinate + CO_2

b) α-ketoglutarate + O_2 + ascorbate $\xrightarrow{Fe^{2+}}$ succinate + CO_2 + dehydroascorbate
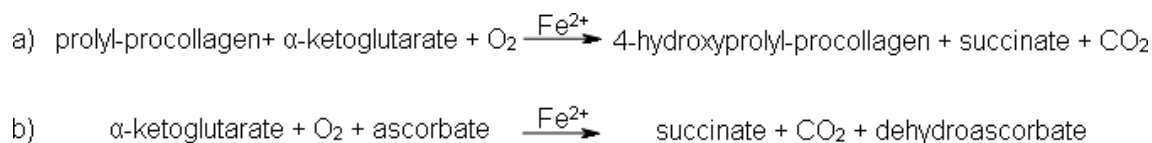
Scheme 12: Reactions catalyzed by prolyl 4-hydroxylase. Reaction a) shows the hydroxylation of a prolyl residue, reaction b) shows the uncoupled decarboxylation of α-ketoglutarate and the role of ascorbate.

Mammalian prolyl 4-hydroxylase is a $\alpha_2\beta_2$ tetramer, the α-subunit (59 kDa) contains the peptide-substrate binding domain and the active site (181;189). The iron is bound in the active site by two histidine residues and an aspartate residue (181). The β-subunit (55 kDa) functions as protein disulfide isomerase, retains the enzyme in the lumen of the endoplasmatic reticulum, and maintains the α-subunit in a soluble and active form (190). Prolyl 4-hydroxylase from the endospore-forming gram-positive bacterium *Bacillus anthracis* was shown to form an α_2 dimer, the enzyme was suggested to play a role in sporulation (191).

6.2   Materials and Methods

6.2.1   Reagents

All chemicals were of highest grade commercially available and purchased from Sigma−Aldrich (St. Louis, MO, USA), Fluka (Buchs, Switzerland), or Merck (Darmstadt, Germany). Nickel−nitrilotriacetic acid agarose (Ni−NTA) was from Qiagen (Hilden, Germany), Sephadex resin from Pharmacia Biotech AB (Uppsala, Sweden).

6.2.2   Cloning and expression in *Escherichia coli*

Streptomyces tendae Tü901/8c was grown in 250 mL LB-Medium at 30 °C for six days. Genomic DNA was isolated using the Illustra™ bacteria genomic Prep Mini Spin Kit from GE Healthcare (Buckinghamshire, UK) and used as a template for PCR using Phusion™ High Fidelity DNA Polymerase from Finnzymes (Espoo, Finland). The PCR products contained an *NdeI* restriction site at the 5'-end and a *XhoI* restriction site at the 3'-end, and were cloned into the *NdeI/XhoI* restriction sites of the pET21a vector (Novagen), generating the expression plasmid pET21a(*nik*I) and pET21a(*nikM*). The *nikI* gene was designed without a stop codon, which allows expression of the protein with a C-terminal hexahistidine tag. The *nikM* gene was designed in a way that allows

expression with an N-terminal hexahistidine tag, with six codons for histidine at the 5'-end and a stop codon at the 3'-end. The sequences on each expression plasmid was verified by DNA-sequencing (Eurofins DNA, Ebersbach, Germany). Chemically competent *E. coli* BL21(DE3) cells were transformed with the expression plasmid pET21a(*nikI*). Chemically competent *E. coli* BL21(DE3) cells were transformed with the chaperone plasmid pG-KJE8 (Takara Bio Inc.), these transformants were made competent and transformed with pET21a(*nikM*). Expression of NikI was achieved by growing a 10 mL preculture in Luria-Bertani (LB) medium containing 100 µg/mL ampicillin over night at 37 °C. The preculture was used to inoculate 750 mL LB medium containing 100 µg/mL ampicillin for plasmid selection. The culture was incubated at 37 °C until an OD600 of 0.5 and IPTG was added to a final concentration of 0.1 mM. The culture was incubated for 3 h at 37 °C and cells were harvested by centrifugation. The pellet was washed with 0.9 % NaCl solution and stored at -20 °C. Expression of NikM with the help of co-expressed chaperones (dnaK, dnaJ, grpE, groES, groEL) was achieved by growing a 10 mL preculture in Luria-Bertani (LB) medium containing 50 µg/mL ampicillin and 20 µg/mL chloramphenicol over night at 37 °C. The preculture was used to inoculate 750 mL LB medium containing 50 µg/mL ampicillin and 20 µg/mL chloramphenicol for plasmid selection, and 0.5 mg/mL L-arabinose and 1 ng/mL tetracycline for chaperone induction. The culture was incubated at 37 °C until an OD600 of 0.5 and IPTG was added to a final concentration of 0.1 mM. The culture was incubated over night at 20 °C and cells were harvested by centrifugation. The pellet was washed with 0.9 % NaCl solution and stored at -20 °C.

6.2.3 Generation of a NikM E47A/E48A/E50A variant by site-specific mutagenesis

Site directed mutagenesis was carried out in two steps according to the QuikChange® XL Site-Directed Mutagenesis Kit from Stratagene (Santa Clara, CA, USA). The pET21a(*nikM*) plasmid served as template to introduce the mutations. The following primer and its complementary counterpart were used: 5'- GAC GGC TTC GCG GCG TCC GCG CGC ACC GAC CTG-3'. The underlined nucleotides denote the mutated codons. After mutagenesis, the sequence of the transformation construct was verified by DNA-sequence analysis. Transformation and expression was carried out as described for wild type NikM.

6.2.4 Cell disruption and purification

The pellet was thawed and resuspended in lysis buffer (100 mM Tris-HCl buffer at pH 8.0, containing 300 mM NaCl and 10 mM imidazole), using 2 mL buffer per gram of wet cells. Cells were disrupted by 30 min incubation with lysozyme and 0.5 s sonication pulses for 10 min while cooling on ice. The cell debris was removed by centrifugation at 18 000 g for 30 min at 4 °C.

The hexahistidine-tagged NikI and NikM enzymes were purified by Ni-NTA affinity chromatography, loading the respective supernatant onto a Ni-NTA column (Qiagen), previously equilibrated with lysis buffer. After loading of the filtered lysate, the column was washed with 10 column volumes of wash buffer (100 mM Tris-HCl, 300 mM NaCl, 20 mM imidazole, pH 8.0 in the case of NikI and 100 mM Tris-HCl, 300 mM NaCl, 10 mM imidazole, pH 8.0 in the case of NikM) and bound protein was recovered with elution buffer (100 mM Tris-HCl, 300 mM NaCl, 150 mM imidazole, pH 8.0). The purity of the eluted 3 mL fractions was determined using SDS-polyacrylamide gel electrophoresis. Fractions containing NikI or NikM were pooled and concentrated using Amicon® Ultra Centrifugal Filter Units (Millipore, Billerica, MA, USA). For NikI, the buffer was exchanged to 100 mM Tris buffer (pH 7.5) using a PD-10 column (GE Healthcare) and the solution of the protein was stored at -20 °C. NikM was always, NikI only when intended for crystallization, further purified by gel filtration chromatography, using a Hi Load™ 16/70 Superdex 75 prep grade column (Pharmacia Biotech AB) which was mounted on a fast protein liquid chromatography (FPLC) system (ÄKTA Explorer, Pharmacia Biotech AB). The column was equilibrated with 50 mM Tris-HCl buffer at pH 7.5.

6.2.5 Native molecular mass determination

The molecular mass of each purified protein was determined by gel filtration chromatography in order to assess the oligomerization state of native NikI and NikM. The analytical column, a Superdex 200 10/300 GL (Pharmacia Biotech AB) was mounted on a fast protein liquid chromatography (FPLC) system (ÄKTA Explorer, Pharmacia Biotech AB). The column was equilibrated with 100 mM Tris-HCl buffer containing 150 mM NaCl at pH 7.5. A 100 μL sample containing 200 μg of the respective protein was applied to the column, and the elution volume was determined by monitoring the absorbance at 280 nm. The column was calibrated using a high-molecular-mass gel-filtration calibration kit (Amersham Biosciences; α-

chymotrypsinogen A, 25 kDa; ovalbumin, 43 kDa; bovine serum albumin, 67 kDa; aldolase, 158 kDa; catalase, 232 kDa; and ferritin, 440 kDa).

6.2.6   Determination of iron bound to NikI or NikM

To determine and quantitate iron bound to NikI and NikM, the rapid colorimetric micromethod developed by W. W. Fish (178) was applied. For a detailed description of the method, see 5.2.10.

6.2.7   Testing 3'-EPUMP and 3'-EP-uridine as potential substrates for NikI and NikM

3'-EPUMP which was generated from UMP and PEP using NikO (see 2.2.5) and 3'-EP-uridine which was generated by incubation of 3'-EPUMP with alkaline phosphatase (see 4.2.6) were tested as substrates for NikI and NikM under various reaction conditions. The reaction mix contained about 1 mM of the respective substrate, 1 mM α-ketoglutarate, 1 mM ammonium iron (II) sulphate, and 1 mM ascorbate in 100 mM Tris-HCl (pH 7.5) and 20 μM NikI or NikM or a combination of both enzymes. After incubation for 1 h or overnight at 20 °C or 30 °C, the reaction mix was diluted with 0.05% TFA and analysed by HPLC, using an Atlantis dC18 column (Waters, Dublin, Ireland), mounted on an UltiMate 3000 HPLC system (Dionex, Germering, Germany). The elution was carried out by applying a linear gradient of 0.05% trifluoroacetic acid to acetonitrile in 25 min, using a flow rate of 1 mL/min. Eluted substances were observed by the absorbance at 260 and 280 nm.

6.3 Results

NikI and NikM were expressed heterologously in *E. coli* in significant amounts and appeared to be stable in solution. In the case of NikM, the co-overexpression of chaperone led to an increase in the amount of protein produced. NikM with the hexahistidine tag either at the C- or at the N-terminus showed a lower affinity to the Ni-NTA column than the other proteins containing a His-tag. An imidazole concentration of 20 mM, which is usually present in the wash buffer, already led to elution of the protein.

Both proteins, NikM and NikI, were shown to exist as monomers in solution. Iron was not detected in preparations of these enzymes by the colorimetric method described.

3'-EPUMP and 3'-EP-uridine were not affected by incubation with NikM, NikI, nor a mix of both.

6.4 Discussion

NikI and NikM share about 45% sequence similarity and show similarity to prolyl 4-hydroxylases. Possibly, they catalyze the hydroxylation of a biosynthetic intermediate, though it is puzzling how such a reaction would fit into the nikkomycin biosynthetic pathway. The expression and purification of both monomeric enzymes turned out to be relatively unproblematic. As prolyl 4-hydroxylases require Fe^{2+} for catalysis, preparations of NikI and NikM were analyzed for their iron content, but no iron was detected. The enzymes did not convert 3´-EPUMP. It is unknown if they are inactive under the tested conditions or if 3´-EPUMP is not their physiological substrate. Their role in nikkomycin biosynthesis remains unclear.

CHAPTER 7

7   Expression and characterization of NikS

7.1 Introduction

7.1.1 D-Alanine-D-alanine ligase

D-Alanine-D-alanine ligase (DDl) (E.C. 6.3.2.4) is an essential enzyme in the biosynthesis of the bacterial cell wall. The assembly of the D-alanyl-D-alanine dipeptide, which is an important cell wall building block, is catalysed in an ATP-dependent manner (192). DDl consists of four domains, and the binding sites for D-Ala and ATP are created by their interfaces. The formation of the dipeptide proceeds via a two-step mechanism. First, an intermediate is generated by phosphorylation of (N-terminal) D-Ala by ATP, which subsequently reacts with the second (C-terminal) D-Ala moiety to form D-alanyl-D-alanine. In this nucleophilic reaction, inorganic phosphate is lost (193). DDl is the second enzyme of the D-Ala branch after alanine racemase in the assembly of peptidoglycan precursors in cytoplasm. Its product D-alanyl-D-alanine is then incorporated into the next cell wall precursor by the action of UDP-*N*-acetylmuramyl-pentapeptide synthetase (MurF) (194). DDl, which is common to Gram-negative and Gram-positive organisms and does not occur in eukaryotes, has emerged as an attractive target to develop novel antibiotics. The enzyme was discovered to be inhibited by D-cycloserine, a structural analog of D-alanine (193), by phosphonate and phosphinate dipeptides, which are transition states analogs that bind to the active site (195) and by several protein kinase inhibitors (196).

7.1.2 The ATP-grasp fold enzyme superfamily

D-Alanine-D-alanine ligase belongs to superfamily of enzymes with an unusual nucleotide-binding fold, the ATP-grasp fold. All the enzymes that belong to this family catalyse a reaction that involves an ATP-dependent ligation of a carboxyl group carbon of one substrate with the nitrogen of an amino or imino group of the other substrate. In each case, it includes the formation of acylphosphate intermediates (195;197;198) (Scheme 13).
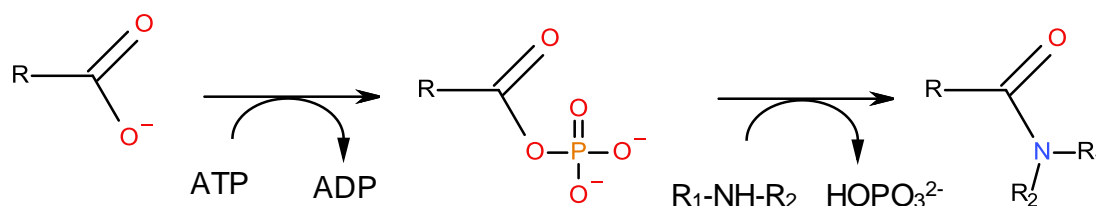
Scheme 13: Summary of the reaction catalysed by carboxylate-amine ligases

Enzymes which contain an ATP-grasp domain are glutathione synthetase, with γ-glutamyl-cysteine and glycine as substrates, and the biotin carboxylase subunit of acetyl-CoA carboxylase (involved in fatty acid biosynthesis), where the nitrogen of the enzyme bound biotin molecule is the amino group containing substrate. Biotin-enzyme is also the amine substrate in propionyl-CoA carboxylase (involved in amino acid catabolism), pyruvate carboxylase (involved in gluconeogenesis), and urea amidolyase (involved in urea hydrolysis). Further examples of enzymes of this superfamily are ATP-citrate lyase (involved in lipid biosynthesis) and succinyl CoA synthetase (involved in the citric acid cycle), where succinate or citrate serves as carboxylate substrate and Coenzyme A as thiol substrate (102).

7.2   Materials and Methods

7.2.1   Reagents

All chemicals were of highest grade commercially available and purchased from Sigma−Aldrich (St. Louis, MO, USA), Fluka (Buchs, Switzerland), or Merck (Darmstadt, Germany). Nickel−nitrilotriacetic acid agarose (Ni−NTA) was from Qiagen (Hilden, Germany), Sephadex resin from Pharmacia Biotech AB (Uppsala, Sweden).

7.2.2   Cloning and expression in *Escherichia coli*

Streptomyces tendae Tü901/8c was grown in 250 mL LB-Medium at 30 °C for six days. Genomic DNA was isolated using the Illustra™ bacteria genomic Prep Mini Spin Kit from GE Healthcare (Buckinghamshire, UK) and served as a template for PCR using Phusion™ High Fidelity DNA Polymerase from Finnzymes (Espoo, Finland). The PCR product contained an *NdeI* restriction site at the 5'-end and a *XhoI* restriction site at the 3'-end, and were cloned into the *NdeI/XhoI* restriction sites of the pET21a vector (Novagen), generating the expression plasmid pET21a(*nik*S). The *nikS* gene was designed without a stop codon, which allows expression of the protein with a C-terminal hexahistidine tag. The sequence on the expression plasmid was verified by DNA-sequencing (Eurofins DNA, Ebersbach, Germany). Chemically competent *E. coli* BL21(DE3) cells were transformed with the expression plasmid pET21a(*nik*S). Expression of NikS was achieved by growing a 10 mL preculture in Luria-Bertani (LB) medium containing 100 µg/mL ampicillin over night at 37 °C. The preculture was used to inoculate 750 mL LB medium, containing 100 µg/mL ampicillin for plasmid

selection. The culture was incubated at 37 °C until an OD600 of 0.5 and IPTG was added to a final concentration of 0.1 mM. The culture was incubated for 3 h at 37 °C and cells were harvested by centrifugation. The pellet was washed with 0.9 % NaCl solution and stored at -20 °C.

7.2.3 Cell disruption and purification

The pellet was thawed and resuspended in lysis buffer (100 mM Tris-HCl buffer at pH 8.0, containing 300 mM NaCl and 10 mM imidazole), using 2 mL buffer per gram of wet cells. Cells were disrupted by 30 min incubation with lysozyme and 0.5 s sonication pulses for 10 min while cooling on ice. The cell debris was removed by centrifugation at 18 000 g for 30 min at 4 °C.

The hexahistidine-tagged NikS was purified by Ni-NTA affinity chromatography, loading the supernatant onto a Ni-NTA column (Qiagen), previously equilibrated with lysis buffer. After loading of the filtered lysate, the column was washed with 10 column volumes of wash buffer (100 mM Tris-HCl, 300 mM NaCl, 20 mM imidazole, pH 8.0) and bound protein was recovered with elution buffer (100 mM Tris-HCl, 300 mM NaCl, 150 mM imidazole, pH 8.0). The purity of the eluted 3 mL fractions was determined using SDS-polyacrylamide gel electrophoresis. Fractions containing NikS were pooled and concentrated using Amicon® Ultra Centrifugal Filter Units (Millipore, Billerica, MA, USA). The buffer was exchanged to 100 mM Tris buffer (pH 7.5) using a PD-10 column (GE Healthcare) and the solution of NikS protein was stored at 4 °C. For crystallization trials, the protein was further purified by gel filtration chromatography, using a Hi Load™ 16/70 Superdex 75 prep grade column (Pharmacia Biotech AB, Uppsala, Sweden) which was mounted on a fast protein liquid chromatography (FPLC) system (ÄKTA Explorer, Pharmacia Biotech AB, Uppsala, Sweden). The column was equilibrated with 20 mM Tris-HCl buffer at pH 7.5.

7.2.4 Testing NikS for enzymatic activity

To find out, if NikS was able to catalyse peptide-bond formation between HPHT (nikkomycin D) and aminohexuronic acid (nikkomycin C_x and C_z), an activity assay developed for D-alanine-D-alanine ligases (196) was adapted to the putative NikS reaction. The reaction mix contained the substrates nikkomycin D and C_x, which were obtained from Bertold Gust and Hans-P. Fiedler (Tübingen), in a concentration of about 1 mM, 10 mM KCl, 10 mM $MgCl_2$, 1 mM ATP, GTP, CTP, or UTP, and 20 µM NikS enzyme in 100 mM Tris-HCl (pH 7.5). Control reactions that did not contain nucleotide

triphosphate, salts, or NikS were also prepared. After two hours of incubation at 37 °C, the samples were diluted with 0.05% trifluoroacetic acid and analysed by HPLC, using an Atlantis dC18 column (Waters, Dublin, Ireland), mounted on an UltiMate 3000 HPLC system (Dionex, Germering, Germany). The elution was carried out by applying a linear gradient of 0.05% trifluoroacetic acid to acetonitrile in 20 min, using a flow rate of 1 mL/min. Eluted substances were observed by the absorbance at 260 and 280 nm.

NikS was also tested for its effect on HPHT and aminohexuronic acid, which were expected to be present in the lyophilized fractions obtained after ion exchange chromatography of *S. tendae* Tü901/8c fermentation broth (see 8.2.5). A milligram of each lyophilized fraction was dissolved in a solution of 10 mM KCl, 10 mM MgCl$_2$, 1 mM ATP, GTP, CTP, or UTP, and 20 µM NikS enzyme in 100 mM Tris-HCl (pH 7.5). These reactions and controls were treated as described above.

7.3 Results

Conversion of HPHT and nikkomycin C$_x$ by NikS could neither be observed with ATP nor with CTP, UTP or GTP present. The peaks of those substances in the HPLC elution profiles did not decrease significantly when NikS was added to the reaction mix, and no new peak was observed.

7.4 Discussion

NikS is expected to catalyze the formation of the peptide bond between the nucleoside and peptide moiety of nikkomycins, as it shows similarities to carboxylate-amine ligases. The enzyme, which was predicted to belong to the ATP-grasp family, is 97% identical to SanS of *Streptomyces ansochromogenes*. The ATPase activity of SanS was demonstrated by Li *et al* (104). We assume that NikS catalyzes an ATP-dependent ligation of the carboxyl group carbon of HPHT with the amino group nitrogen of aminohexuronic acid, but we have not been able to demonstrate that. The substrates we used were nikkomycins C$_x$ and D, obtained from the University of Tübingen, where they had been isolated from *S. tendae* culture broth. Previously to the described experiments, they had been stored for a long time period, so it cannot be excluded that they had already undergone a degradation process. However, freshly prepared extracts of *S. tendae* were also tested for conversion of the nikkomycins C$_x$, C$_z$, and D that they contained. Possibly, the conditions we used for the experiments did not favour the reaction. It might also be possible that NikT-bound HPHT is the substrate for the

condensation step, as was suggested by Lauer *et al* (100) and NikS is unable to ligate free HPHT and aminohexuronic acid.

CHAPTER 8

8 Preservation and growth of *Streptomyces* and isolation of nikkomycins and nikkomycin intermediates

8.1 Introduction

HPLC represents an excellent method to characterize and quantify secondary metabolites in biological fluids, such as culture filtrates of organic extracts. The classification of derivatives of known substances is facilitated by the photodiode array technique, which allows comparing UV spectra of all known and unknown components. The method is much less time consuming than isolation and characterization of all detected peaks, and was used to screen culture filtrates resulting from chemical derivatization, genetic or mutasynthetic programs and to discover new nikkomycins (11;19,20;22;23;199). The methods to extract and characterize nikkomycins developed at the University of Tübingen are expected to be applicable for the identification of intermediates of the nikkomycin biosynthetic pathway produced by *Streptomyces* variants with *nik* gene deletions.

8.2 Materials and Methods

8.2.1 Reagents

All chemicals and resins were of highest grade commercially available and purchased from Sigma−Aldrich (St. Louis, MO, USA), Fluka (Buchs, Switzerland), or Merck (Darmstadt, Germany). Soybean flour (Hensel Voll-Soja, Magstadt, Germany) was purchased at the local health food store. Spores of *Streptomyces tendae* Tü901/8c, *S. tendae* Tü901/S 2566, and kanamycin resistant *S. coelicolor* M512nikKS02 with the whole nikkomycin biosynthetic gene cluster as well as ΔnikI, ΔnikJ, ΔnikK, ΔnikL, and ΔnikM deletion mutants thereof (the respective gene is replaced by the sequence Start-TTT-AAA-Stop), the *S. coelicolor* M512 strain, where the nikkomycin gene cassette has not been introduced, and nikkomycins X, Z, I, J, D, and Cx to be used at HPLC standards, were obtained from Dr. Bertolt Gust (Pharmaceutical Institute Eberhard-Karls-Universität Tübingen, Germany).

8.2.2 Composition of fermentation media

Production medium according to Fiedler: 30 g/L mannitol, 10 g/L soluble starch, 20 g/L soybean flour, 10 g/L yeast extract

YEME medium: 3 g Difco yeast extract, 5 g Difco bacto peptone, 3 g malt extract, 10 g glucose, 340 g sucrose, 1 L H_2O. After autoclaving, $MgCl_2$ is added to an end concentration of 5 mM.

SFM agar plates: 20 g/L soybean flour, 20 g/L mannitol, 15 g/L agar

GYM medium: 4 g glucose, 4 g yeast extract, 10 g malt extract, 1 L H_2O; pH 7.2;

8.2.3 Preservation of sporulating *Streptomyces* strains

5 µL of a spore suspension of the respective strain were diluted in 200 µL of sterile H_2O, and streaked onto two plates of SFM medium. In case of *S. coelicolor* M512nikKS02 and its deletion mutants, the plates were supplemented with 20 µg/mL kanamycin. The plates were incubated for 5 days at 30 °C. 5 mL of water were added to each plate, the spores were gently rubbed off the surface with a sterile cotton bud and the suspension was centrifuged in a sterile falcon tube at 5000g for 5 min. The supernatant was discarded and the re-suspended spores were stored in 100 µL of 20% glycerol, at -20 °C.

8.2.4 Fermentation of *Streptomyces* cultures

Baffled flasks were used for cultivation in the respective medium (150 mL medium in each 500 mL flask). In fermentation of *S. coelicolor* M512nikKS02 cultures, the medium contained 20 µg kanamycin per mL. The medium was inoculated with 50 µL of a spore suspension and incubated at 30 °C and shaking at 170 rpm for 6-7 days. The production medium according to Fiedler was used for *S. tendae* strains, *S. coelicolor* M512nikKS02 was grown in the same medium, as well as in GYM and YEME media. In order to produce and identify the bicyclic nikkomycins S_x and S_z, *S. tendae* Tü901/S 2566 was grown in production medium according to Fiedler supplemented with 0-7 mg $FeSO_4*7H_2O$ per liter.

8.2.5 Extraction of secondary metabolites from the culture broth

The fermentation broth was centrifuged at 4600 rpm for 30 min and the pH of the supernatant was adjusted to 8.0, before it was purified by ion exchange chromatography. A column was packed with 20 g Dowex 1x2 resin (50-100 mesh, Cl⁻

form) and mounted on a fast protein liquid chromatography (FPLC) system (ÄKTA Explorer, Pharmacia Biotech AB, Uppsala, Sweden). The column was activated with 60 mL 5 N acetic acid, and washed with 100 mL H_2O before 400 mL of the previously filtered raw extract were loaded onto the column at a flow rate of 5 mL/min (3 mL/min when YEME was the culture medium). Nikkomycins were eluted with 50 mM formic acid and collected in 10 mL fractions. The fractions were frozen in liquid nitrogen and dried in a Virtis Sentry™ lyophilisation device.

8.2.6   HPLC analysis of the ion exchange chromatography fractions

A few milligrams of each fraction from ion exchange chromatography were dissolved in 0.05% trifluoroacetic acid and analysed by HPLC, using an Atlantis dC18 column (Waters, Dublin, Ireland), mounted on an UltiMate 3000 HPLC system (Dionex, Germering, Germany). The elution was carried out by applying several linear gradients of 0.05% trifluoroacetic acid to acetonitrile, using a flow rate of 1 mL/min. Eluted substances were observed by the absorbance at 260 and 280 nm. The elution profiles were compared to those of nikkomycin standards.

8.2.7   Production and identification of bicyclic nikkomycins Sx and Sz and their exposition to the NikJ enzyme

After centrifugation of the fermentation broth of *S. tendae* Tü901/S 2566 in Fiedler´s medium supplemented with $FeSO_4*7H_2O$ at concentrations of 0, 1, 2, 4 and 7 mg/L, the supernatant was directly analysed by HPLC (see 8.2.6).

Samples of the fermentation broth were incubated with NikJ (in concentrations between 10 and 20 μM, freshly purified with addition of S-adenosylhomocysteine), 50 mM KCl, 1 mM SAM, 3 mM sodium dithionite and 5 mM DTT. Controls were prepared without addition of NikJ, SAM, or DTT. The reactions were incubated at 25 ºC and after 1 h or 15 h they were analysed by HPLC (see 8.2.6).

8.2.8   Attempts to identify nikkomycin intermediates from *S. coelicolor* M512nikKS01 deletion mutants

Several ion exchange fractions of each *S. coelicolor* M512nikKS01 deletion mutant which was grown in YEME medium were incubated with the respective heterologously expressed protein to check for changes in the HPLC elution profile. The compositions of the reaction mixes were chosen in consideration of the potential cofactors or cosubstrates each enzyme might require. Controls were prepared without the addition of

enzyme. Incubation times varied from 1 h to overnight. HPLC runs were performed as described above.

Each reaction mix contained a few milligrams of lyophilisate from the fractions expected to contain the intermediate of the biosynthetic pathway and substrate for the respective enzyme and 10-40 μM of the respective enzyme. For the NikK reaction, 1-10 mM L-glutamate was added, the buffer was 50 mM potassium phosphate, pH 8.0 and pH 9.0. The reaction mix for NikI and NikM contained 100 mM Tris-HCl (pH 8.0), 10 mM α-ketoglutarate, 10 mM Fe^{2+}, and 10 mM ascorbic acid. The NikL reaction contained the MBP-NikL fusion protein or the fusion protein previously incubated with 0.2 ng enterokinase for 1 h. The buffer was 100 mM Tris-HCl, at a pH of 7.0, 8.0, and 9.0.

8.3 Results

Nikkomycins could be detected in *S. tendae* culture filtrate processed using the described methods. The HPLC elution profiles of several fractions resulting from their extraction via ion exchange chromatography can be well compared to those of nikkomycin standards obtained from Tübingen (see Figure 18).

In the similarly processed fermentation broth of *S. coelicolor* M512nikKS02, no nikkomycins could be detected, regardless of the used medium. The pattern of peaks in the HPLC elution profiles obtained after fermentation of *S. coelicolor* M512nikKS02 and the deletion mutants is similar to that of the fermentation broth of *S. coelicolor* M512, which does not contain the *nik* gene cluster.

Addition of heterologously expressed nikkomycin biosynthetic proteins to the lyophilized preparations did not alter their HPLC elution profiles, except in the case of NikK. The intensities of several peaks are altered by NikK. This is the case with fermentation broth of *S. coelicolor* M512nikKS02, the Δ*nikK* deletion mutant and *S. coelicolor* M512.
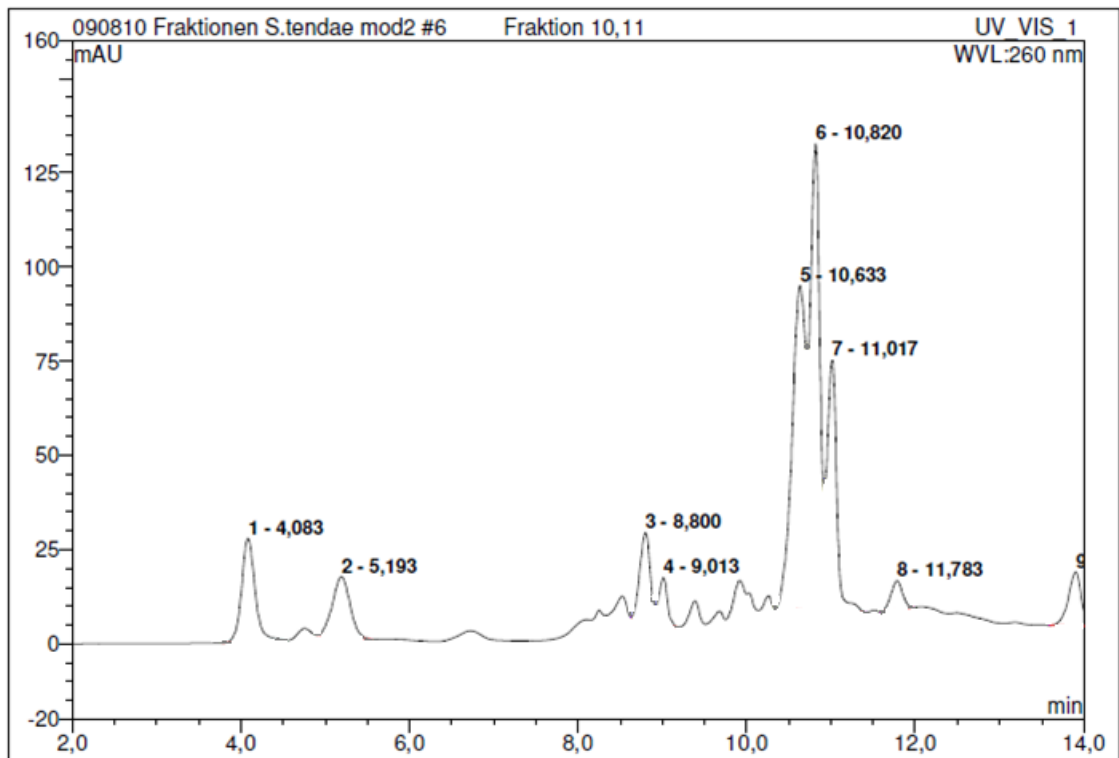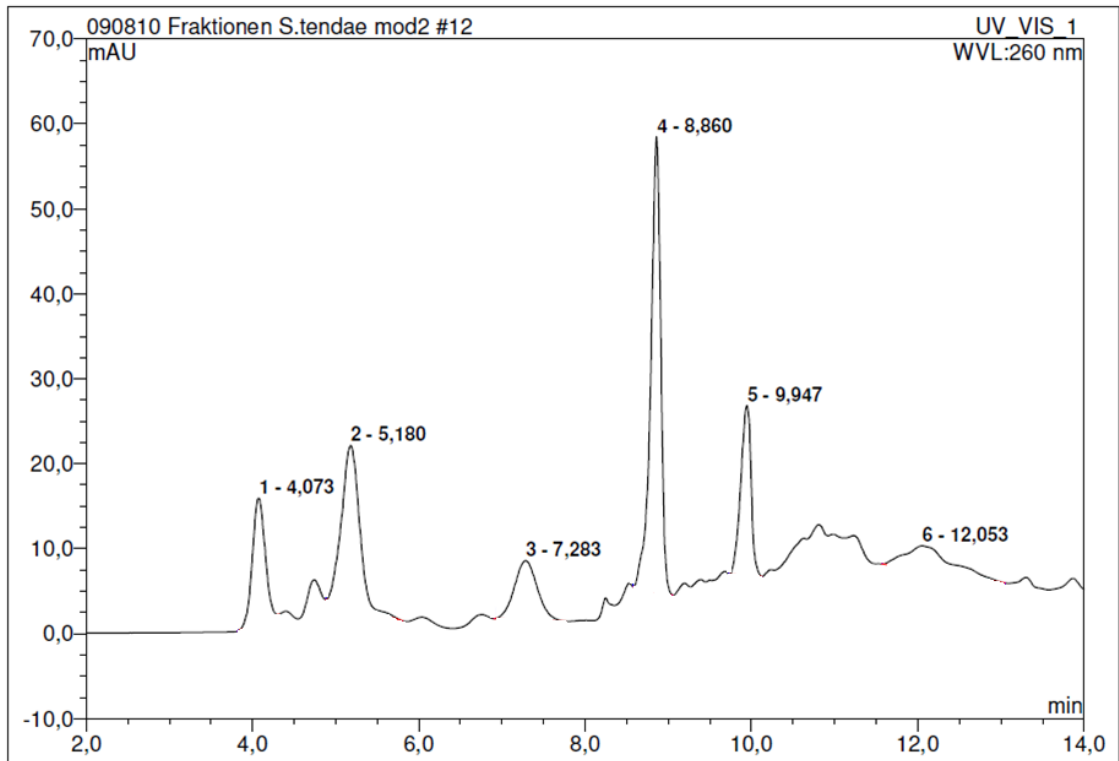
Figure 18: HPLC elution profiles of the nikkomycin standard mix obtained from Tübingen (upper panel) and of a lyophilized fraction of ion exchange eluate of *S. tendae* fermentation medium (lower panel). The peaks at 4.07 min, 5.19 min and 8.86 min correspond to nikkomycin C_x, D, and X or Z, respectively.

8.4 Discussion

Nikkomycins could be extracted from *Streptomyces tendae* fermentation medium and detected by HPLC. The elution profiles of several fractions obtained after ion exchange chromatography and lyophilization were very similar to the elution profile of the nikkomycin standard mix obtained from Tübingen. The methods we used should also be appropriate for identification and isolation of intermediates of the nikkomycin biosynthetic pathway, provided that those intermediates are stable and secreted into the fermentation medium in significant amounts. In addition to the expression and characterization of enzymes which are involved in the biosynthesis of nikkomycins, the identification of intermediates produced by deletion mutants would provide another approach to elucidate the biosynthetic reaction pathway.

Our collaborator at the University of Tübingen, Dr. Bertolt Gust, provided us with spores of *S. coelicolor* M512nikKS02. This strain contains a cassette with the whole nikkomycin biosynthetic gene cluster. Furthermore, we obtained ΔnikI, ΔnikJ, ΔnikK, ΔnikL, and ΔnikM deletion mutants of *S. coelicolor* M512nikKS02. We intended to analyse the culture filtrates of these deletion strains for the occurrence of nikkomycin intermediates, isolate accumulating compounds by HPLC, and determine their structure by MS and NMR spectroscopy. Unfortunately, *S. coelicolor* M512nikKS02 turned out to be a very poor producer of nikkomycins and we were not able to detect them with the methods we used. This was not a very promising precondition for the intended isolation of intermediates, as we did not expect them to be produced by the deletion mutants in higher amounts than the completed nikkomycins by the mutant containing the whole gene cluster. Regardless of this situation we tried it with several production media and conditions but we were not able to identify any peaks in the HPLC profile that could be ascribed to nikkomycin intermediates. The detected peaks apparently derive from media components or other metabolites and were not affected by treatment with the enzymes NikI, NikM, or NikL. NikK, however, seems to convert several substances in the lyophilisate. Most likely, it deaminates amino acids from the culture broth, as the elution profiles obtained from the experiments with the Δ*nikK* deletion mutants are identical to the elution profiles obtained from *S. coelicolor* M512, which does not contain any nikkomycin biosynthetic genes. Due to the incapacity of *S. coelicolor* M512nikKS02 and its deletion mutants to produce nikkomycins and biosynthetic intermediates, it was not possible to elucidate the biosynthetic pathway by this

approach. The generation of *nik* gene deletion mutants directly in the native producer of nikkomycins, *Streptomyces tendae*, could potentially lead to strains that produce these intermediates in amounts sufficient for analysis. To continue the efforts to throw light on the biosynthesis of nikkomycins, the generation of such disruption mutants by the use of a PCR targeting system is planned for the future.

Regarding the production of bicyclic nikkomycins S_x and S_z by *S. tendae* Tü901/S2566, we could not detect the conversion of any peak in the respective HPLC profile. One peak was assumed to derive from nikkomycins S_x and S_z, as its size decreased with an increasing iron concentration in the fermentation medium, but it could not be confirmed that the bicyclic substances were really present and gave rise to that peak.

CHAPTER 9

General discussion and conclusions

Nikkomycins have a great potential as fungicidal antibiotics, due to their inhibition of chitin synthase. Especially for treatment of fungal diseases in immunocompromised patients these peptide nucleosides can be considered as very promising compounds. However, their use is limited by cellular uptake, which is rather poor in most fungal pathogens. Furthermore, the production costs are very high and biologically active nikkomycins have to be purified from other contaminants in a complex process. These difficulties might be overcome, for example by genetic engineering of the producing strains, by combining enzymatic steps with chemical synthesis, or by supplying novel substrates and intermediates. An extensive knowledge of the biosynthetic pathway that leads to the generation of nikkomycins, and of the properties of the enzymes involved would certainly be a benefit for further approaches to establish nikkomycins or nikkomycin derivatives as antifungal drugs.

Initially, enzymes involved in nikkomycin biosynthesis were identified in expression studies, comparing producing and non-producing mutants of *Streptomyces tendae,* and nikkomycin biosynthetic genes were isolated (80). Biosynthetic functions were assigned to the gene products by the detection of sequence similarities to proteins in databases, by the characterization of disruption mutants and by the heterologous expression of the genes and the determination of enzymatic activities. While biosynthesis of the peptidyl moiety of nikkomycins is quite well investigated, the biosynthetic steps leading to the generation of the nucleoside or aminohexuronic acid moiety are still unclear. The enzymes NikO, NikI, NikJ, NikK, NikL, and NikM are predicted to be involved in that biosynthetic pathway (82). Sequence similarities to known proteins (listed in Table 1) could give an idea on the reactions they might catalyze.

Based on such sequence similarities a reaction pathway could be proposed (see Scheme 14), but it has to be kept in mind that this pathway is highly hypothetical and was only intended to serve for rough orientation during attempts to experimentally determine the biosynthetic steps leading to the aminohexuronic acid moiety of nikkomycins.

Table 1: Overview on the enzymes involved in biosynthesis of the aminohexuronic acid moiety and assembly of nikkomycins

Enzyme	MW (kDa)	Calculated pI	Sequence Similarity
NikO	50.4	5.61	enolpyruvyl transferases
NikI	24.5	4.87	prolyl 4-hydroxylases
NikJ	50.5	5.38	Fe-S oxidoreductase/radical SAM protein
NikK	39.5	6.61	histidinol phosphate aminotransferases
NikL	25.9	10.15	tyrosine phosphatases
NikM	24.1	5.16	prolyl 4-hydroxylases
NikS	46.9	5.88	carboxylate-amine ligases/ATP grasp

Biosynthesis of aminohexuronic acid begins with formation of 3'-*enol*pruvyl-UMP. The reaction, which is catalyzed by NikO, was well investigated *in vitro* (98). To find out how 3´-EPUMP is further converted into the aminohexuronic acid moiety, is the aim of this work. The bicyclic structures nikkomycins S_x and S_z form one of the central intermediates in our hypothetic pathway. They were found by Schüz *et al* in the culture filtrate of the *Streptomyces tendae* Tü901/S 2566 strain. Upon addition of iron to the medium, they were produced in smaller amounts, with a subsequent increase in production of nikkomycins X and Z (99). Nikkomycins S_x and S_z possibly represent intermediates of the biosynthetic pathway that are converted to aminohexuronic acid in an iron-dependent manner. The iron-sulfur protein NikJ could be a candidate for such a conversion. It is puzzling, though, that nikkomycins S_x and S_z were not reported to be found in the culture filtrate of the main producer of nikkomycins, *Streptomyces tendae* Tü901/8c, but only in the culture filtrate of *nikK*, *nikL* and *nikM* deletion mutants (82). C. Bormann proposed that they were side products of nikkomycin biosynthesis, but that was before the discovery was made that 3´-EPUMP was the product of the NikO reaction, and not 5´-EP-uridine (98). The occurrence of bicyclic structures as intermediate would be a step towards explanation how the carbon skeleton is rearranged. Possibly, analysis of the *nik* genes of *Streptomyces tendae* Tü901/S 2566 and comparison to those of *Streptomyces tendae* Tü901/8c would give some hints on the role of nikkomycins S_x and S_z.
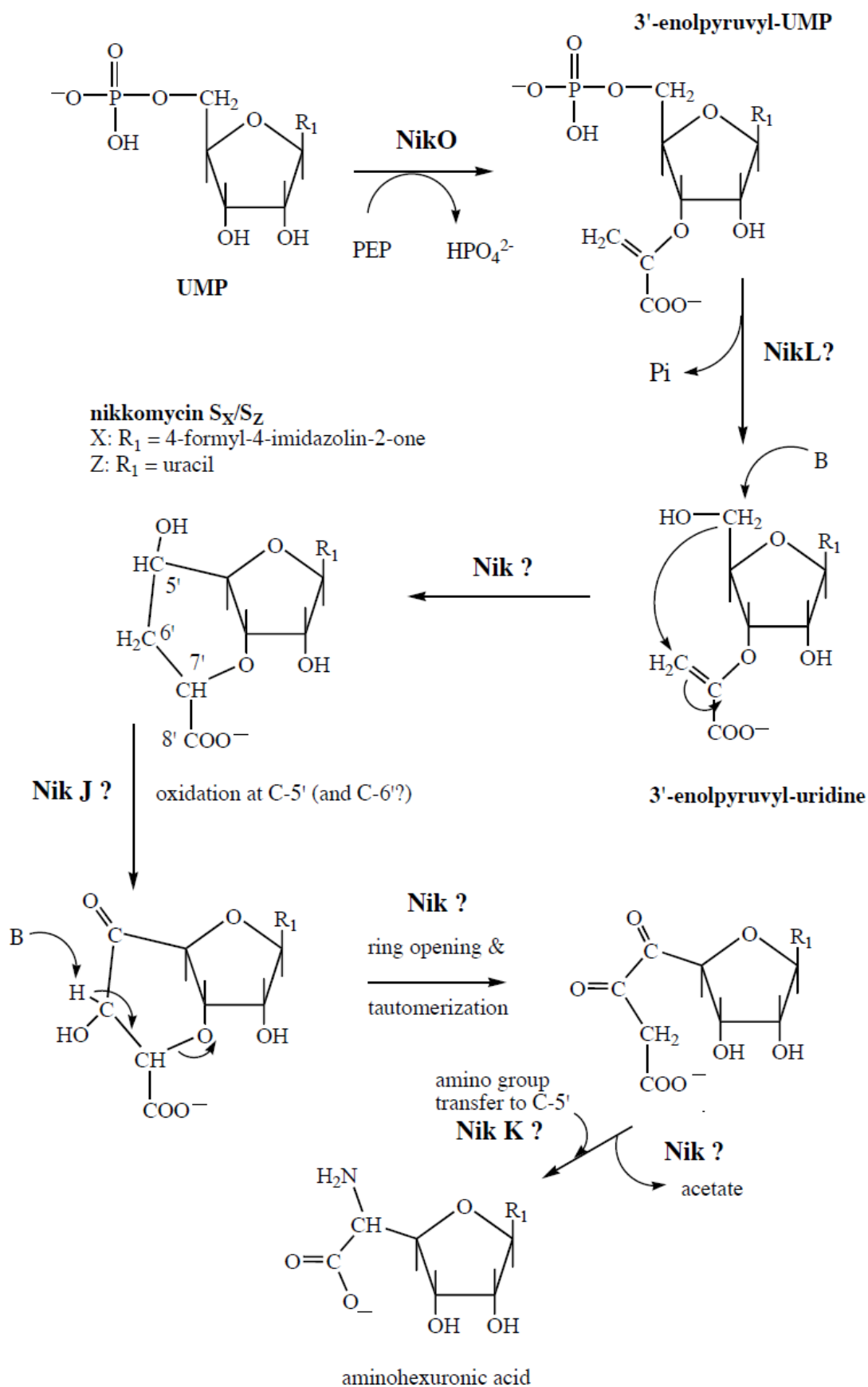
Scheme 14: Hypothetic pathway of biosynthesis of the aminohexuronic acid moiety of nikkomycins

Considering sequence similarities to tyrosine phosphatases, NikL was predicted to catalyze a dephosphorylation reaction. In our hypothetical pathway it catalyzes the dephosphorylation of 3´-EPUMP. However, as C. Bormann reported to have detected the bicyclic nikkomycins S_x and S_z in the culture filtrate of *nikL* deletion mutants (82), it is very doubtful that NikL represents the enzyme that follows NikO in the reaction cascade. In *S. ansochromogenes* the analogous gene to *nikL* and *nikK* is *sanB*, which encodes for a protein almost identical to a fusion protein of NikL and NikK. This gives rise to the speculation that NikL might have a regulating or stabilizing function on the NikK enzyme or that the reactions catalyzed by those enzymes are consecutive steps in the reaction pathway.

NikK shows sequence similarities to histidinol phosphate aminotransferases and is therefore expected to introduce the amino group into aminohexuronic acid. Indeed, aminotransferase activity of the PLP-dependent enzyme was observed. Several amino acids were shown to function as amino group donors. Unfortunately, attempts to synthesise the putative keto acid substrate were unsuccessful. Due to the lack of this substrate this hypothetic step could not be proven.

The biosynthetic pathway of the aminohexuronic acid moiety of nikkomycins was planned be elucidated by two different approaches. Disruption mutants of *Streptomyces tendae* were intended to produce biosynthetic intermediates, which would be isolated and identified. Furthermore, the structural *nik* genes were expressed in order to be characterized and tested for activity. A combination of both approaches, producing intermediates and using them as substrates for the heterologously expressed enzymes, was expected to shed light onto the biosynthetic steps leading to aminohexuronic acid. Unfortunately, both methods had their drawbacks. The *nik* gene disruption mutants available to us did not produce nikkomycin intermediates in detectable amounts. After some efforts it was possible to produce all the enzymes supposed to be involved in aminohexuronic acid biosynthesis. Their substrates were not known, and neither were potential cosubstrates, special requirements and preferred reaction conditions. These could only be guessed, considering sequence similarities with known and well investigated enzymes. That the product of the reaction catalyzed by NikO, 3´-EPUMP, was the only potential substrate available, proved to be a real bottleneck in our approaches to investigate the biosynthesis of nikkomycins. 3´-EPUMP should be the substrate for one of the enzymes encoded on the *nikIJKLMNO* gene cluster. The product

of this enzyme would serve as substrate for the subsequent enzyme in the reaction cascade, leading to the next intermediate and so on. The problem was, none of the enzymes was observed to convert 3´-EPUMP. This lack of substrates impaired a proper biochemical characterization of the enzymes. Most likely, the candidate for 3´-EPUMP conversion was inactive due to improper folding, inappropriate reaction conditions or the lack of a cosubstrate. Another explanation for the failure to convert 3´-EPUMP could be that the assumption that this substance is an intermediate of the nikkomycin biosynthetic pathway is not correct, and that the transfer of an enolpyruvyl moiety to the C-3´of UMP that is observed *in vitro*, is not the reaction that occurs in *Streptomyces tendae* during nikkomycin biosynthesis.

To finally be able to elucidate the biosynthetic pathway leading to the aminohexuronic acid of nikkomycins, it would be essential to obtain disruption mutants which secrete biosynthetic intermediates into the fermentation medium. It is hoped, that the application of a PCR targeting system, which was initially developed for *S. coelicolor* by Bertolt Gust *et al* (200), will serve to generate disruption mutants of the excellent nikkomycin producer *S. tendae* Tü901/8c.

CHAPTER 10

References

1. Latge, J. P. (2007) The cell wall: a carbohydrate armour for the fungal cell, *Mol. Microbiol. 66*, 279-290.

2. Lesage, G. and Bussey, H. (2006) Cell wall assembly in *Saccharomyces cerevisiae*, *Microbiol. Mol. Biol. Rev. 70*, 317-343.

3. Lorand, T. and Kocsis, B. (2007) Recent advances in antifungal agents, *Mini. Rev. Med. Chem. 7*, 900-911.

4. Dähn, U., Hagenmaier, H., Höhne, H., König, W. A., Wolf, G., and Zähner, H. (1976) Stoffwechselprodukte von Mikroorganismen. 154. Mitteilung. Nikkomycin, ein neuer Hemmstoff der Chitinsynthese bei Pilzen, *Arch. Microbiol. 107*, 143-160.

5. Winn, M., Goss, R. J., Kimura, K., and Bugg, T. D. (2010) Antimicrobial nucleoside antibiotics targeting cell wall assembly: recent advances in structure-function studies and nucleoside biosynthesis, *Nat. Prod. Rep. 27*, 279-304.

6. Suzuki, S., Isono, K., Nagatsu, J., Mizutani, T., Kawashima, Y., and Mizuno, T. (1965) A new antibiotic, polyoxin A, *J. Antibiot. (Tokyo) 18*, 131.

7. Isono, K., Asahi, K., and Suzuki, S. (1969) Studies on polyoxins, antifungal antibiotics. 13. The structure of polyoxins, *J. Am. Chem. Soc. 91*, 7490-7505.

8. Hector, R. F. (1993) Compounds active against cell walls of medically important fungi, *Clin. Microbiol. Rev. 6*, 1-21.

9. Uramoto, M., Kobinata, K., Isono, K., Jenkins, E. E., McCloskey, J. A., Higashijima, T., and Miyazawa, T. (1980) Neopolyoxins A, B, and C: new inhibitors of fungal cell wall chitin synthetase, *Nucleic Acids Symp. Ser.* s69-s71.

10. Chen, W., Zeng, H., and Tan, H. (2000) Cloning, sequencing, and function of sanF: A gene involved in nikkomycin biosynthesis of *Streptomyces ansochromogenes*, *Curr. Microbiol. 41*, 312-316.

11. Decker, H., Bormann, C., Fiedler, H. P., Zahner, H., Heitsch, H., and Konig, W. A. (1989) Metabolic products of microorganisms. 252. Isolation of new nikkomycins from *Streptomyces tendae*, *J. Antibiot. (Tokyo) 42*, 230-235.

12. Hagenmaier, H., Keckeisen, A., Zahner, H., and Konig, W. A. (1979) Metabolites of Microorganisms .182. Structure Elucidation of the Nucleoside Antibiotic Nikkomycin-X, *Liebigs Annalen der Chemie* 1494-1502.

13. Heitsch, H., Konig, W. A., Decker, H., Bormann, C., Fiedler, H. P., and Zahner, H. (1989) Metabolic products of microorganisms. 254. Structure of the new nikkomycins pseudo-Z and pseudo-J, *J. Antibiot. (Tokyo) 42*, 711-717.

14. Isono, K., Nagatsu, J., Kawashima, Y., and Suzuki, S. (1965) Studies on Polyoxins Antifungal Antibiotics .I. Isolation and Characterization of Polyoxins A and B, *Agricultural and Biological Chemistry 29*, 848-&.

15. Isono, K., Kobinata, K., and Suzuki, S. (1968) Isolation and Characterization of Polyoxins J, K and l New Components of Polyoxin Complex, *Agricultural and Biological Chemistry 32*, 792-&.

16. Isono, K. N. J., Kobinata, K., Sasaki, K., and Suzuki, S. (1967) Studies on Polyoxins Antifungal Antibiotics .V. Isolation and Characterization of Polyoxins C,D,E,F,G,H and I, *Agricultural and Biological Chemistry 31*, 190-&.

17. Obi, K., Uda, J., Iwase, K., Sugimoto, O., Ebisu, H., and Matsuda, A. (2000) Novel nikkomycin analogues: inhibitors of the fungal cell wall biosynthesis enzyme chitin synthase, *Bioorg. Med. Chem. Lett. 10*, 1451-1454.

18. Stauffer, C. S., Bhaket, P., Fothergill, A. W., Rinaldi, M. G., and Datta, A. (2007) Total synthesis and antifungal activity of a carbohydrate ring-expanded pyranosyl nucleoside analogue of nikkomycin B, *J. Org. Chem. 72*, 9991-9997.

19. Bormann, C., Lauer, B., Kalmanczhelyi, A., Süssmuth, R., and Jung, G. (1999) Novel nikkomycins Lx and Lz produced by genetically engineered *Streptomyces tendae* Tu901, *J. Antibiot. (Tokyo) 52*, 582-585.

20. Bormann, C., Huhn, W., Zähner, H., Rathmann, R., Hahn, H., and König, W. A. (1985) Metabolic products of microorganisms. 228. New nikkomycins produced by mutants of *Streptomyces tendae*, *J. Antibiot. (Tokyo) 38*, 9-16.

21.   Bormann, C., Mattern, S., Schrempf, H., Fiedler, H. P., and Zähner, H. (1989) Isolation of *Streptomyces tendae* mutants with an altered nikkomycin spectrum, *J. Antibiot. (Tokyo) 42*, 913-918.

22.   Decker, H., Walz, F., Bormann, C., Zähner, H., Fiedler, H. P., Heitsch, H., and König, W. A. (1990) Metabolic products of microorganisms. 255. Nikkomycins Wz and Wx, new chitin synthetase inhibitors from *Streptomyces tendae*, *J. Antibiot. (Tokyo) 43*, 43-48.

23.   Bormann, C., Kalmanczhelyi, A., Süssmuth, R., and Jung, G. (1999) Production of nikkomycins Bx and Bz by mutasynthesis with genetically engineered *Streptomyces tendae* Tu901, *J. Antibiot. (Tokyo) 52*, 102-108.

24.   Isono, K., Nagatsu, J., Kobinata, K., Sasaki, K., and Suzuki, S. (1967) Studies on Polyoxins Antifungal Antibiotics .V. Isolation and Characterization of Polyoxins C,D,E,F,G,H and I, *Agricultural and Biological Chemistry 31*, 190-&.

25.   Isono, K. (1988) Nucleoside antibiotics: structure, biological activity, and biosynthesis, *J. Antibiot. (Tokyo) 41*, 1711-1739.

26.   Endo, A. and Misato, T. (1969) Polyoxin D, a competitive inhibitor of UDP-N-acetylglucosamine: chitin N-acetylglucosaminyltransferase in *Neurospora crassa*, *Biochem. Biophys. Res. Commun. 37*, 718-722.

27.   Endo, A., Kakiki, K., and Misato, T. (1970) Mechanism of action of the antifugal agent polyoxin D, *J. Bacteriol. 104*, 189-196.

28.   Fox, J. J., Watanabe, K. A., and Bloch, A. (1966) Nucleoside antibiotics, *Prog. Nucleic Acid Res. Mol. Biol. 5*, 251-313.

29.   Gow, L. A. and Selitrennikoff, C. P. (1984) Chitin Synthetase of *Neurospora-Crassa* - Inhibition by Nikkomycin, Polyoxin-B, and Udp, *Current Microbiology 11*, 211-216.

30.   Müller, H., Furter, R., Zähner, H., and Rast, D. M. (1981) Metabolic Products of Microorganisms .203. Inhibition of Chitosomal Chitin Synthetase and Growth of *Mucor-Rouxii* by Nikkomycin-Z, Nikkomycin-X, and Polyoxin-A - A Comparison, *Archives of Microbiology 130*, 195-197.

31. Decker, H., Zähner, H., Heitsch, H., König, W. A., and Fiedler, H. P. (1991) Structure-activity relationships of the nikkomycins, *J. Gen. Microbiol. 137*, 1805-1813.

32. Hori, M., Kakiki, K., and Misato, T. (1974) Studies on Mode of Action of Polyoxins .4. Further Study on Relation of Polyoxin Structure to Chitin Synthetase Inhibition, *Agricultural and Biological Chemistry 38*, 691-698.

33. Mitani, M. and Inoue, Y. (1968) Antagonists of an antifungal substance, polyoxin, *J. Antibiot. (Tokyo) 21*, 492-496.

34. Yadan, J. C., Gonneau, M., Sarthou, P., and Legoffic, F. (1984) Sensitivity to Nikkomycin-Z in *Candida-Albicans* - Role of Peptide Permeases, *Journal of Bacteriology 160*, 884-888.

35. Emmer, G., Ryder, N. S., and Grassberger, M. A. (1985) Synthesis of new polyoxin derivatives and their activity against chitin synthase from *Candida albicans*, *J. Med. Chem. 28*, 278-281.

36. Khare, R. K., Becker, J. M., and Naider, F. R. (1988) Synthesis and anticandidal properties of polyoxin L analogues containing alpha-amino fatty acids, *J. Med. Chem. 31*, 650-656.

37. Krainer, E., Becker, J. M., and Naider, F. (1991) Synthesis and biological evaluation of dipeptidyl and tripeptidyl polyoxin and nikkomycin analogues as anticandidal prodrugs, *J. Med. Chem. 34*, 174-180.

38. Shenbagamurthi, P., Smith, H. A., Becker, J. M., Steinfeld, A., and Naider, F. (1983) Design of anticandidal agents: synthesis and biological properties of analogues of polyoxin L, *J. Med. Chem. 26*, 1518-1522.

39. Shenbagamurthi, P., Smith, H. A., Becker, J. M., and Naider, F. (1986) Synthesis and biological properties of chitin synthetase inhibitors resistant to cellular peptidases, *J. Med. Chem. 29*, 802-809.

40. Delzer, J., Fiedler, H. P., Müller, H., Zähner, H., Rathmann, R., Ernst, K., and König, W. A. (1984) New nikkomycins by mutasynthesis and directed fermentation, *J. Antibiot. (Tokyo) 37*, 80-82.

41. Bowen, A. R., Chenwu, J. L., Momany, M., Young, R., Szaniszlo, P. J., and Robbins, P. W. (1992) Classification of Fungal Chitin Synthases, *Proceedings of the National Academy of Sciences of the United States of America 89*, 519-523.

42. Cabib, E. (1991) Differential inhibition of chitin synthetases 1 and 2 from *Saccharomyces cerevisiae* by polyoxin D and nikkomycins, *Antimicrob. Agents Chemother. 35*, 170-173.

43. Bowers, B., Levin, G., and Cabib, E. (1974) Effect of polyoxin D on chitin synthesis and septum formation in *Saccharomyces cerevisiae*, *J. Bacteriol. 119*, 564-575.

44. Gooday, B. W. (1977) Biosynthesis of the fungal wall - mechanisms and implications. The first Fleming Lecture, *J. Gen. Microbiol. 99*, 1-11.

45. Hector, R. F. and Pappagianis, D. (1983) Inhibition of chitin synthesis in the cell wall of *Coccidioides immitis* by polyoxin D, *J. Bacteriol. 154*, 488-498.

46. Braun, P. C. and Calderone, R. A. (1978) Chitin synthesis in *Candida albicans*: comparison of yeast and hyphal forms, *J. Bacteriol. 133*, 1472-1477.

47. Chattaway, F. W., Holmes, M. R., and Barlow, A. J. (1968) Cell wall composition of the mycelial and blastospore forms of *Candida albicans*, *J. Gen. Microbiol. 51*, 367-376.

48. Hector, R. F., Zimmer, B. L., and Pappagianis, D. (1990) Evaluation of nikkomycins X and Z in murine models of coccidioidomycosis, histoplasmosis, and blastomycosis, *Antimicrob. Agents Chemother. 34*, 587-593.

49. Davis, T. E., Jr., Domer, J. E., and Li, Y. T. (1977) Cell wall studies of *Histoplasma capsulatum* and *Blastomyces dermatitidis* using autologous and heterologous enzymes, *Infect. Immun. 15*, 978-987.

50. Domer, J. E., Hamilton, J. G., and Harkin, J. C. (1967) Comparative study of the cell walls of the yeastlike and mycelial phases of *Histoplasma capsulatum*, *J. Bacteriol. 94*, 466-474.

51. Kanetsuna, F., Carbonell, L. M., Gil, F., and Azuma, I. (1974) Chemical and ultrastructural studies on the cell walls of the yeastlike and mycelial forms of *Histoplasma capsulatum*, *Mycopathol. Mycol. Appl. 54*, 1-13.

52. Reiss, E. (1977) Serial Enzymatic-Hydrolysis of Cell-Walls of 2 Serotypes of Yeast-Form *Histoplasma-Capsulatum* with Alpha(1-]3)-Glucanase, Beta(1-]3)-Glucanase, Pronase, and Chitinase, *Infection and Immunity 16*, 181-188.

53. Wheat, R. W., Tritschler, C., Conant, N. F., and Lowe, E. P. (1977) Comparison of *Coccidioides immitis* arthrospore, mycelium, and spherule cell walls, and influence of growth medium on mycelial cell wall composition, *Infect. Immun. 17*, 91-97.

54. McCarthy, P. J., Troke, P. F., and Gull, K. (1985) Mechanism of action of nikkomycin and the peptide transport system of *Candida albicans*, *J. Gen. Microbiol. 131*, 775-780.

55. Becker, J. M., Marcus, S., Tullock, J., Miller, D., Krainer, E., Khare, R. K., and Naider, F. (1988) Use of the Chitin-Synthesis Inhibitor Nikkomycin to Treat Disseminated Candidiasis in Mice, *Journal of Infectious Diseases 157*, 212-214.

56. Nix, D. E., Swezey, R. R., Hector, R., and Galgiani, J. N. (2009) Pharmacokinetics of Nikkomycin Z after Single Rising Oral Doses, *Antimicrobial Agents and Chemotherapy 53*, 2517-2521.

57. Clemons, K. V. and Stevens, D. A. (1997) Efficacy of nikkomycin Z against experimental pulmonary blastomycosis, *Antimicrob. Agents Chemother. 41*, 2026-2028.

58. Sandovsky-Losica, H., Shwartzman, R., Lahat, Y., and Segal, E. (2008) Antifungal activity against *Candida albicans* of nikkomycin Z in combination with caspofungin, voriconazole or amphotericin B, *J. Antimicrob. Chemother. 62*, 635-637.

59. Hector, R. F. and Laniado-Laborin, R. (2005) Coccidioidomycosis--a fungal disease of the Americas, *PLoS Med. 2*, e2.

60. Ampel, N. M., Mosley, D. G., England, B., Vertz, P. D., Komatsu, K., and Hajjeh, R. A. (1998) Coccidioidomycosis in Arizona: Increase in incidence from 1990 to 1995, *Clinical Infectious Diseases 27*, 1528-1530.

61. Cortez, K. J., Walsh, T. J., and Bennett, J. E. (2003) Successful treatment of coccidioidal meningitis with voriconazole, *Clinical Infectious Diseases 36*, 1619-1622.

62. Galgiani, J. N., Ampel, N. M., Catanzaro, A., Johnson, R. H., Stevens, D. A., and Williams, P. L. (2000) Practice guideline for the treatment of coccidioidomycosis. Infectious Diseases Society of America, *Clin. Infect. Dis. 30*, 658-661.

63. Galgiani, J. N., Catanzaro, A., Cloud, G. A., Johnson, R. H., Williams, P. L., Mirels, L. F., Nassar, F., Lutz, J. E., Stevens, D. A., Sharkey, P. K., Singh, V. R., Larsen, R. A., Delgado, K. L., Flanigan, C., and Rinaldi, M. G. (2000) Comparison of oral fluconazole and itraconazole for progressive, nonmeningeal coccidioidomycosis. A randomized, double-blind trial. Mycoses Study Group, *Ann. Intern. Med. 133*, 676-686.

64. Bakerspigel, A., Kane, J., and Schaus, D. (1986) Isolation of Blastomyces-Dermatitidis from An Earthen Floor in Southwestern Ontario, Canada, *Journal of Clinical Microbiology 24*, 890-891.

65. Denton, J. F., Mcdonough, E. S., Ajello, L., and Ausherman, R. J. (1961) Isolation of Blastomyces Dermatitidis from Soil, *Science 133*, 1126-&.

66. Denton, J. F. and Disalvo, A. F. (1964) Isolation of Blastomyces Dermatitidis from Natural Sites at Augusta Georgia, *American Journal of Tropical Medicine and Hygiene 13*, 716-&.

67. Denton, J. F. and Disalvo, A. F. (1979) Isolation of *Histoplasma-Capsulatum*, *Cryptococcus-Neoformans* and *Blastomyces-Dermatitidis* from the Same Natural Site, *Sabouraudia-Journal of Medical and Veterinary Mycology 17*, 193-195.

68. Dixon, D. M., Shadomy, H. J., and Shadomy, S. (1977) Invitro Growth and Sporulation of *Blastomyces-Dermatitidis* on Woody Plant Material, *Mycologia 69*, 1193-1195.

69. Crampton, T. L., Light, R. B., Berg, G. M., Meyers, M. P., Schroeder, G. C., Hershfield, E. S., and Embil, J. M. (2002) Epidemiology and clinical spectrum of blastomycosis diagnosed at Manitoba hospitals, *Clinical Infectious Diseases 34*, 1310-1316.

70. Medoff, G., Painter, A., and Kobayashi, G. S. (1987) Mycelial-Phase to Yeast-Phase Transitions of the Dimorphic Fungi *Blastomyces-Dermatitidis* and *Paracoccidioides-Brasiliensis*, *Journal of Bacteriology 169*, 4055-4060.

71. Chapman, S. W., Lin, A. C., Hendricks, K. A., Nolan, R. L., Currier, M. M., Morris, K. R., and Turner, H. R. (1997) Endemic blastomycosis in Mississippi: epidemiological and clinical studies, *Semin. Respir. Infect. 12*, 219-228.

72. Clinton, T. S. and Timko, A. L. (2003) Cutaneous blastomycosis without evidence of pulmonary involvement, *Mil. Med. 168*, 651-653.

73. Saccente, M. and Woods, G. L. (2010) Clinical and Laboratory Update on Blastomycosis, *Clinical Microbiology Reviews 23*, 367-+.

74. Lim, C. S., Rosli, R., Seow, H. F., and Chong, P. P. (2011) Candida and invasive candidiasis: back to basics, *Eur. J. Clin. Microbiol. Infect. Dis.*

75. Moosa, M. Y., Sobel, J. D., Elhalis, H., Du, W., and Akins, R. A. (2004) Fungicidal activity of fluconazole against *Candida albicans* in a synthetic vagina-simulative medium, *Antimicrob. Agents Chemother. 48*, 161-167.

76. Cowen, L. E., Nantel, A., Whiteway, M. S., Thomas, D. Y., Tessier, D. C., Kohn, L. M., and Anderson, J. B. (2002) Population genomics of drug resistance in *Candida albicans*, *Proc. Natl. Acad. Sci. U. S. A 99*, 9284-9289.

77. Drew, S. W. and Demain, A. L. (1977) Effect of Primary Metabolites on Secondary Metabolism, *Annual Review of Microbiology 31*, 343-356.

78. Martin, J. F. and Demain, A. L. (1980) Control of antibiotic biosynthesis, *Microbiol. Rev. 44*, 230-251.

79. Motamedi, H. and Hutchinson, C. R. (1987) Cloning and heterologous expression of a gene cluster for the biosynthesis of tetracenomycin C, the anthracycline antitumor antibiotic of *Streptomyces glaucescens*, *Proc. Natl. Acad. Sci. U. S. A 84*, 4445-4449.

80. Möhrle, V., Roos, U., and Bormann, C. (1995) Identification of cellular proteins involved in nikkomycin production in *Streptomyces tendae* Tu901, *Mol. Microbiol. 15*, 561-571.

81. Bormann, C., Möhrle, V., and Bruntner, C. (1996) Cloning and heterologous expression of the entire set of structural genes for nikkomycin synthesis from Streptomyces tendae Tu901 in *Streptomyces lividans*, *J. Bacteriol. 178*, 1216-1218.

82. Bormann, C. (2002) Biosynthesis of the peptidyl nucleoside antibiotic nikkomycin in *Streptomyces tendae* Tü901 deduced from the analysis of the gene cluster and mutational studies, in *Microbial Secondary Metabolites: Biosynthesis, Genetics and Regulation* (Fierro, F. and Martin J.F., Eds.) pp 43-61.

83. Bruntner, C., Lauer, B., Schwarz, W., Mohrle, V., and Bormann, C. (1999) Molecular characterization of co-transcribed genes from *Streptomyces tendae* Tu901 involved in the biosynthesis of the peptidyl moiety of the peptidyl nucleoside antibiotic nikkomycin, *Mol. Gen. Genet. 262*, 102-114.

84. Lauer, B., Russwurm, R., and Bormann, C. (2000) Molecular characterization of two genes from *Streptomyces tendae* Tü901 required for the formation of the 4-formyl-4-imidazolin-2-one-containing nucleoside moiety of the peptidyl nucleoside antibiotic nikkomycin, *Eur. J. Biochem. 267*, 1698-1706.

85. Bruntner, C. and Bormann, C. (1998) The *Streptomyces tendae* Tu901 L-lysine 2-aminotransferase catalyzes the initial reaction in nikkomycin D biosynthesis, *Eur. J. Biochem. 254*, 347-355.

86. Nishina, Y., Sato, K., and Shiga, K. (1991) Isomerization of delta 1-piperideine-2-carboxylate to delta 2-piperideine-2-carboxylate on complexation with flavoprotein D-amino acid oxidase, *J. Biochem. 109*, 705-710.

87. Venci, D., Zhao, G., and Jorns, M. S. (2002) Molecular characterization of NikD, a new flavoenzyme important in the biosynthesis of nikkomycin antibiotics, *Biochemistry 41*, 15795-15802.

88. Bruckner, R. C., Zhao, G., Venci, D., and Jorns, M. S. (2004) Nikkomycin biosynthesis: formation of a 4-electron oxidation product during turnover of NikD with its physiological substrate, *Biochemistry 43*, 9160-9167.

89. Moon, M. and Van Lanen, S. G. (2010) Characterization of a dual specificity aryl acid adenylation enzyme with dual function in nikkomycin biosynthesis, *Biopolymers 93*, 791-801.

90. Niu, G., Liu, G., Tian, Y., and Tan, H. (2006) SanJ, an ATP-dependent picolinate-CoA ligase, catalyzes the conversion of picolinate to picolinate-CoA during nikkomycin biosynthesis in *Streptomyces ansochromogenes*, *Metab Eng 8*, 183-195.

91. Ling, H. B., Wang, G. J., Li, J. E., and Tan, H. R. (2008) sanN encoding a dehydrogenase is essential for Nikkomycin biosynthesis in *Streptomyces ansochromogenes*, *J. Microbiol. Biotechnol. 18*, 397-403.

92. Ling, H., Wang, G., Tian, Y., Liu, G., and Tan, H. (2007) SanM catalyzes the formation of 4-pyridyl-2-oxo-4-hydroxyisovalerate in nikkomycin biosynthesis by interacting with SanN, *Biochem. Biophys. Res. Commun. 361*, 196-201.

93. Li, Y., Ling, H., Li, W., and Tan, H. (2005) Improvement of nikkomycin production by enhanced copy of sanU and sanV in *Streptomyces ansochromogenes* and characterization of a novel glutamate mutase encoded by sanU and sanV, *Metab Eng 7*, 165-173.

94. Jia, L., Tian, Y., and Tan, H. (2007) SanT, a bidomain protein, is essential for nikkomycin biosynthesis of *Streptomyces ansochromogenes*, *Biochem. Biophys. Res. Commun. 362*, 1031-1036.

95. Xie, Z., Niu, G., Li, R., Liu, G., and Tan, H. (2007) Identification and characterization of sanH and sanI involved in the hydroxylation of pyridyl residue during nikkomycin biosynthesis in *Streptomyces ansochromogenes*, *Curr. Microbiol. 55*, 537-542.

96. Chen, H., Hubbard, B. K., O'Connor, S. E., and Walsh, C. T. (2002) Formation of beta-hydroxy histidine in the biosynthesis of nikkomycin antibiotics, *Chem. Biol. 9*, 103-112.

97.   Lauer, B., Süssmuth, R., Kaiser, D., Jung, G., and Bormann, C. (2000) A putative enolpyruvyl transferase gene involved in nikkomycin biosynthesis, *J. Antibiot. (Tokyo) 53*, 385-392.

98.   Ginj, C., Ruegger, H., Amrhein, N., and Macheroux, P. (2005) 3'-Enolpyruvyl-UMP, a novel and unexpected metabolite in nikkomycin biosynthesis, *Chembiochem. 6*, 1974-1976.

99.   Schüz, T. C., Fiedler, H. P., Zähner, H., Rieck, M., and König, W. A. (1992) Metabolic products of microorganisms. 263. Nikkomycins S_Z, S_X, So_Z and So_X, new intermediates associated to the nikkomycin biosynthesis of *Streptomyces tendae*, *J. Antibiot. (Tokyo) 45*, 199-206.

100.   Lauer, B., Russwurm, R., Schwarz, W., Kalmanczhelyi, A., Bruntner, C., Rosemeier, A., and Bormann, C. (2001) Molecular characterization of co-transcribed genes from *Streptomyces tendae* Tü901 involved in the biosynthesis of the peptidyl moiety and assembly of the peptidyl nucleoside antibiotic nikkomycin, *Molecular and General Genetics 264*, 662-673.

101.   Artymiuk, P. J., Poirrette, A. R., Rice, D. W., and Willett, P. (1996) Biotin carboxylase comes into the fold, *Nature Structural Biology 3*, 128-132.

102.   Galperin, M. Y. and Koonin, E. V. (1997) A diverse superfamily of enzymes with ATP-dependent carboxylate-amine/thiol ligase activity, *Protein Science 6*, 2639-2643.

103.   Healy, V. L., Mullins, L. S., Li, X., Hall, S. E., Raushel, F. M., and Walsh, C. T. (2000) D-Ala-D-X ligases: evaluation of D-alanyl phosphate intermediate by MIX, PIX and rapid quench studies, *Chem. Biol. 7*, 505-514.

104.   Li, Y., Zeng, H., and Tan, H. (2004) Cloning, function, and expression of sanS: a gene essential for nikkomycin biosynthesis of *Streptomyces ansochromogenes*, *Curr. Microbiol. 49*, 128-132.

105.   Bibb, M. J. (2005) Regulation of secondary metabolism in streptomycetes, *Current Opinion in Microbiology 8*, 208-215.

106.   Takano, E. (2006) γ-Butyrolactones: *Streptomyces* signalling molecules regulating antibiotic production and differentiation, *Current Opinion in Microbiology 9*, 287-294.

107.   Wietzorrek, A. and Bibb, M. (1997) A novel family of proteins that regulates antibiotic production in streptomycetes appears to contain an OmpR-like DNA-binding fold, *Molecular Microbiology 25*, 1181-1184.

108.   Tanaka, A., Takano, Y., Ohnishi, Y., and Horinouchi, S. (2007) AfsR recruits RNA polymerase to the *afsS* promoter: A model for transcriptional activation by SARPs, *Journal of Molecular Biology 369*, 322-333.

109.   Anton, N., Mendes, M. V., Martin, J. F., and Aparicio, J. F. (2004) Identification of PimR as a positive regulator of pimaricin biosynthesis in *Streptomyces natalensis*, *Journal of Bacteriology 186*, 2567-2575.

110.   Ikeda, H., Ishikawa, J., Hanamoto, A., Shinose, M., Kikuchi, H., Shiba, T., Sakaki, Y., Hattori, M., and Omura, S. (2003) Complete genome sequence and comparative analysis of the industrial microorganism *Streptomyces avermitilis*, *Nat. Biotechnol. 21*, 526-531.

111.   He, X., Li, R., Pan, Y., Liu, G., and Tan, H. (2010) SanG, a transcriptional activator, controls nikkomycin biosynthesis through binding to the sanN-sanO intergenic region in *Streptomyces ansochromogenes*, *Microbiology 156*, 828-837.

112.   Liu, G., Tian, Y., Yang, H., and Tan, H. (2005) A pathway-specific transcriptional regulatory gene for nikkomycin biosynthesis in *Streptomyces ansochromogenes* that also influences colony development, *Mol. Microbiol. 55*, 1855-1866.

113.   Li, W., Liu, G., and Tan, H. (2003) Disruption of sabR affects nikkomycin biosynthesis and morphogenesis in *Streptomyces ansochromogenes*, *Biotechnol. Lett. 25*, 1491-1497.

114.   Chater, K. F. and Horinouchi, S. (2003) Signalling early developmental events in two highly diverged *Streptomyces species*, *Mol. Microbiol. 48*, 9-15.

115. Liao, G., Li, J., Li, L., Yang, H., Tian, Y., and Tan, H. (2009) Selectively improving nikkomycin Z production by blocking the imidazolone biosynthetic pathway of nikkomycin X and uracil feeding in *Streptomyces ansochromogenes*, *Microb. Cell Fact. 8*, 61.

116. Olano, C., Lombo, F., Mendez, C., and Salas, J. A. (2008) Improving production of bioactive secondary metabolites in actinomycetes by metabolic engineering, *Metab Eng 10*, 281-292.

117. Santos, C. N. and Stephanopoulos, G. (2008) Combinatorial engineering of microbes for optimizing cellular phenotype, *Curr. Opin. Chem. Biol. 12*, 168-176.

118. Liao, G., Li, J., Li, L., Yang, H., Tian, Y., and Tan, H. (2010) Cloning, reassembling and integration of the entire nikkomycin biosynthetic gene cluster into *Streptomyces ansochromogenes* lead to an improved nikkomycin production, *Microb. Cell Fact. 9*, 6.

119. Gustav Oberdorfer (2011) Structural Studies on Enzymes of Nikkomycin Biosynthesis, Doctoral Thesis.

120. Iacob Cristian Ginj (2005) Biochemical Characterization of NikO, a New *Enol*pyruvyltransferase from *Streptomyces tendae* Tü901/8c.

121. Bugg, T. D. H. and Walsh, C. T. (1992) Intracellular Steps of Bacterial-Cell Wall Peptidoglycan Biosynthesis - Enzymology, Antibiotics, and Antibiotic-Resistance, *Natural Product Reports 9*, 199-215.

122. Arca, P., Reguera, G., and Hardisson, C. (1997) Plasmid-encoded fosfomycin resistance in bacteria isolated from the urinary tract in a multicentre survey, *Journal of Antimicrobial Chemotherapy 40*, 393-399.

123. Katayama, N., Tsubotani, S., Nozaki, Y., Harada, S., and Ono, H. (1990) Fosfadecin and fosfocytocin, new nucleotide antibiotics produced by bacteria, *J. Antibiot. (Tokyo) 43*, 238-246.

124. Kahan, F. M., Kahan, J. S., Cassidy, P. J., and Kropp, H. (1974) The mechanism of action of fosfomycin (phosphonomycin), *Ann. N. Y. Acad. Sci. 235*, 364-386.

125. Campbell, S. A., Richards, T. A., Mui, E. J., Samuel, B. U., Coggins, J. R., McLeod, R., and Roberts, C. W. (2004) A complete shikimate pathway in *Toxoplasma gondii:* an ancient eukaryotic innovation, *International Journal for Parasitology 34*, 5-13.

126. Roberts, C. W., Roberts, F., Lyons, R. E., Kirisits, M. J., Mui, E. J., Finnerty, J., Johnson, J. J., Ferguson, D. J. P., Coggins, J. R., Krell, T., Coombs, G. H., Milhous, W. K., Kyle, D. E., Tzipori, S., Barnwell, J., Dame, J. B., Carlton, J., and McLeod, R. (2002) The shikimate pathway and its branches in apicomplexan parasites, *Journal of Infectious Diseases 185*, S25-S36.

127. Roberts, F., Roberts, C. W., Johnson, J. J., Kyle, D. E., Krell, T., Coggins, J. R., Coombs, G. H., Milhous, W. K., Tzipori, S., Ferguson, D. J. P., Chakrabarti, D., and McLeod, R. (1998) Evidence for the shikimate pathway in apicomplexan parasites, *Nature 393*, 801-805.

128. Mousdale, D. M. and Coggins, J. R. (1987) 3-Phosphoshikimate 1-Carboxyvinyltransferase from *Pisum-Sativum*, *Methods in Enzymology 142*, 348-354.

129. Steinrucken, H. C. and Amrhein, N. (1984) 5-Enolpyruvylshikimate-3-Phosphate Synthase of *Klebsiella-Pneumoniae* .2. Inhibition by Glyphosate [N-(Phosphonomethyl)Glycine], *European Journal of Biochemistry 143*, 351-357.

130. Schonbrunn, E., Sack, S., Eschenburg, S., Perrakis, A., Krekel, F., Amrhein, N., and Mandelkow, E. (1996) Crystal structure of UDP-N-acetylglucosamine enolpyruvyltransferase, the target of the antibiotic fosfomycin, *Structure 4*, 1065-1075.

131. Skarzynski, T., Mistry, A., Wonacott, A., Hutchinson, S. E., Kelly, V. A., and Duncan, K. (1996) Structure of UDP-N-acetylglucosamine enolpyruvyl transferase, an enzyme essential for the synthesis of bacterial peptidoglycan, complexed with substrate UDP-N-acetylglucosamine and the drug fosfomycin, *Structure 4*, 1465-1474.

132. Skarzynski, T., Kim, D. H., Lees, W. J., Walsh, C. T., and Duncan, K. (1998) Stereochemical course of enzymatic enolpyruvyl transfer and catalytic conformation of the active site revealed by the crystal structure of the fluorinated analogue of the reaction tetrahedral intermediate bound to the active site of the C115A mutant of MurA, *Biochemistry 37*, 2572-2577.

133.   Krekel, F., Oecking, C., Amrhein, N., and Macheroux, P. (1999) Substrate and inhibitor-induced conformational changes in the structurally related enzymes UDP-N-acetylglucosamine enolpyruvyl transferase (MurA) and 5-enolpyruvylshikimate 3-phosphate synthase (EPSPS), *Biochemistry 38*, 8864-8878.

134.   Marquardt, J. L., Brown, E. D., Lane, W. S., Haley, T. M., Ichikawa, Y., Wong, C. H., and Walsh, C. T. (1994) Kinetics, stoichiometry, and identification of the reactive thiolate in the inactivation of UDP-GlcNAc enolpyruvoyl transferase by the antibiotic fosfomycin, *Biochemistry 33*, 10646-10651.

135.   Krekel, F., Samland, A. K., Macheroux, P., Amrhein, N., and Evans, J. N. (2000) Determination of the pKa value of C115 in MurA (UDP-N-acetylglucosamine enolpyruvyltransferase) from *Enterobacter cloacae*, *Biochemistry 39*, 12671-12677.

136.   Isono, K., Sato, T., Hirasawa, K., Funayama, S., and Suzuki, S. (1978) Biosynthesis of Polyoxins, Nucleoside Peptide Antibiotics - Biosynthesis of Nucleoside Skeleton of Polyoxins, *Journal of the American Chemical Society 100*, 3937-3939.

137.   Paul, S. and Lombroso, P. J. (2003) Receptor and nonreceptor protein tyrosine phosphatases in the nervous system, *Cell Mol. Life Sci. 60*, 2465-2482.

138.   Wang, W. Q., Sun, J. P., and Zhang, Z. Y. (2003) An overview of the protein tyrosine phosphatase superfamily, *Curr. Top. Med. Chem. 3*, 739-748.

139.   Beinert, H. (2000) Iron-sulfur proteins: ancient structures, still full of surprises, *Journal of Biological Inorganic Chemistry 5*, 2-15.

140.   Noodleman, L., Lovell, T., Liu, T. Q., Himo, F., and Torres, R. A. (2002) Insights into properties and energetics of iron-sulfur proteins from simple clusters to nitrogenase, *Current Opinion in Chemical Biology 6*, 259-273.

141.   Beinert, H., Holm, R. H., and Munck, E. (1997) Iron-sulfur clusters: nature's modular, multipurpose structures, *Science 277*, 653-659.

142.   Peters, J. W., Lanzilotta, W. N., Lemon, B. J., and Seefeldt, L. C. (1998) X-ray crystal structure of the Fe-only hydrogenase (CpI) from *Clostridium pasteurianum* to 1.8 angstrom resolution, *Science 282*, 1853-1858.

143. Werst, M. M., Kennedy, M. C., Houseman, A. L. P., Beinert, H., and Hoffman, B. M. (1990) Characterization of the [4Fe-4S]+ Cluster at the Active-Site of Aconitase by Fe-57, S-33, and N-14 Electron Nuclear Double-Resonance Spectroscopy, *Biochemistry 29*, 10533-10540.

144. Beinert, H. and Kennedy, M. C. (1993) Aconitase, a two-faced protein: enzyme and iron regulatory factor, *FASEB J. 7*, 1442-1449.

145. Wang, S. C. and Frey, P. A. (2007) S-adenosylmethionine as an oxidant: the radical SAM superfamily, *Trends in Biochemical Sciences 32*, 101-110.

146. Hidalgo, E., Ding, H., and Demple, B. (1997) Redox signal transduction via iron-sulfur clusters in the SoxR transcription activator, *Trends Biochem. Sci. 22*, 207-210.

147. Haile, D. J., Rouault, T. A., Harford, J. B., Kennedy, M. C., Blondin, G. A., Beinert, H., and Klausner, R. D. (1992) Cellular regulation of the iron-responsive element binding protein: disassembly of the cubane iron-sulfur cluster results in high-affinity RNA binding, *Proc. Natl. Acad. Sci. U. S. A 89*, 11735-11739.

148. Hentze, M. W. and Kuhn, L. C. (1996) Molecular control of vertebrate iron metabolism: mRNA-based regulatory circuits operated by iron, nitric oxide, and oxidative stress, *Proc. Natl. Acad. Sci. U. S. A 93*, 8175-8182.

149. Bandyopadhyay, S., Chandramouli, K., and Johnson, M. K. (2008) Iron-sulfur cluster biosynthesis, *Biochem. Soc. Trans. 36*, 1112-1119.

150. Fontecave, M., Choudens, S. O., Py, B., and Barras, F. (2005) Mechanisms of iron-sulfur cluster assembly: the SUF machinery, *J. Biol. Inorg. Chem. 10*, 713-721.

151. Takahashi, Y. and Nakamura, M. (1999) Functional assignment of the ORF2-iscS-iscU-iscA-hscB-hscA-fdx-ORF3 gene cluster involved in the assembly of Fe-S clusters in *Escherichia coli*, *Journal of Biochemistry 126*, 917-926.

152. Zheng, L. M., Cash, V. L., Flint, D. H., and Dean, D. R. (1998) Assembly of iron-sulfur clusters - Identification of an iscSUA-hscBA-fdx gene cluster from *Azotobacter vinelandii*, *Journal of Biological Chemistry 273*, 13264-13272.

153.   Balk, J. and Lobreaux, S. (2005) Biogenesis of iron-sulfur proteins in plants, *Trends in Plant Science 10*, 324-331.

154.   Lill, R. and Mühlenhoff, U. (2006) Iron-sulfur protein biogenesis in eukaryotes: Components and mechanisms, *Annual Review of Cell and Developmental Biology 22*, 457-486.

155.   Takahashi, Y. and Tokumoto, U. (2002) A third bacterial system for the assembly of iron-sulfur clusters with homologs in archaea and plastids, *Journal of Biological Chemistry 277*, 28380-28383.

156.   Mihara, H. and Esaki, N. (2002) Bacterial cysteine desulfurases: their function and mechanisms, *Applied Microbiology and Biotechnology 60*, 12-23.

157.   Sendra, M., de Choudens, S. O., Lascoux, D., Sanakis, Y., and Fontecave, M. (2007) The SUF iron-sulfur cluster biosynthetic machinery: Sulfur transfer from the SUFS-SUFE complex to SUFA, *Febs Letters 581*, 1362-1368.

158.   Smith, A. D., Agar, J. N., Johnson, K. A., Frazzon, J., Amster, I. J., Dean, D. R., and Johnson, M. K. (2001) Sulfur transfer from IscS to IscU: The first step in iron-sulfur cluster biosynthesis, *Journal of the American Chemical Society 123*, 11103-11104.

159.   Agar, J. N., Krebs, C., Frazzon, J., Huynh, B. H., Dean, D. R., and Johnson, M. K. (2000) IscU as a scaffold for iron-sulfur cluster biosynthesis: Sequential assembly of [2Fe-2S] and [4Fe-4S] clusters in IscU, *Biochemistry 39*, 7856-7862.

160.   Krebs, C., Agar, J. N., Smith, A. D., Frazzon, J., Dean, D. R., Huynh, B. H., and Johnson, M. K. (2001) IscA, an alternate scaffold for Fe-S cluster biosynthesis, *Biochemistry 40*, 14069-14080.

161.   Ollagnier-de-Choudens, S., Mattioli, T., Tagahashi, Y., and Fontecave, M. (2001) Iron-sulfur cluster assembly - Characterization of IscA and evidence for a specific and functional complex with ferredoxin, *Journal of Biological Chemistry 276*, 22604-22607.

162. Yuvaniyama, P., Agar, J. N., Cash, V. L., Johnson, M. K., and Dean, D. R. (2000) NifS-directed assembly of a transient [2Fe-2S] cluster within the NifU protein, *Proceedings of the National Academy of Sciences of the United States of America 97*, 599-604.

163. Layer, G., Ollagnier-de Choudens, S., Sanakis, Y., and Fontecave, M. (2006) Iron-sulfur cluster biosynthesis - Characterization of *Escherichia coli* CyaY as an iron donor for the assembly of [2Fe-2S] clusters in the scaffold IscU, *Journal of Biological Chemistry 281*, 16256-16263.

164. Chen, D. W., Walsby, C., Hoffman, B. M., and Frey, P. A. (2003) Coordination and mechanism of reversible cleavage of S-adenosylmethionine by the [4Fe-4S] center in lysine 2,3-aminomutase, *Journal of the American Chemical Society 125*, 11788-11789.

165. Cosper, M. M., Jameson, G. N. L., Davydov, R., Eidsness, M. K., Hoffman, B. M., Huynh, B. H., and Johnson, M. K. (2002) The [4Fe-4S](2+) cluster in reconstituted biotin synthase binds S-adenosyl-L-methionine, *Journal of the American Chemical Society 124*, 14006-14007.

166. Hanzelmann, P. and Schindelin, H. (2004) Crystal structure of the S-adenosylmethionine-dependent enzyme MoaA and its implications for molybdenum cofactor deficiency in humans, *Proceedings of the National Academy of Sciences of the United States of America 101*, 12870-12875.

167. Krebs, C., Broderick, W. E., Henshaw, T. F., Broderick, J. B., and Huynh, B. H. (2002) Coordination of adenosylmethionine to a unique iron site of the [4Fe-4S] of pyruvate formate-lyase activating enzyme: A Mossbauer spectroscopic study, *Journal of the American Chemical Society 124*, 912-913.

168. Layer, G., Moser, J., Heinz, D. W., Jahn, D., and Schubert, W. D. (2003) Crystal structure of coproporphyrinogen III oxidase reveals cofactor geometry of Radical SAM enzymes, *Embo Journal 22*, 6214-6224.

169.   Walsby, C. J., Ortillo, D., Broderick, W. E., Broderick, J. B., and Hoffman, B. M. (2002) An anchoring role for FeS clusters: Chelation of the amino acid moiety of S-adenosylmethionine to the unique iron site of the [4Fe-4S] cluster of pyruvate formate-lyase activating enzyme, *Journal of the American Chemical Society 124*, 11270-11271.

170.   Walsby, C. J., Hong, W., Broderick, W. E., Cheek, J., Ortillo, D., Broderick, J. B., and Hoffman, B. M. (2002) Electron-nuclear double resonance spectroscopic evidence that S-adenosylmethionine binds in contact with the catalytically active [4Fe-4S](+) cluster of pyruvate formate-lyase activating enzyme, *Journal of the American Chemical Society 124*, 3143-3151.

171.   Chirpich, T. P., Zappia, V., Costilow, R. N., and Barker, H. A. (1970) Lysine 2,3-Aminomutase - Purification and Properties of A Pyridoxal Phosphate and S-Adenosylmethionine-Activated Enzyme, *Journal of Biological Chemistry 245*, 1778-89.

172.   Sofia, H. J., Chen, G., Hetzler, B. G., Reyes-Spindola, J. F., and Miller, N. E. (2001) Radical SAM, a novel protein superfamily linking unresolved steps in familiar biosynthetic pathways with radical mechanisms: functional characterization using new analysis and information visualization methods, *Nucleic Acids Research 29*, 1097-1106.

173.   Frey, P. A. and Magnusson, O. T. (2003) S-Adenosylmethionine: A wolf in sheep's clothing, or a rich man's adenosylcobalamin? *Chemical Reviews 103*, 2129-2148.

174.   Jarrett, J. T. (2003) The generation of 5 '-deoxyadenosyl radicals by adenosylmethionine-dependent radical enzymes, *Current Opinion in Chemical Biology 7*, 174-182.

175.   Gräwert, T., Kaiser, J., Zepeck, F., Laupitz, R., Hecht, S., Amslinger, S., Schramek, N., Schleicher, E., Weber, S., Haslbeck, M., Buchner, J., Rieder, C., Arigoni, D., Bacher, A., Eisenreich, W., and Rohdich, F. (2004) IspH protein of *Escherichia coli*: Studies on iron-sulfur cluster implementation and catalysis, *Journal of the American Chemical Society 126*, 12847-12855.

176.   Khoroshilova, N., Beinert, H., and Kiley, P. J. (1995) Association of a polynuclear iron-sulfur center with a mutant FNR protein enhances DNA binding, *Proc. Natl. Acad. Sci. U. S. A 92*, 2499-2503.

177. Tran, Q. H., Arras, T., Becker, S., Holighaus, G., Ohlberger, G., and Unden, G. (2000) Role of glutathione in the formation of the active form of the oxygen sensor FNR ([4Fe-4S].FNR) and in the control of FNR function, *Eur. J. Biochem. 267*, 4817-4824.

178. Fish, W. W. (1988) Rapid Colorimetric Micromethod for the Quantitation of Complexed Iron in Biological Samples, *Methods in Enzymology 158*, 357-364.

179. Rubach, J. K., Brazzolotto, X., Gaillard, J., and Fontecave, M. (2005) Biochemical characterization of the HydE and HydG iron-only hydrogenase maturation enzymes from *Thermatoga maritima*, *FEBS Lett. 579*, 5055-5060.

180. Kivirikko, K. I., Myllylä, R., and Pihlajaniemi, T. (1989) Protein hydroxylation: prolyl 4-hydroxylase, an enzyme with four cosubstrates and a multifunctional subunit, *FASEB J. 3*, 1609-1617.

181. Gorres, K. L. and Raines, R. T. (2010) Prolyl 4-hydroxylase, *Crit Rev. Biochem. Mol. Biol. 45*, 106-124.

182. Shoulders, M. D. and Raines, R. T. (2009) Collagen structure and stability, *Annu. Rev. Biochem. 78*, 929-958.

183. Wu, H., de, G. B., Mariani, C., and Cheung, A. Y. (2001) Hydroxyproline-rich glycoproteins in plant reproductive tissues: structure, functions and regulation, *Cell Mol. Life Sci. 58*, 1418-1429.

184. Baldwin, J. E., Field, R. A., Lawrence, C. C., Merritt, K. D., and Schofield, C. J. (1993) Proline 4-Hydroxylase - Stereochemical Course of the Reaction, *Tetrahedron Letters 34*, 7489-7492.

185. Adefarati, A. A., Giacobbe, R. A., Hensens, O. D., and Tkacz, J. S. (1991) Biosynthesis of L-671,329, An Echinocandin-Type Antibiotic Produced by *Zalerion-Arboricola* - Origins of Some of the Unusual Amino-Acids and the Dimethylmyristic Acid Side-Chain, *Journal of the American Chemical Society 113*, 3542-3545.

186. Rhoads, R. E. and Udenfriend, S. (1968) Decarboxylation of alpha-ketoglutarate coupled to collagen proline hydroxylase, *Proc. Natl. Acad. Sci. U. S. A 60*, 1473-1478.

187. Counts, D. F., Cardinale, G. J., and Udenfriend, S. (1978) Prolyl hydroxylase half reaction: peptidyl prolyl-independent decarboxylation of alpha-ketoglutarate, *Proc. Natl. Acad. Sci. U. S. A 75*, 2145-2149.

188. Myllylä, R., Majamaa, K., Gunzler, V., Hanauske-Abel, H. M., and Kivirikko, K. I. (1984) Ascorbate is consumed stoichiometrically in the uncoupled reactions catalyzed by prolyl 4-hydroxylase and lysyl hydroxylase, *J. Biol. Chem. 259*, 5403-5405.

189. Helaakoski, T., Vuori, K., Myllylä, R., Kivirikko, K. I., and Pihlajaniemi, T. (1989) Molecular cloning of the alpha-subunit of human prolyl 4-hydroxylase: the complete cDNA-derived amino acid sequence and evidence for alternative splicing of RNA transcripts, *Proc. Natl. Acad. Sci. U. S. A 86*, 4392-4396.

190. Vuori, K., Pihlajaniemi, T., Myllylä, R., and Kivirikko, K. I. (1992) Site-directed mutagenesis of human protein disulphide isomerase: effect on the assembly, activity and endoplasmic reticulum retention of human prolyl 4-hydroxylase in *Spodoptera frugiperda* insect cells, *EMBO J. 11*, 4213-4217.

191. Culpepper, M. A., Scott, E. E., and Limburg, J. (2010) Crystal structure of prolyl 4-hydroxylase from *Bacillus anthracis*, *Biochemistry 49*, 124-133.

192. Ellsworth, B. A., Tom, N. J., and Bartlett, P. A. (1996) Synthesis and evaluation of inhibitors of bacterial D-alanine:D-alanine ligases, *Chem. Biol. 3*, 37-44.

193. Zawadzke, L. E., Bugg, T. D., and Walsh, C. T. (1991) Existence of two D-alanine: D-alanine ligases in *Escherichia coli*: cloning and sequencing of the *ddlA* gene and purification and characterization of the DdlA and DdlB enzymes, *Biochemistry 30*, 1673-1682.

194. Walsh, C. T. (1989) Enzymes in the D-Alanine Branch of Bacterial-Cell Wall Peptidoglycan Assembly, *Journal of Biological Chemistry 264*, 2393-2396.

195. Fan, C., Moews, P. C., Walsh, C. T., and Knox, J. R. (1994) Vancomycin Resistance - Structure of D-Alanine-D-Alanine Ligase at 2.3-Angstrom Resolution, *Science 266*, 439-443.

196.   Triola, G., Wetzel, S., Ellinger, B., Koch, M. A., Hubel, K., Rauh, D., and Waldmann, H. (2009) ATP competitive inhibitors of D-alanine-D-alanine ligase based on protein kinase inhibitor scaffolds, *Bioorganic & Medicinal Chemistry 17*, 1079-1087.

197.   Gushima, H., Miya, T., Murata, K., and Kimura, A. (1983) Purification and characterization of glutathione synthetase from *Escherichia coli* B, *J. Appl. Biochem. 5*, 210-218.

198.   Ogita, T. and Knowles, J. R. (1988) On the intermediacy of carboxyphosphate in biotin-dependent carboxylations, *Biochemistry 27*, 8028-8033.

199.   Fiedler, H. P. (1984) Screening for New Microbial Products by High-Performance Liquid-Chromatography Using A Photodiode Array Detector, *Journal of Chromatography 316*, 487-494.

200.   Gust, B., Challis, G. L., Fowler, K., Kieser, T., and Chater, K. F. (2003) PCR-targeted *Streptomyces* gene replacement identifies a protein domain needed for biosynthesis of the sesquiterpene soil odor geosmin, *Proc. Natl. Acad. Sci. U. S. A 100*, 1541-1546.

Appendix A:

PLP-dependent enzymes as potential drug targets for protozoan diseases

The following manuscript was submitted to Biochimica et Biophysica Acta (Proteins and Proteomics) in July 2011. I contributed by describing the enzymes in the part "Turning potential into practice: PLP-dependent enzymes as targets for anti-protozoan therapies."

Review

PLP-dependent enzymes as potential drug targets for protozoan diseases

Barbara Kappes[a], Ivo Tews[b], Alexandra Binter[c], Peter Macheroux[c]

[a] University Hospital Heidelberg, Department of Infectious Diseases, Parasitology, Im Neuenheimer Feld 324, 69120 Heidelberg, Germany

[b] University of Southampton, School of Biological Sciences, Institute for Life Sciences (IfLS) B85, Highfield Campus, Southampton SO17 1BJ, UK

[c] Graz University of Technology, Institute of Biochemistry, Petersgasse 12, A-8010 Graz, Austria

Abstract

The chemical properties of the B6 vitamers are uniquely suited for wide use as cofactors in essential reactions, such as decarboxylations and transaminations. This review addresses current efforts to explore vitamin B6 dependent enzymatic reactions as drug targets. Several current targets are described that are found amongst these enzymes. The focus is set on diseases caused by protozoan parasites. Comparison across a range of these organisms allows insight into the distribution of potential targets, many of which may be of interest in the development of broad range anti-protozoan drugs. This article is part of a Special Issue entitled: Pyridoxal Phosphate Enzymology.

1. Introduction

Protozoa synthesize vitamin B6 in the form of PLP from pentose and triose phosphate substrates, utilising in situ generated ammonia as a nitrogen source [1]. Vitamin B6 salvage pathways are also known, and these involve uptake of unphosphorylated precursors with subsequent phosphorylation inside the cells [1]. Drug development based on enzymatic targets in these pathways has recently been discussed for protozoan parasites [2,3]. In this review, we have analyzed PLP-dependent enzymes from 15 protozoan parasites. From the subphylum Mastigophora (Flagellata) the orders Kinetoplastida with *Leishmania major*, *Trypanosoma brucei* and *Trypanosoma cruzi* as representatives, Diplomonadida with *Giardia lamblia* as a member and Trichomonadida with *Trichomonas vaginalis* as associate were selected. The subphylum Sarcodina (Amoebae) is represented by *Entamoeba histolytica*. The phylum Apicomplexa (Sporozoa) which harbours parasites of veterinary importance as well as human pathogens is represented by the following parasites: *Plasmodium falciparum* and *vivax* from the order Haemosporida, *Babesia bigemina*, *Theileria annulata* and *Theileria parva* from the Piroplasmida, and *Eimeria tenella, Cryptosporidium parvum, Cryptosporidium hominis* and *Toxoplasma gondii* from the order Eucoccidiorida. The genomes of these organisms were screened with the metatiger software (http://www.bioinformatics.leeds.ac.uk/metatiger/), using the cofactor search option with the query string "PLP" and by manual inspection of EuPathDB (http://eupathdb.org/ eupathdb/) and GeneDB (http://www.genedb.org/) for the EC numbers and gene product names of PLP-dependent proteins [4] (see Supplement, Table S1). For further information the genome databases of the individual parasites (http://tritrypdb.org/tritrypdb/, http://amoebadb.org/amoeba/, http://giardiadb.org/giardiadb/, http://trichdb.org/trichdb/, http://plasmodb.org/ plasmo/, http://beta.piroplasmadb.org/piro.b10/, http://cryptodb.org/cryptodb/, http://toxodb.org/toxo/) were screened except for *E. tenella*, which was accessed via http://www.genedb.org/Homepage/Etenella, since the genome data is not available on http://eupathdb.org/eupathdb/. As the EC number search for *E. tenella* did not yield any results, the respective database was solely searched for the gene product names. In total, 44 PLP-dependent enzymes were identified (Table 1). The individual gene IDs are provided in Supplemental Fig. 1 and are referring to the gene IDs of the parasite-specific databases, which are listed above. The only exception is *E. tenella*, where the

GeneDB ID has been provided. PLP-dependent enzymes have been classified into seven structural superfamilies named according to their prototype members [5]. Grishin et al. [6] were first to establish this structural classification, which was later refined by Percudani and Peracchi [4].

The prototype superfamilies have developed approximately 1.5 to 1.0 billion years ago [7], well before the three biological kingdoms came into existence. Today, we find a wide functional variety within each of the seven superfamilies. The largest of these families is the aspartate aminotransaminase family (fold-type I), consisting of aminotransferases, decarboxylases as well as of enzymes that catalyze α-, β- or γ-eliminations. The tryptophan synthase β-family (fold-type II) primarily contains enzymes catalyzing β-elimination reactions. Alanine racemase and a subset of amino acid decarboxylases make up the alanine racemase family (fold-type III). The other families are the D-alanine aminotransferase family (fold-type IV), the glycogen phosphorylase family (fold-type V), the D-lysine 5,6-aminomutase family (fold-type VI) and the lysine 2,3-aminomutase family (fold-type VII) (Supplementary Tables 2A and B).

The majority of the proteins identified in this study belong to fold-type I (31 or 70.5%). Less common are fold-types II (6 or 13.6%) and III (3 or 6.8%). Fold-type IVand fold-type V are rare. They contain one member each which is equivalent to 2.3% (see Supplemental Tables 2A and B).

Nomembers of the fold-types VI and VII were identified. The distribution amongst the various fold-types is comparable to that found for other organisms [4,7,8]. The highest numbers of PLP-dependent enzymes were found in the Kinetoplastida (25), followed by the Apicomplexa and Trichomonadida with 19 each and the Amoebida with 15 (Table 2). When scrutinizing the distribution of PLP-dependent enzymes in Apicomplexa, we found significant variation amongst individual orders. Eucoccidiorida contain significantly more PLP-dependent enzymes than Haemosporida or Piroplasmida. In our view, the uneven distribution reflects different metabolic challenges that the individual parasites encounter in their host(s). For example, *Plasmodium* species multiply in hepatocytes, red blood cells or reticulocytes in their vertebrate host as well as extracellularly in the mosquito (http://www.cdc.gov/malaria/about/biology/; [9,10]). *Theileria* infects lymphocytes and/or red blood cells of the vertebrate host as well as cells of the digestive tract or the salivary gland of the vector ([10]). *Babesia* further infects cells of all organs and the eggs of the vector (http://www.cdc.

152

gov/parasites/babesiosis/biology.html; [9,11]). Species of the Eucoccidiorida infect multiple cell types and reside in different parts of the body. *T. gondii*, for example, can infect virtually all nucleated cells and, in its dormant phase, resides in tissue cysts, preferentially in muscles or brain (http://www.cdc.gov/parasites/toxoplasmosis/biology.html; [9,10]). Thus, it is quite likely that the demands associated with the adaption to a certain set of host cells may also influence the set of PLP-dependent enzymes present in the individual parasite.

Several enzymes are found with high prevalence amongst protozoan species analysed (Table 1). These were serine hydroxymethyltransferase (13/15), aspartate transaminase (13/15), alanine transaminase (9/15), branched-chain amino acid transaminase (10/15), and cysteine desulfurase (15/15). On the other hand, a minimal set of three PLP-dependent enzymes was found in the Piroplasmida. Interestingly, these three enzymes belong to the most abundant enzymes which we identified (see above), and are present in all three species of this order. To the best of our knowledge, this is the smallest set of PLP-dependent enzymes being identified in an organism so far. The three enzymes are: serine hydroxymethyltransferase (SHMT, also called glycine hydroxymethyltransferase), aspartate transaminase and cysteine desulfurase. These enzymes together with ornithine decarboxylase are briefly introduced in the following sections.

Table 1: Protozoan PLP-dependent enzymes

#	Enzyme	Sarcomastigophora						Apicomplexa						
	Phylum													
	Order	Kinetoplastida			Diplomonadida	Trichomonadida	Amoebida	Haemosporida		Piroplasmida		Eucoccidiorida		
	Species	*Lm*	*Tb*	*Tc*	*Gl*	*Tv*	*Eh*	*Pf*	*Pv*	*Bb*	*Ta/Tp*	*Et*	*Cp/Ch*	*Tg*
1.	glycine dehydrogenase EC1.4.4.2	+ [66]	+	+	-	-	-	-	-	-	-	-	-	-
2	√ glycine hydroxymethyltransferase (serine HMT) EC 2.1.2.1	+	-	+ [67]	-	+	-	+[a] [50,68,69]	+	+	+/+	+	+/+	+/+
3	glycine C-acetyltransferase EC2.3.1.29	-	+ [70]	+	-	-	-	-	-	-	-	-	-/-	-
4	5-aminolevulinic acid synthase EC2.3.1.37	-	-	-	-	-	-	+[a][71]	+	-	-	+	-	+/+
5	8-amino-7-oxononanoate synthase EC2.3.1.47	-	-	-	-	-	-	-	-	-	-	-	+	
6	serine C-palmitoyltransferase (CW) EC2.3.1.50	+ [72]	+	+	+	+	+	+[a]	+	-	-	+	-	+/+
7	Phosphorylase 2.4.1.1	-	-	-	+	+	+	- [73]	-	-	-	+	+/+	+/+
8	cysteine synthase/(O(3)-acetyl-L-serine acetate-lyase) EC2.5.1.47√	+ [49]	-	+	-	+ [46]	+	-	-	-	-	+	-	+
9	aspartate transaminase EC2.6.1.1	+	+	+	+	+	+	+[a][14]	+	+	+/+	+	-	+/+
10	alanine transaminase EC2.6.1.2	+	+	+	+	+ [74]	+	-	-	-	-	+	-	+/+
11	cysteine amino transferase EC2.6.1.3	+	-	-	-	-	-	-	-	-	-	-	-	-
12	tyrosine transaminase EC2.6.1.5	+	-	+ [75,76]	-	+	-	-	-	-	-	-	-	-
13	kynurenine—oxoglutarate transaminase EC2.6.1.7	-	+	-	-	-	-	-	-	-	-	-	-	-
14	ornithine—oxo-acid transaminase EC2.6.1.13	-	-	-	-	-	-	+[a] [77]	+	-	-	+	-	+/+
15	branched-chain-amino-acid transamininase EC2.6.1.42	+	+	-	+	+	+	+[a]	+	-	-	+	-	+/+
16	alanine—glyoxalate transamininase EC2.6.1.44	+ [78]	-	+	-	-	-	-	-	-	-	-	-	-
17	glutaminase—scyllo-inositol transaminase EC2.6.1.50	-	-	-	-	-	-	-	-	-	-	+	-	-
18	serine—pyruvate transaminase EC2.6.1.51	-	-	-	+	-	-	-	-	-	-	+	-	+/+
19	phosphoserine transaminase EC2.6.1.52	-	-	-	-	+ [46]	+	-	-	-	-	+	-	+/+
20	aromatic amino acid transaminase EC2.6.1.57	-	-	-	-	-	-	-	-	-	-	-	-	+
21	adenosylmethionine—8-amino-7-oxononanoatetransaminase EC2.6.1.62	-	-	-	-	+	-	-	-	-	-	-	+	-
22	cysteine desulfurase EC2.8.1.7	+	+	+	+	+	+	+[a]	+	+	+	+	+	+
23	kynureninase EC3.7.1.3	+	+	+ [59]	-	-	-	-	-	-	-	-	-	-
24	glutamate decarboxylase EC4.1.1.15	-	-	-	-	+	-	-	-	-	-	-	-	-
25	ornithine decarboxylase EC4.1.1.17	+	+ [79]	-	+	+	+	+[a]	+	-	-	-	-	-
26	lysine decarboxylase EC4.1.1.18	-	-	-	-	-	+	+[a]	+	-	-	+	-	+/+
27	diaminopimelate decarboxylase EC4.1.1.20	-	-	-	-	+	-	-	-	-	-	-	-	+/+
28	tyrosine decarboxylase EC4.1.1.25	+	-	-	-	-	-	-	-	-	-	-	-	-
29	aromatic-L-amino-acid decarboxylase EC4.1.1.28	+	+	+	-	-	-	-	-	-	-	-	-	-
30	threonine aldolase EC4.1.2.5	+	-	-	-	+	-	-	-	-	-	-	-	-
31	sphinganine-1-phosphate aldolase EC4.1.2.27	+ [72]	+	+	-	-	+	-	-	-	-	-	-	-
32	aminodeoxychorismate lyase (p-aminobenzoic acid synthetase) EC4.1.3.38	-	-	-	-	-	-	+[a]	+	+	+	+	-	-
33	tryptophanase EC4.1.99.1	-	-	-	-	+	+	-	-	-	-	-	-	-
34	tryptophan synthase EC4.2.1.20	- [49]	-	-	-	-	-	-	-	-	-	-	+/+	-

#	Enzyme													
35	cystathionine beta-synthase EC4.2.1.22	+	+	+	-	-	-	-	-	-	-	+	-	+/+
36	threonine synthase EC4.2.3.1	+	+	+	+	-	-	-	-	-	-	-	-	+/+
37	L-serine ammonia-lyase EC4.3.1.17	-	-	-	+	-	-	-	-	-	-	-	-	-
38	threonine ammonia-lyase (threonine dehydratase) EC4.3.1.19	+	-	+ [81]	+	+	+	-	-	-	-	-	-	-
39	cystathionine gamma-lyase EC4.4.1.1	+	+	+	-	-	+	-	-	-	-	-	-	-
40	cystathionine beta-lyase EC4.4.1.8	+	-	-	-	-	-	-	-	-	-	+	-	+/+
41	methionine gamma-lyase EC4.4.1.11	-	-	-	-	+[38,82]	+ [39]	-	-	-	-	-	-	-
42	cysteine-S-conjugate beta-lyase EC4.4.1.13	+	-	-	-	-	-	-	-	-	-	-	-	-
43	1-aminocyclopropane-1-carboxylate synthase EC4.4.1.14	-	-	-	-	+	-	-	-	-	-	-	-	-
44	selenocysteine lyase EC4.4.1.16	+	+ [21]	+	-	-	-	-	-	-	-	+	-	+
45	alanine racemase EC5.1.1.1	+ [83]	+	+	-	-	-	+	+	-	-	-	-	-
	totals of 45	25	17	19	11	19	15	11	11	4	4	18	6	19

Cobimed results of METATIGER/EC/AMIGO and Blastsearches using Metatiger, GeneDB, trypdb, giardiadb, trichdb.org, amoebadb, plasmodb, beta.piroplasmadb, cryptodb, toxodb, NCBI protein blast. Lm = *Leishmania major*, T.b. = *Trypanosoma brucei*, Tc = *Trypanosoma cruzi* , Eh = *Entamoeba histolytica*, Gl = *Giardia lamblia*, Tv = *Trichinella vaginalis*, Pf = *Plasmodium falciparum*, Pv = *Plasmodium vivax*, Bb = Babesia bovis, Ta = *Theileria annulata*, Tp = *Theileria parva*, Et = *Eimeria tenella*, Cp = *Cryptosporidum parvum*, Ch = *Cryptosporidum hominis*, Tg = *Toxoplasma gondii*. [a]published by Müller et al., 2010

Table 2: Number of PLP-dependent enzymes among the investigated protozoan taxa

Taxonomic allocation	Number	%
Kinetoplastida	25	56.8
Amoebozoa	15	34.1
Diplomonadida	11	25.0
Trichomonadida	19	43.2
Apicomplexa	19	43.2
Apicomplexa (Eucoccidiorida)	19	43.2
Apicomplexa (Haemosporida)	10	22.7
Apicomplexa (Piroplasmida)	3	6.82

.

2. A minimal set of PLP-dependent enzymes

2.1 Serine hydroxymethyltransferase (EC 2.1.2.1)

SHMT is involved in folate and amino acid metabolism. It produces 5,10-methylenetetrahydrofolate from serine [12] and is required for folate recycling [13]. In apicomplexan parasites, folate is a cofactor that is required to convert deoxyuridine 5′-monophosphate (dUMP) to deoxythymidine 5′-monophosphate (dTMP), which is then incorporated into DNA via dTTP. In the methylation reaction, 5,10-methylene tetrahydrofolate is oxidised to dihydrofolate, which needs to be regenerated to tetrahydrofolate by dihydrofolate reductase. Hence, apicomplexan parasites such as *Plasmodium* and *T. gondii* are entirely dependent on an adequate dihydrofolate reductase activity for dihydrofolate reduction.

In contrast to the apicomplexan species *Plasmodium* and *Toxoplasma*, *C. parvum* and *C. hominis* are deficient in de novo pyrimidine biosynthesis and have compensated this loss by the salvage pathway enzymes monofunctional uracil phosphoribosyltransferase, bifunctional uracil phosphoribosyltransferase and uridine as well as thymidine kinase, the latter two being unique to *Cryptosporidium* [12].

2.2 Aspartate aminotransferase (E.C. 2.6.1.1)

Aspartate aminotransferases are key enzymes in the nitrogen metabolism of all organisms. They catalyze the reversible reaction of L-aspartate and α-ketoglutarate into oxaloacetate and L-glutamate [14]. Protozoal aspartate transaminases have been cloned and expressed from *Crithidia fasciculata, T. brucei brucei, Giardia intestinalis*, and *P. falciparum* [15]. Those enzymes were shown to catalyze aspartate-ketoglutarate, tyrosine-ketoglutarate, and amino acid-α-ketomethiobutyrate (KMTB) aminotransfer reactions with glutamate, phenylalanine, tyrosine, tryptophan and histidine as effective amino donors. Berger et al. [15] observed that the kinetic constants were broadly similar in all the enzymes, with the exception of the plasmodial enzyme, which catalyzed the transamination of ketomethiobutyrate significantly more slowly than aspartate-ketoglutarate aminotransfer. Furthermore, total ketomethiobutyrate transamination activity in malarial homogenates is much lower than in other organisms like *T. vaginalis*

and *G. intestinalis*, where lysine-ketomethiobutyrate aminotransferase activity is also involved in KMTB transamination.

The transamination of KMTB is the final step in the methionine regeneration pathway. This unique pathway prevents depletion of free methionine, which is required for polyamine biosynthesis. Thus, it is of particular importance in rapidly growing cells, such as most parasites [16]. As regeneration of methionine was shown to be essential for cellular survival of *P. falciparum* [17] and the KMTB transamination reaction catalyzed by *Pf*AspAT is much less readily catalyzed than byAspAT of other protozoa, the malaria parasite may be uniquely susceptible to interference with the last step of the Met recycling pathway [15]. However, the role of *Pf*AspAT in methionine regeneration is a matter of debate, and some authors claim that *P. falciparum* does not possess the full complement of enzymes necessary for methionine regeneration [18].

The *Pf*AspAT enzyme was also suggested to play a role in oxidative phosphorylation [14]. PfAspAT was shown to be present only in the parasite cytosol and there it is the only enzyme capable of generating oxaloacetate [19], which is further converted to malate by *P. falciparum* malate dehydrogenase and then imported into the mitochondria by the malate-oxaloacetate shuttle [20].

The catalytic site of *Pf*AspAT is highly conserved, which makes specific inhibition of plasmodial AspAT without affecting the host AspAT difficult. However, the conformation of the N-terminal residues of *Pf*AspAT diverges significantly from that of other AspAT. Deletion of the divergent N-terminal residues leads to a loss of activity in recombinant *Pf*AspAT, and addition of a peptide containing the N-terminal residues leads to inhibition of the parasite enzyme, while human cytosolic AspAT is unaffected [14].

2.3 Cysteine desulfurase (EC 2.8.1.7)

Cysteine desulfurases remove elemental sulfur from cysteine to provide it for iron–sulfur cluster assembly and thiolation of tRNAs. They also show selenocysteine lyase activity in vitro, by cleaving selenocysteine into alanine and elemental selenium. All organisms studied to date encode cysteine desulfurases. They are termed NikS, IscS, CsdA or SufS in bacteria and Nfs in mitochondria [21]. In eukaryotes, Nfs-like proteins interact with the scaffold protein IscU, upon which iron–sulfur clusters are formed [22]. In the apicomplexan protist *Plasmodium*, two Nfs-like proteins have been identified,

one of them being localized to the apicoplast [23]. The *T. brucei* genome also encodes two Nfs-like proteins. One is localized in the mitochondrion, the other one in the nucleus and cytoplasm. Down-regulation of either leads to a significant decrease in cysteine desulfurase and selenocysteine lyase activities [21]. Furthermore, in trypanosomes ablated for Nfs, tRNA thiolation is disrupted [24]. *Giardia* and *Trichomonas* lack the standard mitochondria but contain mitochondrial-type α-proteobacterium-derived assembly proteins for iron–sulfur clusters, located to mitosomes in *Giardia* and to hydrogenosomes in *Trichomonas* [25]. The cysteine desulfurase (*Tv*iscS-2) of the hydrogenosomes of *T. vaginalis* was shown to be phylogenetically related to its mitochondrial homologs [26]. *E. histolytica* possesses a simplified and non-redundant NIF (nitrogen fixation)-like system for formation of iron–sulfur clusters, which is composed only of a catalytical (NifS) and a scaffold component (NifU). Interestingly, ectopic expression of *Eh*NifS and *Eh*NifU in an *Escherichia coli* strain in which both the *isc* and *suf* operons were deleted, successfully complemented the growth defect under anaerobic conditions. This suggests that those enzymes are sufficient for the formation of iron–sulfur clusters under anaerobic conditions [27].

3.   A prototype enzyme: Ornithine decarboxylase (EC 4.1.1.17)

Polyamines are ubiquitous supercations characterized by a charge distribution along the entire length of the carbon backbone. They are essential for a variety of cellular processes ranging from nucleic acid packaging and stabilization, to DNA replication, transcription, translation, protein stabilization, cell differentiation and signalling [28]. The two key enzymes in polyamine biosynthesis are ornithine decarboxylase (ODC) and S-adenosylmethionine decarboxylase (AdoMetDC), which provide putrescine and decarboxylated S-adenosyl-L-methionine for the synthesis of spermidine. Both enzymes are regulated by feedback mechanisms on several levels [29]. ODC is commonly found in protozoan parasites and only absent in *T. cruzi*, the Piroplasmida and Eucoccidiorida. The eucoccidian parasite *C. parvum* bypasses ODC activity by employing a plant-like pathway that utilizes arginine decarboxylase (ADC), through the conversion of arginine to agmantine which is then further converted to putrescine by agmantine iminohydrolase [30–32]. For *T. gondii* and *T. cruzi* neither ODC nor ADC activities were detected in [30–33]. *T. gondii* possesses a highly active backconversion pathway for formation of spermidine from spermine and putrescine from spermidine via

158

spermidine-spermine and spermidine-N1-acetyltransferases and polyamine oxidase. To our knowledge, *T. gondii* and *T. cruzi* are the only eukaryotic organisms that are auxotrophic for polyamines. Except for plants and eucoccidians, polyamines are synthesized via the forward-directed biosynthetic pathway using ODC. However, ODC of plasmodial species displays some unique features. It is combined with AdoMetDC in a bifunctional enzyme forming a heterotetrameric complex consisting of heterotetrameric N-terminal AdoMetDC and C-terminal dimeric ODC. The K_m value of the *P. falciparum* ODC for ornithine is 41 μM and its overall enzymatic characteristics are similar to those of its mammalian orthologs. In contrast to the short half-life of the mammalian monofunctional counterparts, the plasmodial bifunctional enzyme has a half-life of more than 2 h. Moreover, putrescine inhibits the plasmodial enzyme ten-fold more efficiently than the mammalian enzyme [34].

4. Turning potential into practice: PLP-dependent enzymes as targets for anti-protozoan therapies

These four PLP-dependent enzymes may present an attractive set of targets for general drug design against protozoan parasites. However, so far only two of these candidates, SHMT and ODC, have been targeted to develop clinically useful drugs. Future studies are required to explore the potential of the other enzymes as anti-protozoan drug targets. This section follows a rather distinct approach as it focuses on PLP-dependent enzymes that appear to have crucial importance for some specific parasites rather than being ubiquitous for the entire range of parasites.

In this category, sulfur-containing amino acid metabolism is one of the most promising pathways for the development of new chemotherapeutic agents against protozoan parasites, particularly those causing amoebiasis and trichomoniasis. Importantly, the metabolic pathways of sulphur-containing amino acid metabolism diverge remarkably between the parasites and their hosts. The forward trans-sulfuration pathway is involved in the formation of methionine from cysteine. It was demonstrated in bacteria, fungi and plants. Cysteine is converted to cystathionine by the PLP-dependent cystathionine γ-synthase, followed by an α,β-elimination reaction catalysed by cystathionine β-lyase (also PLP-dependent), generating homocysteine. The final step is catalysed by homocysteine methyltransferase (methionine synthase). Importantly, the metabolic pathways of sulphur-containing amino acid metabolism diverge remarkably between the

parasites and their hosts. For example, the forward trans-sulfuration pathway (cysteine to methionine) is lacking in mammals, which utilize only the part of the pathway, which is catalysed by homocysteine methyltransferase for the recycling of methionine. The reverse trans-sulfuration pathway, which has been demonstrated in fungi and mammals, generates cysteine from methionine. After methionine is activated to S-adenosylmethionine by methionine adenosyltransferase, transmethylation to S-adenosylhomocysteine and hydrolysis to homocysteine occur. The following two reactions are catalyzed by the PLP-dependent enzymes, cystathionine β-synthase and cystathionine γ-lyase, to finally form cysteine [35].

Further PLP-dependent enzymes involved in sulphur-containing amino acid metabolism include methionine γ-lyase (MGL) and cysteine synthase (CS), which are involved in the degradation of cysteine and methionine and in the generation of cysteine from serine, respectively [35,36].

4.1   Methionine-γ-lyase (EC 4.4.1.11)

The PLP-dependent enzyme L-methionine-γ-lyase (MGL) is involved in the degradation of cysteine, methionine and related compounds (Fig. 1). MGL is biologically significant for the production of propionic acid for energy metabolism and the degradation of toxic sulphur-containing amino acids [35,37]. Since mammalian cells lack MGL, it is a promising drug target against infections caused by the primitive protozoa *E. histolytica* and *Trichomonas vaginalis* [38,39].

E. histolytica causes ameobiasis, which takes second place with respect to incidence as a parasitic disease after malaria. *E. histolytica* is unable to interconvert methionine and cysteine, as it is deficient of the trans-sulfuration pathway. However, in *E. histolytica*, L-methionine-γ-lyase is involved in the metabolism of sulphur-containing amino acids [39]. MGL catalyzes α,γ- or α,β-elimination reactions and β- or γ-replacement reactions of sulphur-containing amino acids, thereby producing ammonia, α-keto acids and volatile thiols [40]. Two isotypes of distinct substrate specificities were identified in *E. histolytica* (*Eh*MGL1 and *Eh*MGL2) and *T. vaginalis* [38,39].

The halogenated methionine analog S-trifluoromethyl-L-homocysteine (trifluoromethionine, TFM) and various amide derivatives of TFM were shown to have severe cytotoxic effects on *T. vaginalis* and *E. histolytica* in vitro [39,41,42]. The

toxicity of TFM against amoeba and mammalian cells is remarkably different (IC_{50} for *E. histolytica* trophozoites or Chinese hamster ovary cells, 18 μM or 865 μM, respectively), which makes it a promising lead compound for the development of chemotherapeutic drugs against amoebiasis. However, the mechanism of action of the inhibitor remains to be elucidated [43].
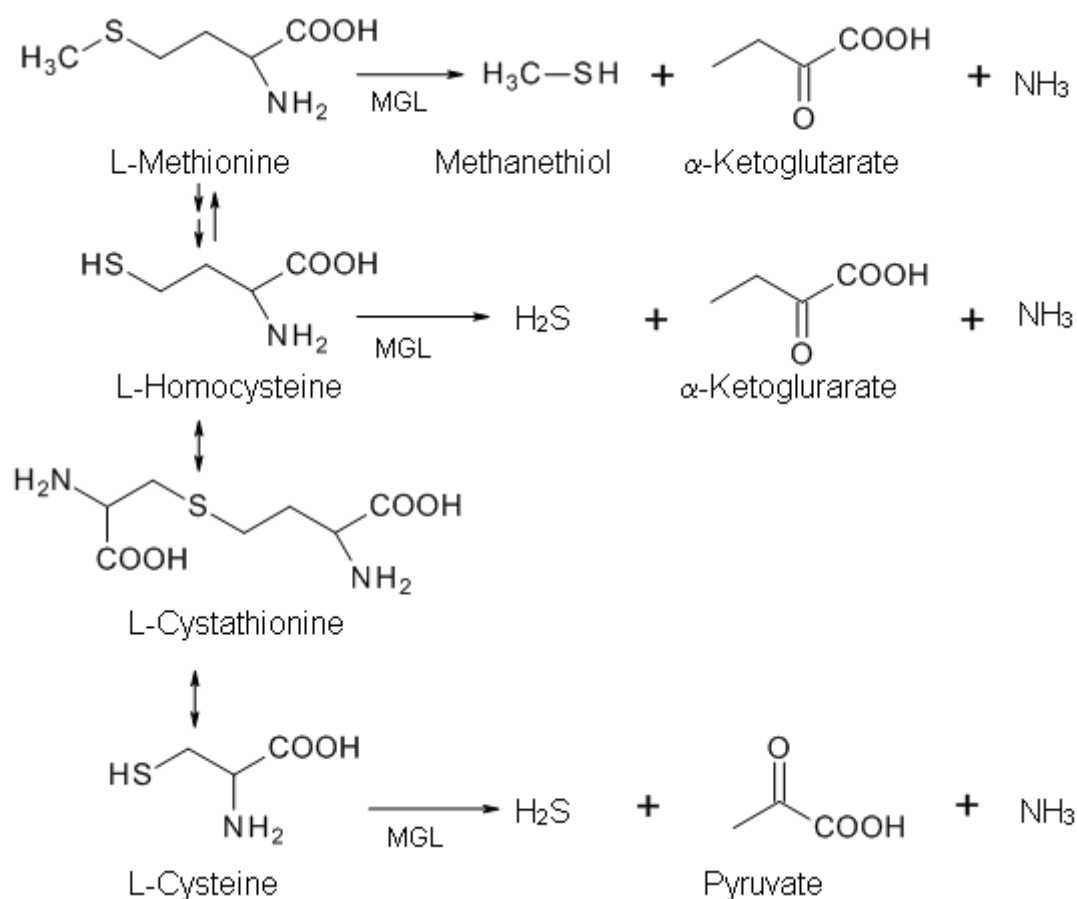

Figure 1: The role of methionine-γ-lyase (MGL) in sulphur amino acid metabolism

4.2 Cysteine synthase (EC 2.5.1.47)

In bacteria, plants and parasitic protists, the pathways of cysteine biosynthesis play an important role for the incorporation of sulphur into organic compounds. O-acetylserine, which in bacteria and plants is generated from serine and acetyl-CoA by serine O-acetyltransferase (SAT), is the substrate for cysteine synthase (CS) [44]. The PLP-dependent CS catalyzes the production of L-cysteine by transferring the alanyl moiety of O-acetylserine to sulphide [45]. Hence, *E. histolytica* and *T. vaginalis* lacking a

sulphate reduction pathway depend on sulphide sequestration from iron–sulfur proteins released by ingested bacteria. In contrast, animals are deficient of a sulphur-assimilatory pathway and require exogenous methionine as a source for sulphur [36]. Sulphur assimilatory biosynthesis of cysteine was characterized in *T. vaginalis* [46]. Analysis of the *T. vaginalis* genome revealed six copies of CS, but no SAT. Apparently, *T. vaginalis* cysteine synthase is able to utilize O-phosphoserine as well as O-acetylserine as an alanyl donor substrate (Fig. 2).
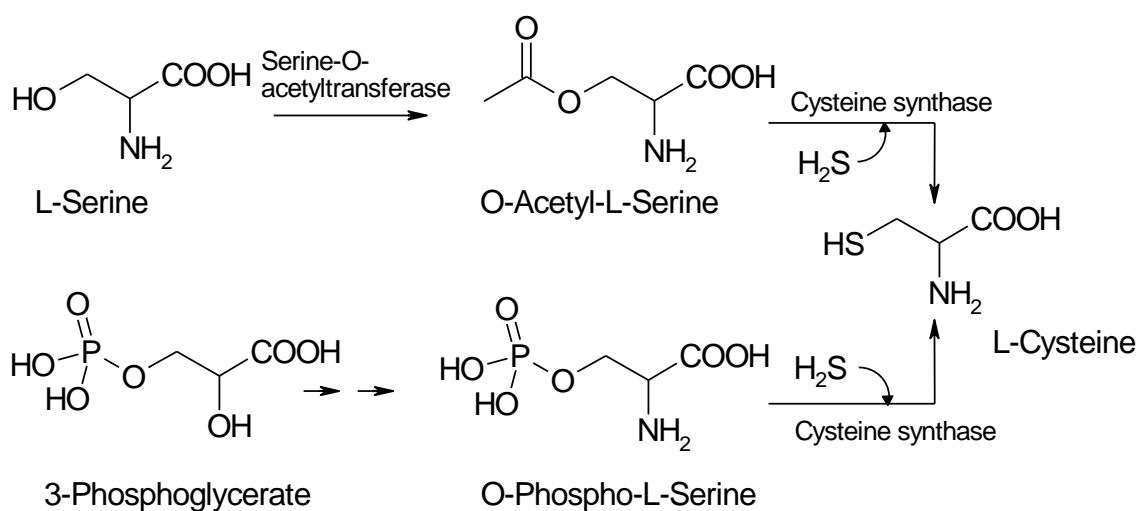

Figure 2: The role of *Trichomonas vaginalis* cysteine synthase in the biosynthesis of L-cysteine

O-phosphoserine, which is derived from the glycolytic intermediate 3-phosphoglycerate, is likely to be the physiological substrate for *T. vaginalis* CS. As *T. vaginalis* lacks glutathione and related thiols, it is thought to rely heavily on cysteine as a redox buffer and antioxidant [47]. Cysteine synthase is not present in humans. This makes the parasitic enzyme a promising target for the rational design of drugs against trichomoniasis, as well as amoebiasis [36]. *E. histolytica* CS utilizes various alanyl acceptors beside sulphide, including 1,2,4-triazole, isoxazolin-5-one, pyrazole, and cyanide. Thiol derivatives of tetrazole and triazole are highly cytotoxic for *E. histolytica* in vitro. Further investigations on CS substrates with amoebacidal activity are necessary [45]. Reduced forms of pyrazole, pyrazolines, and their derivatives show remarkable effects against amoebiasis [48]. Their mode of action and toxicity againstmammals remains to be elucidated. It is possible that some of these derivatives target cysteine synthase or methionine γ-lyase. The protozoan parasite *L. major* possesses two

pathways for cysteine synthesis. The de novo biosynthesis pathway comprises SAT and CS, and the reverse trans-sulfuration pathway comprises cystathionine β-synthase (CBS) and cystathionine γ-lyase (CGL). CBS from *L. major* catalyzes the synthesis of cystathionine from homocysteine and possesses high cysteine synthase activity, which distinguishes it from mammalian CBS. The differences between mammalian and *L. major* CBS and the absence of CS from mammals suggest that both parasitic enzymes are suitable drug targets [49].

In addition to sulfur metabolism, the folate cycle represents another very appealing metabolic process [50], in which the PLP-dependent serine hydroxymethyltransferase plays a major role (see also previous section). Furthermore, the kynurenine pathway of tryptophane degradation [51,52], Fig. 3, and polyamine biosynthesis [53], Fig. 4, require PLP-dependent enzymes that are discussed in more detail in the next paragraphs.

4.3   Serine hydroxymethyltransferase (EC 2.1.2.1)

Serine and tetrahydrofolate are reversibly converted to glycine and 5,10-methylenetetrahydrofolate by serine hydroxymethyltransferase (SHMT), which was recently identified as a potential drug target [50]. In 2006, Mukherjee *et al*. postulated a distinct active site of the *T. vaginalis* serine hydroxymethyltransferase from its human counterpart [54]. SHMT is involved in the biosynthetic pathway of dTMP, a nucleotide precursor for DNA synthesis. For *P. falciparum*, the two other enzymes in the deoxythymidylate synthesis cycle, dihydrofolate reductase and thymidylate synthase, have been well investigated for antimalarial drug design purposes [55]. Protozoan parasites are characterized by the bifunctional enzyme dihydrofolate reductase-thymidylate synthase (DFHR-TS). Parasitic protozoa and humans show several differences in their biosynthetic pathway of folate.

Apicomplexa possess an endogenous folate biosynthetic pathway, which is susceptible to antifolate inhibitors, whereas humans do not synthesize folates de novo. Throughout evolution, the sequence of the DHFR gene has significantly diverged resulting in major differences in amino acid sequences of the encoded DHFR, which has the potential to increase the feasibility for the development of species-specific DHFR inhibitors [56]. SHMT was postulated as an antitumor target, due to its essential role in supplying C-1 units for the biosynthesis of dTMP [57]. However, it was not explored as a target for the

development of antimalarial drugs until 2009, when Maenpuen *et al*. postulated that, in addition to folate derivatives, D-amino acid analogs could be potential specific inhibitors for *P. falciparum* SHMT. Unlike the mammalian enzyme, His-tagged *Pf*SHMT shows broader stereospecificity with catalytic activity toward D-serine as well as L-serine, a property that may be explored in drug design.

4.4   *T. cruzi* kynureninase (EC 3.7.1.3)

The protozoan parasite *T. cruzi* causes Chagas disease, a potentially life-threatening illness, which is found mainly in South America with ten million people infected worldwide and more than 25 million people at risk of. A transcriptomics project was carried out in order to identify genes that are upregulated in infective (metacyclic trypomastigotes) forms of *T. cruzi* [58]. One such gene identified is kynureninase that hydrolyzes L-kynurenine and 3-hydroxykynurenine to L-alanine and anthranilic or 3-hydroxyanthranilic acid, respectively (Fig. 3).
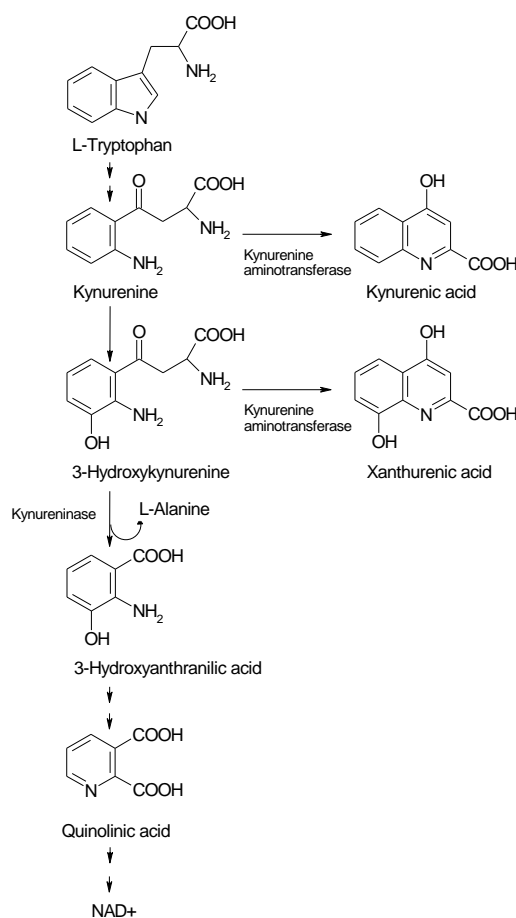

Figure 3: Kynurenine pathway of tryptophan degradation in vertebrates

164

The enzyme from *T. cruzi* shows 35% sequence identity to human kynureninase. Sequence alignment shows replacements at critical amino acids required for PLP cofactor coordination, the significance of which need to be verified by further biochemical and structural analyses [59].

4.5   Ornithine decarboxylase (EC 4.1.1.17)

Protozoan parasites have an unusually high demand of polyamines as essential components for cell growth, proliferation and differentiation due to their rapid proliferation rates during infections. Ornithine decarboxylase (ODC) catalyzes the decarboxylation of ornithine to putrescine in the initial step of polyamine biosynthesis [53] (Fig. 4).
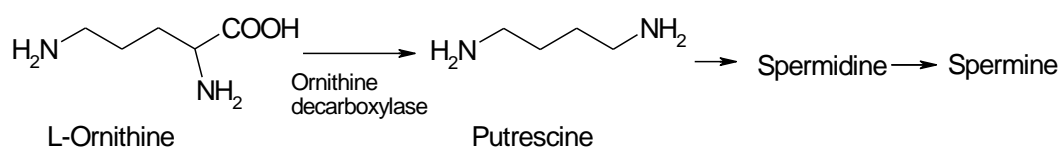

Figure 4: The role of ornithine decarboxylase in polyamine biosynthesis

As α-difluoromethylornithine (DFMO, eflornithine, Fig. 5) irreversibly inhibits ODC, the blockade of polyamine biosynthesis by DFMO is successfully exploited against trypanosomes, and eflornithine is administered as a drug against human African trypanosomiasis [60]. The success of DFMO encouraged further investigations into structurally related ODC inhibitors. So far, attempts to use DFMO in the treatment of other protozoan infections have failed [53,61].

P. falciparum ODC inhibitors are 3-aminooxy-1-propane (APA) and its derivatives CGP 52622A and CGP 54169A with K_i values in the low nanomolar range (Fig. 5). These compounds possess an aminooxy group and form an oxime with the PLP cofactor in the active site of ODC. Due to the structural analogy to putrescine, the inhibitory effect is very specific, whereas the activities of other PLP-dependent enzymes are hardly affected. APA and some of its derivatives were shown to be far more potent antimalarials than the classic agents, at least in culture [62,63].
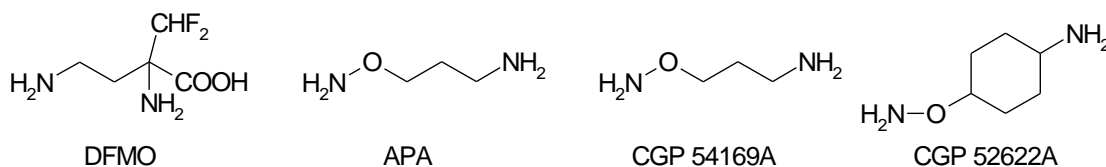
Figure 5: Inhibitors of ornithine decarboxylase (DFMO: α-difluoromethylornithine, APA: 3-aminooxy-1-aminopropane)

E. histolytica ODC was shown to be largely insensitive towards inhibition by DFMO, but is inhibited by APA and 2,4-diamino-2-butanone [64]. APA was shown to inhibit *Leishmania donovani* ODC with a K_i of 1 nM. Since the three-dimensional structure of *L. donovani* ODC in complex with APA is available, we may expect more specific inhibitors to treat leishmaniasis [65].

5.   Conclusions

Screening and analysis of parasite genomes is a powerful tool to establish an inventory of protein families with common features, such as vitamin dependence. As these sets of enzymes are presumably required for viability or infectivity of the parasite, they represent an array of potential drug targets. Our analysis for PLP-dependent enzymes suggests two types of emergent drug targets: (1) enzymes common to most parasites and (2) those related to a specialized parasitic life style (particular hosts, host cells and/or life cycle).While the first group identifies targets that may be of interest in the development of broad range anti-protozoan drugs, the second group may be attractive in the design of species-specific therapeutics. At any rate, the current state of affairs is such that many potential targets await getting hit by powerful compounds to be designed and synthesized in the future.

References

[1] T. Mukherjee, J.W. Hanes, I. Tews, S.E. Ealick, T.P. Begley, Pyridoxal phosphate: biosynthesis and catabolism, Biochim Biophys Acta this volume (2011).

[2] I.B. Muller, J.E. Hyde, C. Wrenger, Vitamin B metabolism in *Plasmodium falciparum* as a source of drug targets, Trends Parasit 26 (2010) 35-43.

[3] S. Muller, B. Kappes, Vitamin and cofactor biosynthesis pathways in Plasmodium and other apicomplexan parasites, Trends Parasit 23 (2007) 112-121.

[4] R. Percudani, A. Peracchi, The B6 database: a tool for the description and classification of vitamin B6-dependent enzymatic activities and of the corresponding protein families, BMC Bioinformatics 10 (2009) 273.

[5] A. Amadasi, M. Bertoldi, R. Contestabile, S. Bettati, B. Cellini, M.L. di Salvo, C. Borri-Voltattorni, F. Bossa, A. Mozzarelli, Pyridoxal 5'-phosphate enzymes as targets for therapeutic agents, Curr Med Chem 14 (2007) 1291- 1324.

[6] N.V. Grishin, M.A. Phillips, E.J. Goldsmith, Modeling of the spatial structure of eukaryotic ornithine decarboxylases, Protein Sci 4 (1995) 1291-1304.

[7] P. Christen, P.K. Mehta, From cofactor to enzymes. The molecular evolution of pyridoxal-5'-phosphate-dependent enzymes, Chem Rec 1 (2001) 436-447.

[8] R. Percudani, A. Peracchi, A genomic overview of pyridoxal phosphatedependent enzymes, EMBO Rep 4 (2003) 850-854.

[9] Parasitology in focus, facts and trends, Springer Verlag, Berlin, Heidelberg, New York, London, Paris, Tokyo, 1988.

[10] K. Matthews, B. Kappes, D. Chakrabarti, C. Doerig, Cell cycle in parasitic protozoans, in: L. Meijer, A. Jezequal, B. Ducommun (Eds.), Progress in cell cycle research, vol. 4th, Kluwer Academic / Plenum Publishers, New York, 2000, pp. 163 183.

[11] A.S. Young, S.P. Morzaria, Biology of babesia, Parasitology today (Personal ed 2 (1986) 211-219.

[12] J.E. Hyde, Targeting purine and pyrimidine metabolism in human apicomplexan parasites, Curr Drug Targets 8 (2007) 31-47.

[13] J.E. Hyde, Exploring the folate pathway in *Plasmodium falciparum*, Acta Trop 94 (2005) 191-206.

[14] C. Wrenger, I.B. Muller, A.J. Schifferdecker, R. Jain, R. Jordanova, M.R. Groves, Specific inhibition of the aspartate aminotransferase of *Plasmodium falciparum*, Journal of molecular biology 405 (2011) 956-971. 12

[15] L.C. Berger, J. Wilson, P. Wood, B.J. Berger, Methionine regeneration and aspartate aminotransferase in parasitic protozoa, J Bact 183 (2001) 4421- 4434.

[16] L.J. Marton, A.E. Pegg, Polyamines as targets for therapeutic intervention, Ann Rev Pharm Toxicol 35 (1995) 55-91.

[17] J.R. Sufrin, S.R. Meshnick, A.J. Spiess, J. Garofalo-Hannan, X.Q. Pan, C.J. Bacchi, Methionine recycling pathways and antimalarial drug design, Antimicrob Agents Chemother 39 (1995) 2511-2515.

[18] L.M. Ting, W. Shi, A. Lewandowicz, V. Singh, A. Mwakingwe, M.R. Birck, E.A. Ringia, G. Bench, D.C. Madrid, P.C. Tyler, G.B. Evans, R.H. Furneaux, V.L. Schramm, K. Kim, Targeting a novel *Plasmodium falciparum* purine recycling pathway with specific immucillins, J Biol Chem 280 (2005) 9547-9554.

[19] M.J. Gardner, N. Hall, E. Fung, O. White, M. Berriman, R.W. Hyman, J.M. Carlton, A. Pain, K.E. Nelson, S. Bowman, I.T. Paulsen, K. James, J.A. Eisen, K. Rutherford, S.L. Salzberg, A. Craig, S. Kyes, M.S. Chan, V. Nene, S.J. Shallom, B. Suh, J. Peterson, S. Angiuoli, M. Pertea, J. Allen, J. Selengut, D. Haft, M.W. Mather, A.B. Vaidya, D.M. Martin, A.H. Fairlamb, M.J. Fraunholz, D.S. Roos, S.A. Ralph, G.I. McFadden, L.M. Cummings, G.M. Subramanian, C. Mungall, J.C. Venter, D.J. Carucci, S.L. Hoffman, C. Newbold, R.W. Davis, C.M. Fraser, B. Barrell, Genome sequence of the human malaria parasite *Plasmodium falciparum*, Nature 419 (2002) 498-511.

[20] C.R. Goward, D.J. Nicholls, Malate dehydrogenase: a model for structure, evolution, and catalysis, Protein Sci 3 (1994) 1883-1888.

[21] P. Poliak, D. Van Hoewyk, M. Obornik, A. Zikova, K.D. Stuart, J. Tachezy, M. Pilon, J. Lukes, Functions and cellular localization of cysteine desulfurase and selenocysteine lyase in *Trypanosoma brucei*, FEBS J 277 (2010) 383- 393.

[22] J. Gerber, U. Muhlenhoff, R. Lill, An interaction between frataxin and Isu1/Nfs1 that is crucial for Fe/S cluster synthesis on Isu1, EMBO Rep 4 (2003) 906-911.

[23] K.E. Ellis, B. Clough, J.W. Saldanha, R.J. Wilson, Nifs and Sufs in malaria, Mol Microbiol 41 (2001) 973-981.

[24] J.M. Wohlgamuth-Benedum, M.A. Rubio, Z. Paris, S. Long, P. Poliak, J. Lukes, J.D. Alfonzo, Thiolation controls cytoplasmic tRNA stability and acts as a negative determinant for tRNA editing in mitochondria, J Biol Chem 284 (2009) 23947-23953.

[25] T.A. Richards, M. van der Giezen, Evolution of the Isd11-IscS complex reveals a single alpha-proteobacterial endosymbiosis for all eukaryotes, Mol Biol Evo 23 (2006) 1341-1344.

[26] R. Sutak, P. Dolezal, H.L. Fiumera, I. Hrdy, A. Dancis, M. Delgadillo-Correa, P.J. Johnson, M. Muller, J. Tachezy, Mitochondrial-type assembly of FeS centers in the hydrogenosomes of the amitochondriate eukaryote *Trichomonas vaginalis*, Proc Nat Acad Sci U.S.A. 101 (2004) 10368-10373. 13

[27] V. Ali, Y. Shigeta, U. Tokumoto, Y. Takahashi, T. Nozaki, An intestinal parasitic protist, *Entamoeba histolytica*, possesses a non-redundant nitrogen fixation-like system for iron-sulfur cluster assembly under anaerobic conditions, J Biol Chem 279 (2004) 16863-16874.

[28] H.M. Wallace, A.V. Fraser, A. Hughes, A perspective of polyamine metabolism, Biochem J 376 (2003) 1-14.

[29] L. Persson, Polyamine homoeostasis, Essays Biochem 46 (2009) 11-24.

[30] T. Cook, D. Roos, M. Morada, G. Zhu, J.S. Keithly, J.E. Feagin, G. Wu, N. Yarlett, Divergent polyamine metabolism in the Apicomplexa, Microbiology 153 (2007) 1123-1130.

[31] J.S. Keithly, G. Zhu, S.J. Upton, K.M. Woods, M.P. Martinez, N. Yarlett, Polyamine biosynthesis in *Cryptosporidium parvum* and its implications for chemotherapy, Molec Biochem Parasit 88 (1997) 35-42.

[32] S.D. Rider, Jr., G. Zhu, *Cryptosporidium*: genomic and biochemical features, Exp Parasit 124 (2010) 2-9.

[33] M.R. Ariyanayagam, A.H. Fairlamb, Diamine auxotrophy may be a universal feature of *Trypanosoma cruzi* epimastigotes, Molec Biochem Parasit 84 (1997) 111-121.

[34] C. Wrenger, K. Luersen, T. Krause, S. Muller, R.D. Walter, The *Plasmodium falciparum* bifunctional ornithine decarboxylase, *S*-adenosyl-Lmethionine decarboxylase, enables a well balanced polyamine synthesis without domain-domain interaction, J Biol Chem 276 (2001) 29651- 29656.

[35] T. Nozaki, V. Ali, M. Tokoro, Sulfur-containing amino acid metabolism in parasitic protozoa, Adv Parasitol 60 (2005) 1-99.

[36] V. Ali, T. Nozaki, Current therapeutics, their problems, and sulfurcontaining-amino-acid metabolism as a novel target against infections by "amitochondriate" protozoan parasites, Clin Microbiol Rev 20 (2007) 164-187.

[37] I.J. Anderson, B.J. Loftus, Entamoeba histolytica: observations on metabolism based on the genome sequence, Exp Parasit 110 (2005) 173-177.

[38] A.E. McKie, T. Edlind, J. Walker, J.C. Mottram, G.H. Coombs, The primitive protozoon *Trichomonas vaginalis* contains two methionine gamma-lyase genes that encode members of the gamma-family of pyridoxal 5'- phosphate-dependent enzymes, J Biol Chem 273 (1998) 5549-5556.

[39] M. Tokoro, T. Asai, S. Kobayashi, T. Takeuchi, T. Nozaki, Identification and characterization of two isoenzymes of methionine gamma-lyase from *Entamoeba histolytica*: a key enzyme of sulfur-amino acid degradation in an anaerobic parasitic protist that lacks forward and reverse transsulfuration pathways, J Biol Chem 278 (2003) 42717-42727.

[40] H. Tanaka, N. Esaki, K. Soda, A versatile bacterial enzyme: L-methionine gammy-lyase, Enz Microb Techn 7 (1985) 530-537. 14

[41] G.H. Coombs, J.C. Mottram, Trifluoromethionine, a prodrug designed against methionine gamma-lyase-containing pathogens, has efficacy *in vitro* and *in vivo* against *Trichomonas vaginalis*, Antimicrob Agents Chemother 45 (2001) 1743-1745.

[42] D. Sato, S. Kobayashi, H. Yasui, N. Shibata, T. Toru, M. Yamamoto, G. Tokoro, V. Ali, T. Soga, T. Takeuchi, M. Suematsu, T. Nozaki, Cytotoxic effect of amide derivatives of trifluoromethionine against the enteric protozoan parasite Entamoeba histolytica, Int J Antimicrob Agents 35 (2010) 56-61.

[43] D. Sato, W. Yamagata, S. Harada, T. Nozaki, Kinetic characterization of methionine gamma-lyases from the enteric protozoan parasite *Entamoeba histolytica* against physiological substrates and trifluoromethionine, a promising lead compound against amoebiasis, FEBS J 275 (2008) 548- 560.

[44] T. Nozaki, T. Asai, L.B. Sanchez, S. Kobayashi, M. Nakazawa, T. Takeuchi, Characterization of the gene encoding serine acetyltransferase, a regulated enzyme of cysteine biosynthesis from the protist parasites *Entamoeba histolytica* and *Entamoeba dispar*. Regulation and possible function of the cysteine biosynthetic pathway in *Entamoeb*a, J Biol Chem 274 (1999) 32445-32452.

[45] T. Nozaki, T. Asai, S. Kobayashi, F. Ikegami, M. Noji, K. Saito, T. Takeuchi, Molecular cloning and characterization of the genes encoding two isoforms of cysteine synthase in the enteric protozoan parasite *Entamoeba histolytica*, Molec Biochem Parasit 97 (1998) 33-44.

[46] G.D. Westrop, G. Goodall, J.C. Mottram, G.H. Coombs, Cysteine biosynthesis in *Trichomonas vaginalis* involves cysteine synthase utilizing *O*phosphoserine, J Biol Chem 281 (2006) 25062-25075.

[47] J.E. Ellis, N. Yarlett, D. Cole, M.J. Humphreys, D. Lloyd, Antioxidant defences in the microaerophilic protozoan *Trichomonas vaginalis*: comparison of metronidazole-resistant and sensitive strains, Microbiology 140 (1994) 2489-2494.

[48] M. Abid, A.R. Bhat, F. Athar, A. Azam, Synthesis, spectral studies and antiamoebic activity of new 1-N-substituted thiocarbamoyl-3-phenyl-2- pyrazolines, Eur J Biochem 44 (2009) 417-425.

[49] R.A. Williams, G.D. Westrop, G.H. Coombs, Two pathways for cysteine biosynthesis in *Leishmania major*, Biochem J 420 (2009) 451-462.

[50] C.K. Pang, J.H. Hunter, R. Gujjar, R. Podutoori, J. Bowman, D.G. Mudeppa, P.K. Rathod, Catalytic and ligand-binding characteristics of *Plasmodium falciparum* serine hydroxymethyltransferase, Molec Biochem Parasit 168 (2009) 74-83.

[51] F. Rossi, S. Garavaglia, G.B. Giovenzana, B. Arca, J. Li, M. Rizzi, Crystal structure of the *Anopheles gambiae* 3-hydroxykynurenine transaminase, Proc Natl Acad Sci U.S.A. 103 (2006) 5711-5716. 15

[52] F. Rossi, F. Lombardo, A. Paglino, C. Cassani, G. Miglio, B. Arca, M. Rizzi, Identification and biochemical characterization of the *Anopheles gambiae* 3-hydroxykynurenine transaminase, FEBS J 272 (2005) 5653-5662.

[53] I.B. Muller, R. Das Gupta, K. Luersen, C. Wrenger, R.D. Walter, Assessing the polyamine metabolism of *Plasmodium falciparum* as chemotherapeutic target, Molec Biochem Parasit 160 (2008) 1-7.

[54] M. Mukherjee, S.A. Sievers, M.T. Brown, P.J. Johnson, Identification and biochemical characterization of serine hydroxymethyl transferase in the hydrogenosome of *Trichomonas vaginalis*, Eukaryot Cell 5 (2006) 2072- 2078.

[55] Y. Yuthavong, S. Kamchonwongpaisan, U. Leartsakulpanich, P. Chitnumsub, Folate metabolism as a source of molecular targets for antimalarials, Future Microbiol 1 (2006) 113-125.

[56] A.C. Anderson, Targeting DHFR in parasitic protozoa, Drug Discov Today 10 (2005) 121-128.

[57] S. Agrawal, A. Kumar, V. Srivastava, B.N. Mishra, Cloning, expression, activity and folding studies of serine hydroxymethyltransferase: a target enzyme for cancer chemotherapy, J Mol Microbiol Biotechnol 6 (2003) 67- 75.

[58] A.A. Figueiredo da Silva, L. de Carvalho Vieira, M.A. Krieger, S. Goldenberg, N.I. Zanchin, B.G. Guimaraes, Crystal structure of chagasin, the endogenous cysteine-protease inhibitor from *Trypanosoma cruzi*, J Struct Biol 157 (2007) 416-423.

[59] G. Ecco, J. Vernal, G. Razzera, C. Tavares, V.I. Serpa, S. Arias, F.K. Marchini, M.A. Krieger, S. Goldenberg, H. Terenzi, Initial characterization of a recombinant kynureninase from *Trypanosoma cruzi* identified from an EST database, Gene 448 (2009) 1-6.

[60] C. Burri, R. Brun, Eflornithine for the treatment of human African trypanosomiasis, Parasitol Res 90 Supp 1 (2003) S49-52.

[61] S. Muller, G.H. Coombs, R.D. Walter, Targeting polyamines of parasitic protozoa in chemotherapy, Trends Parasit 17 (2001) 242-249.

[62] R. Das Gupta, T. Krause-Ihle, B. Bergmann, I.B. Muller, A.R. Khomutov, S. Muller, R.D. Walter, K. Luersen, 3-Aminooxy-1-aminopropane and derivatives have an antiproliferative effect on cultured Plasmodium falciparum by decreasing intracellular polyamine concentrations, Antimicrob Agents Chemother 49 (2005) 2857-2864.

[63] R.M. Khomutov, T. Hyvonen, E. Karvonen, L. Kauppinen, T. Paalanen, L. Paulin, T. Eloranta, R.L. Pajula, L.C. Andersson, H. Poso, 1-Aminooxy-3- aminopropane, a new and potent inhibitor of polyamine biosynthesis that inhibits ornithine

decarboxylase, adenosylmethionine decarboxylase and spermidine synthase, Biochem Biophys Res Commun 130 (1985) 596- 602.

[64] P. Arteaga-Nieto, E. Lopez-Romero, Y. Teran-Figueroa, C. Cano-Canchola, J.P. Luna Arias, A. Flores-Carreon, C. Calvo-Mendez, *Entamoeba histolytica*: 16 purification and characterization of ornithine decarboxylase, Exp Parasit 101 (2002) 215-222.

[65] V.T. Dufe, D. Ingner, O. Heby, A.R. Khomutov, L. Persson, S. Al-Karadaghi, A structural insight into the inhibition of human and *Leishmania donovani* ornithine decarboxylases by 1-amino-oxy-3-aminopropane, Biochem J 405 (2007) 261-268.

[66] D.A. Scott, S.M. Hickerson, T.J. Vickers, S.M. Beverley, The role of the mitochondrial glycine cleavage complex in the metabolism and virulence of the protozoan parasite *Leishmania major*, J Biol Chem 283 (2008) 155- 165.

[67] C. Nosei, J.L. Avila, Serine hydroxymethyltransferase activity in *Trypanosoma cruzi*, *Trypanosoma rangeli* and American *Leishmania* spp, Comp Biochem Physiol 81 (1985) 701-704.

[68] S. Alfadhli, P.K. Rathod, Gene organization of a *Plasmodium falciparu*m serine hydroxymethyltransferase and its functional expression in *Escherichia coli*, Molec Biochem Parasit 110 (2000) 283-291.

[69] E. Salcedo, P.F. Sims, J.E. Hyde, A glycine-cleavage complex as part of the folate one-carbon metabolism of *Plasmodium falciparum*, Trends Parasit 21 (2005) 406-411.

[70] D.J. Linstead, R.A. Klein, G.A. Cross, Threonine catabolism in *Trypanosoma bruce*i, J Gen Microbiol 101 (1977) 243-251.

[71] S. Sato, B. Clough, L. Coates, R.J. Wilson, Enzymes for heme biosynthesis are found in both the mitochondrion and plastid of the malaria parasite *Plasmodium falciparum*, Protist 155 (2004) 117-125.

[72] K. Zhang, J.M. Pompey, F.F. Hsu, P. Key, P. Bandhuvula, J.D. Saba, J. Turk, S.M. Beverley, Redirection of sphingolipid metabolism toward *de novo* synthesis of ethanolamine in Leishmania, EMBO J 26 (2007) 1094-1104.

[73] H. Cui, G.F. Ruda, J. Carrero-Lerida, L.M. Ruiz-Perez, I.H. Gilbert, D. Gonzalez-Pacanowska, Exploring new inhibitors of *Plasmodium falciparum* purine nucleoside phosphorylase, Eur J Med Chem 45 (2010) 5140-5149.

[74] P.N. Lowe, A.F. Rowe, Aminotransferase activities in *Trichomonas vaginalis*, Molec Biochem Parasit 21 (1986) 65-74.

[75] W. Blankenfeldt, C. Nowicki, M. Montemartini-Kalisz, H.M. Kalisz, H.J. Hecht, Crystal structure of *Trypanosoma cruzi* tyrosine aminotransferase: substrate specificity is influenced by cofactor binding mode, Protein Sci 8 (1999) 2406-2417.

[76] J.V. Rego, S.M. Murta, P. Nirde, F.B. Nogueira, H.M. de Andrade, A.J. Romanha, *Trypanosoma cruzi*: characterisation of the gene encoding tyrosine aminotransferase in benznidazole-resistant and susceptible populations, Exp Parasit 118 (2008) 111-117.

[77] C. Gafan, J. Wilson, L.C. Berger, B.J. Berger, Characterization of the ornithine aminotransferase from *Plasmodium falciparum*, Molec Biochem Parasit118 (2001) 1-10. 17

[78] M.W. Simon, E. Martin, A.J. Mukkada, Evidence for a functional glyoxylate cycle in the leishmaniae, J Bac 135 (1978) 895-899.

[79] N.V. Grishin, A.L. Osterman, H.B. Brooks, M.A. Phillips, E.J. Goldsmith, Xray structure of ornithine decarboxylase from *Trypanosoma brucei*: the native structure and the structure in complex with alphadifluoromethylornithine, Biochemistry 38 (1999) 15174-15184.

[80] J.V. Becker, L. Mtwisha, B.G. Crampton, S. Stoychev, A.C. van Brummelen, S. Reeksting, A.I. Louw, L.M. Birkholtz, D.T. Mancama, *Plasmodium falciparum* spermidine synthase inhibition results in unique perturbationspecific effects observed on transcript, protein and metabolite levels, BMC Genomics 11 (2010) 235.

[81] S.C. Alfieri, E.P. Camargo, Trypanosomatidae: isoleucine requirement and threonine deaminase in species with and without endosymbionts, Exp Parasit 53 (1982) 371-380.

[82] I.A. Moya, G.D. Westrop, G.H. Coombs, J.F. Honek, Mechanistic studies on the enzymatic processing of fluorinated methionine analogs by *Trichomonas vaginalis* methionine gamma-lyase, Biochem J (2011).

[83] R. Panizzutti, M. de Souza Leite, C.M. Pinheiro, J.R. Meyer-Fernandes, The occurrence of free D-alanine and an alanine racemase activity in *Leishmania amazonensis*, FEMS Microbiol Lett 256 (2006) 16-21.

Appendix B:

Curriculum Vitae

CURRICULUM VITAE

Contact Information and Personal Information

Name:	Alexandra Binter
Address:	Hubert-Hoffmann-Ring 30e; 8044 Graz
Phone:	0676/9646764
Email:	alexandra.binter@tugraz.at
Date and place of birth:	21st of October, 1981; Villach, Austria
Citizenship:	Austrian

Education

1988 – 1992	Elementary School in Görtschach/Gailtal, Austria
1992 – 1996	Secondary School in Hermagor, Austria
1996 – 2001	Federal College of Kindergarten Pedagogy, Klagenfurt, Austria
06/2001	Matura ("mit ausgezeichnetem Erfolg")
2001 – 2004	Studies of Technical Chemistry (F800) at University of Technology, Graz
10/2004	First section of the diploma completed
2004 – 2007	Studies of Biochemistry, Biotechnology and Food Chemistry (F809) at University of Technology, Graz
06/2005 – 08/2005	Summer School at Syracuse University, Syracuse, NY
09/2005 – 06/2006	Studies at Universidad de Sevilla, Seville, Spain, as part of the Erasmus Student Exchange Program
09/2006 – 06/2007	Diploma thesis at the Institute of Biochemistry, with Prof. Peter Macheroux: "*Characterization of Bacillus subtilis* NADPH:FMN *Oxidoreductase* YhdA *in Respect of Oligomerization, Activity and Thermostability*"
09/2007	Diploma completed
10/2007-09/2011	Work on doctoral thesis at the Institute of Biochemistry

Research Activities

07/2004	Project at the Department of Inorganic Chemistry, TUG, with Prof. Karl Hassler
06/2005 – 08/2005	Project at the Bioinorganic Chemistry Research Group, Syracuse University, NY, with Prof. James Dabrowiak: "*Formation of monofunctional cisplatin-DNA adducts in carbonate buffer.*"
07/2006	Project at the Department of Biotechnology, TUG, with Prof. Bernd Nidetzky: *"Kinetic and temperature*

inactivation studies on Sucrose phosphorylase from Leuconostoc mesenteroides"

09/2006 – 06/2007:   Work on my Diploma thesis at the Institute of Biochemistry, Prof. Peter Macheroux: "*Characterization of Bacillus subtilis* NADPH:FMN *Oxidoreductase* YhdA *in Respect of Oligomerization, Activity and Thermostability"*

10/2007-09/2011   Work on doctoral thesis on Nikkomycin biosynthesis at the Institute of Biochemistry, TU Graz

Other Qualifications

Languages: German as mother tongue,
                      fluent in English and Spanish

Computer Skills: Microsoft Office
                      Bioinformatics (databases, sequence alignments,
                      protein analysis etc.)

Publications

1. *Formation of monofunctional cisplatin-DNA adducts in carbonate buffer.*
   Binter, A.; Goodisman, J.; Dabrowiak, J.C.
   J. Inorg. Biochem. 2006**,** *100,* 1219-1224.

2. *Chair, Boat and Twist Conformation of Dodecamethylcyclohexasilane and Undecamethylcyclohexasilane: A Combined DFT and Raman Spectroscopic Study*
   Günter Tekauz, Alexandra Binter, Karl Hassler, Michaela Flock
   Chemphyschem. 2006 Jan 13;:1641126

3. *A single intersubunit salt bridge affects oligomerization and catalytic activity in a bacterial quinone reductase*
   Binter, A.; Staunig, N.; Jelesarov, I.; Lohner, K.; Palfey, B.A.; Deller S.; Gruber, K.; Macheroux,
   FEBS JOURNAL 2009; 276; 18: 5263-5274